



# UNIVERSITÀ DEGLI STUDI DI MILANO

Doctorate in Pharmacological, Experimental and Clinical Sciences  
Department of Pharmacological and Biomolecular Sciences  
XXXI Cycle

PhD Thesis

## A spine to nucleus signaling pathway in Alzheimer's disease

BIO/14

Ana Cláudia da Rocha RIBEIRO  
Student Number: R11496

TUTOR: Prof. Fabrizio Gardoni

CO-TUTORS: Prof. Elena Marcello and Prof. Monica Di Luca

COORDINATOR: Prof. Alberico L. Catapano

Academic year: 2017-2018

"Para ser grande, sê inteiro: nada  
Teu exagera ou exclui.  
Sê todo em cada coisa. Põe quanto és  
No mínimo que fazes.  
Assim em cada lago a lua toda  
Brilha, porque alta vive."  
Fernando Pessoa

Scientists have become the bearers of the torch of discovery in our quest for  
knowledge.

Stephen Hawking

# Acknowledgements

First, I would like to thank my supervisors, Professor Fabrizio Gardoni, Professor Elena Marcello and Professor Monica Di Luca for having accepted me and received me in their lab, for all the discussions, ideas, and the very close relationship that we built while developing this project –it wouldn't be a reality without you;

To all my lab mates: Nicolò Carrano, Sebastien Therin, Lina Vandermeulen, Elisa Zianni, Manuela Mellone, Silvia Pelucchi, Francesca Palese, Luca Franchini and Annalisa Longhi – for all the good and not so good times, for all that we overcame, for all the joyful laughs we had and all the numerous moments and memories - my many many thanks, this work could have not been done without all your contributions;

To the Marie Curie SyDAD program, to all my fellow PhD colleagues and to all the connections we made, places we visited and memories we shared – it certainly helped me grow, not only as a scientist but as a person;

To our collaborators – Christophe Mulle and Gäel Barthelet in Bordeaux and Nico Mitro and Matteo Audano in Milan – your contributions, your ideas and your work were vital for us to get this project to a good port;

To all my friends, to the Portuguese community in Milan and in Bordeaux and to those that were there for me when I needed help seeing things with better eyes – my thanks will never be enough;

To my Hulk and Torre family – when a “distraction” becomes part of your life and helps you find the strength to go on and conquer it;

To my Ben Davis – because without you I could have not done it, because you were and you are always there for me, for loving me and showing me that great things can be achieved and deserved, and all I could add but would run out of space to... ♥;

To my mom, my dad, my sister and my grandma – for never letting me give up, for always listening to me either in happiness or in sadness, for allowing me the completion of this dream, for giving what you have and what you don't have for me and for simply being the best family I could possibly have – this one is for you! ♥;

*À minha mãe, ao meu pai, à minha irmã e à minha avó - por nunca me deixarem desistir, por me ouvirem sempre, quer nas situações de alegria quer nas situações de tristeza, por me proporcionarem o realizar deste sonho, por darem o que têm e o que não têm por mim, e por serem simplesmente a melhor família que alguma vez poderia ter - esta é para vocês!;*

And last, but not the least, to all that, even though not specifically mentioned in here, are a part of my life, a very big “thank you!” for all your help and comprehension!

# I. Index

Acknowledgements .....	iii
II. List of illustrations.....	vi
III. List of tables.....	vii
IV. Abstract .....	viii
V. Abstract (Italiano) .....	ix
Introduction.....	1
1. Synapses .....	2
1.1. Excitatory synapses.....	2
2. Ionotropic glutamate receptors.....	3
2.1. Receptors: NMDA .....	4
2.2. Receptors: AMPA and Kainate .....	7
2.3. Receptors: Metabotropic.....	10
3. Synapse-to-nucleus communication pathways .....	11
a. Electrochemical signaling .....	13
b. Regenerative ER calcium waves.....	13
c. Signaling endosomes .....	14
d. Diffusion/facilitated diffusion of soluble proteins .....	14
e. Synapse to nucleus messengers .....	15
3.1. Abelson interacting protein-1 (Abi-1) .....	17
3.2. Amyloid precursor protein intracellular domain-associated protein-1 (AIDA-1d) ...	17
3.3. cAMP responsive element binding protein-2 (CREB2).....	18
3.4. Juxtasyntaptic attractor of Caldendrin on dendritic buttons (Jacob) .....	18
3.5. Nuclear factor kappa of light chain enhancer of activated B-cells (Nf-κB).....	20
3.6. CREB-regulated transcriptional coactivator-1 (CRTC1) .....	21
3.7. RING Finger Protein 10 (RNF10) .....	21
4. Synaptopathies .....	25
4.1. Alzheimer's disease .....	26
4.2. Synapse-to-nucleus impact in synaptopathies.....	32
a) RNF10 .....	35
b) ProSAP2/Shank3 .....	35
c) Jacob.....	35
d) AIDA-1.....	36
e) CREB2/ATF4.....	36
f) CRTC1 .....	37

g) MAPK/ERK.....	37
h) NF- $\kappa$ B .....	37
i) $\gamma$ CaMKII.....	38
Aims.....	40
Materials and Methods .....	42
1. Animals .....	43
2. Genotyping procedures .....	43
3. Immunohistochemistry.....	44
4. RNA extraction and Real Time PCR (qPCR) .....	44
5. Food intake, insulin and glucose tolerance tests .....	45
6. Purification of triton insoluble postsynaptic fractions and crude nuclear fractions .....	45
7. Western Blot.....	46
8. Antibodies.....	47
9. Spine analysis procedures.....	47
10. Confocal imaging .....	48
11. ELISA .....	48
12. Behavioral testing .....	49
12.1. Rotarod.....	49
12.2. Y-Maze .....	49
12.3. Novel Object Recognition Test (NORT) .....	50
13. Electrophysiology.....	51
14. Statistical Analysis.....	53
Results .....	54
1. Genotypic confirmation of RNF10 .....	55
2. RNF10 KO animals have lower body weight and increased food intake .....	56
3. Metabolic studies in RNF10 KO animals .....	57
4. KO animals show altered spine morphology in the hippocampus .....	59
5. KO animals display differences in the molecular composition of the synapse .....	61
6. KO animals show a decreased level of A $\beta$ in the hippocampus .....	65
7. KO animals do not present any difference in the locomotion .....	65
8. KO animals display slightly altered exploratory behavior .....	66
9. KO animals display impaired long memory functionality.....	67
10. KO animals present normal basal synaptic transmission .....	69
Discussion .....	74
References.....	82

## II. List of illustrations

Figure 1 Glutamate receptors and synaptic plasticity .....	4
Figure 2 Structural mechanism of NMDAR activation .....	6
Figure 3 Scaffolding and Trafficking Proteins Involved in AMPAR Membrane Trafficking and Synaptic Plasticity .....	8
Figure 4 mGlu receptor families.....	10
Figure 5 The different mechanisms of synapse-to-nucleus signaling .....	12
Figure 6 Long-distance transport from synapse to nucleus .....	16
Figure 7 Time-Lapse Imaging of Jacob's Nuclear Translocation .....	20
Figure 8 Characterizing the RNF10 binding region of MEOX2 .....	22
Figure 9 Disease proteins dysregulating spine morphology .....	26
Figure 10 Alzheimer's disease: histopathology, mechanisms and progression .....	27
Figure 11 APP processing pathways .....	29
Figure 12 Synapse-to-nucleus signaling regulates neuronal excitability and synapse plasticity .....	34
Figure 13 $\alpha$ CaMKII is dysregulated in the Alzheimer's disease hippocampus.....	39
Figure 14 Representative scheme of the fractionation, with all the steps from half brain to TIF fraction .....	46
Figure 15 Model used to count dendritic spines.....	48
Figure 16 Representative scheme of the maze setup for the familiarization phase of the NORT .....	50
Figure 17 Representative scheme of the maze setup for the 2 hours test of the NORT ....	51
Figure 18 Representative scheme of the maze setup for the 24 hours test of the NORT ..	51
Figure 19 Schematics of the protocol used to record the excitatory inputs from the perforant path to the dentate cells .....	53
Figure 20 Immunocytochemistry of the CA1 region of the hippocampus in RNF10 KO and WT mice .....	55
Figure 21 Determination and confirmation of RNF10 genotype .....	56
Figure 22 Assessment of body weight and food intake of the animals.....	57
Figure 23 Measurements of basal temperature (A), total glucose levels (B), and insulin (C) and FGF-21 (D) by ELISA.....	58
Figure 24 Glucose (A) and Insulin (B) Tolerance tests .....	59
Figure 25 Immunohistochemistry in brain slices of WT and KO animals .....	60
Figure 26 Spine morphology count and categorization results .....	61
Figure 27 Western Blot assessment in proteins involved in AD pathogenesis.....	62
Figure 28 Western Blot analysis of the synaptic proteins in the hippocampus.....	63
Figure 29 Western Blot on the target gene of RNF10 .....	63
Figure 30 Western Blots in the proteins involved in AD pathogenesis in the hippocampus .....	64
Figure 31 Western Blot in a synaptic plasticity protein, and in an adhesion molecule cleaved by ADAM10.....	64
Figure 32 ELISA performed to detect amyloid-beta in the hippocampus.....	65
Figure 33 Rotarod and Accelerated Rotarod testing in adult 6-months old animals .....	66

Figure 34 Rotarod and Accelerated Rotarod testing in aged 18-months old animals.....	66
Figure 35 Testing the exploratory activity in a Y-Maze test.....	67
Figure 36 NORT 2 hours after familiarization in adult and aged WT and RNF10 KO mice ..	68
Figure 37 NORT 24 hours after familiarization in adult and aged WT and RNF10 KO mice	69
Figure 38 Electrophysiology model used to record EPSCs .....	70
Figure 39 Results of the electrophysiological studies.....	70
Figure 40 Decay Time Measures in WT and KO in NMDAR currents.....	71
Figure 41 Miniature EPSCs measurements .....	72
Figure 42 Induction of LTP by theta burst stimulation the CA1 area of the hippocampus.	73
Figure 43 A $\beta$ 42 treatment induces RNF10-tdEOS translocation from distal dendrites to the nucleus in hippocampal neurons .....	75
Figure 44 RNF10 expression and localization are affected in AD patients .....	76
Figure 45 Represents the effects of FGF21 on the brain.....	77

### III. List of tables

Table 1: Synaptonuclear messengers, related pathologies and their molecular mechanisms .....	32
Table 2 All proteins assessed in the molecular characterization, in both total brain and hippocampus.....	62

## IV. Abstract

RING Finger Protein 10 (RNF10) is a novel synapse-to-nucleus protein messenger, enriched at the excitatory synapses and associated with the GluN2A subunit of NMDA receptors. RNF10 translocates from synapses to the nucleus, upon the activation of synaptic GluN2A-containing NMDA receptors, inducing the expression of specific target genes that have a role in Alzheimer's disease (AD) pathogenesis or that are associated with the regulation of dendritic spine morphology. Notably, RNF10 expression is reduced in AD patients' hippocampi at the earlier stages of the disease and A $\beta$  oligomers trigger RNF10 translocation from the synapse to the nucleus.

The main objective of the PhD project is to characterize the role of RNF10 in cognitive function and synaptic plasticity, using the RNF10 KO mice as an experimental model.

RNF10 KO mice present reduced body weight with an increase in food intake, and no alterations in glucose, insulin or FGF-21 levels. The molecular characterization shows downregulation of the amyloid cascade players in the hippocampus, and a consequent decrease in amyloid levels. Concerning morphological analysis, RNF10 KO animals show a significant increase in mushroom-type dendritic spines and a decrease in thin-type spines. In the behavioral characterization, both adult and aged KO animals have normal locomotion, but displayed slightly altered exploratory behavior, as well as an impaired long-term memory function. Moreover, RNF10 KO animals present a complete loss of long-term potentiation in CA1 area of the hippocampus.

Overall, these data suggest an involvement of RNF10 in AD pathogenesis, pointing towards a possible role for RNF10 in cognitive dysfunction along aging.

*Keywords:* RNF10, synaptonuclear messenger, NMDA receptor, Alzheimer's disease

## V. Abstract (Italiano)

Ring Finger Protein 10 (RNF10) è una proteina messaggero sinaptonucleare localizzata a livello delle sinapsi eccitatorie e associata con la subunità GluN2A del recettore NMDA. Stimolazione dei recettori NMDA contenenti la subunità GluN2A induce il trasporto di RNF10 dalla sinapsi al nucleo e la conseguente espressione di specifici geni bersaglio, alcuni dei quali svolgono un ruolo nella patogenesi della malattia di Alzheimer o nella modulazione della morfologia delle spine dendritiche. E' inoltre importante osservare come l'espressione di RNF10 sia ridotta negli ippocampi di pazienti con malattia di Alzheimer e come oligomeri di A $\beta$  siano in grado di indurre il trasporto di RNF10 dalla sinapsi al nucleo.

Il principale obiettivo del progetto di dottorato è la caratterizzazione del ruolo di RNF10 nei processi cognitivi e la plasticità sinaptica utilizzando gli animali RNF10 KO quale modello sperimentale.

I topi RNF10 KO sono caratterizzati da una riduzione del peso corporeo e da un concomitante aumento dell'assunzione di cibo in assenza di modificazioni significative dei livelli di glucosio, insulina e FGF-21. L'analisi molecolare ha mostrato una riduzione nell'animale RNF10 delle proteine coinvolte nel metabolismo di APP nell'ippocampo e una conseguente riduzione dei livelli di A $\beta$ . L'analisi morfologica ha mostrato un aumento significativo delle spine dendritiche mushroom e una concomitante riduzione delle spine sottili. Una approfondita analisi del comportamento ha rilevato come gli animali RNF10 KO non presentino modificazioni del comportamento motorio, sia in animali adulti che anziani, mentre è stata osservata una moderata alterata alterazione sia dell'esplorazione che della memoria a lungo termine. Inoltre, gli animali RNF10 sono caratterizzati dalla completa assenza di potenziamento a lungo termine nell'area CA1 dell'ippocampo.

In conclusione, questi risultati suggeriscono il coinvolgimento di RNF10 nella patogenesi della malattia di Alzheimer e indicano un possibile ruolo di questa proteina nelle alterazioni delle capacità cognitive associate all'invecchiamento.

# INTRODUCTION

The human brain has always been the target of many studies, to uncover more of what is behind our functioning and reasoning. Over the years, much has been brought to light, starting with Santiago Ramón y Cajal and with his investigations on the microscopic structures of the brain. He was the first to give the idea that neurons communicate with each other, yet are not continuous in the body (Cajal 1954), laying the path to the term “synapse”, that later appeared by the hands of Michael Foster and Charles Sherrington in 1897 (Foster & Sherrington 1897). The word "synapse" is derived from the Greek words "syn" and "haptein" that mean "together" and "to clasp", respectively.

## 1. Synapses

Synapses are junctions between the end terminal of one neuron (presynaptic) and the membrane of another neuron (postsynaptic). The space in between is called synaptic cleft, a gap of approximately 20 nm. After stimulation, the neurotransmitters that are contained in the presynaptic vesicles inside the presynaptic neuron, are released in this synaptic cleft and captured by the receptors that exist in the membrane of the postsynaptic neuron. This binding will initiate an action potential, caused by the opening of ion channels and the subsequent alteration of the membrane potential and conductance. The type of neurotransmitter released will determine the type of synapse, that can be excitatory, inhibitory or modulatory. While inhibitory synapses are formed on the shaft of the synapses, on cell bodies or axon initial segments (Sheng & Kim 2011), excitatory synapses occur mainly at the dendritic spines (Bourne & Harris 2008).

### 1.1. Excitatory synapses

As described before, synapses are characterized as polarized neuronal cell junctions with specific membrane specialties at the transmitter-releasing presynaptic site and the afferent postsynaptic part (Boeckers 2006). Considering specifically the excitatory synapses, that use glutamate as a neurotransmitter, this afferent membrane appeared thickened and more electron-dense than other neuronal substructures (De Robertis & Bennett 1955; Palade & Palay 1954) being therefore called the postsynaptic thickening or the postsynaptic density (PSD).

While the PSD presents itself as a dynamic structure, the constituent proteins are organized in a precise and hierarchical manner, determined by the targeting and binding characteristics of the individual proteins. This leads to the division of the PSD into several groups, including scaffolding proteins like post-synaptic density protein 95 (PSD-95), Shank and Homer; cytoplasmic signaling molecules such as kinases (for example, calcium-calmodulin-dependent kinase II alpha (CaMKII $\alpha$ ) and nonreceptor tyrosine kinases) and membrane receptors, being the glutamate receptors (GluRs) the most relevant (Sheng & Kim 2011). Ionotropic and metabotropic glutamate receptors, for instance, have different locations within the postsynaptic membrane and PSD. The ionotropic N-methyl-D-aspartic acid (NMDA) and non-NMDA  $\alpha$ -amino-3-hydroxy-5-methyl-4-isoxazolepropionic acid (AMPA) glutamate receptors are primarily in the center along the PSD, while the metabotropic glutamate receptors (mGluRs) are peripheral in their location (Cohen 2016), characterizing the excitatory synapses.

## 2. Ionotropic glutamate receptors

L-glutamate is the main excitatory neurotransmitter in the mammalian nervous system and is detected at postsynaptic terminals by both G-protein-coupled and ionotropic glutamate receptors (iGluRs) (Voglis & Tavernarakis 2006). There are also metabotropic glutamate receptors (mGluRs), found in 8 different subtypes, divided in 3 major groups (for more, see Page 10). Up to today, four iGluR subtypes were distinguished based on their pharmacology and sequence similarity (Collingridge et al. 2009): AMPA receptors (AMPA; GluA1–4), kainate receptors (KARs; GluK1–5), NMDA receptors (NMDARs; GluN1, GluN2A–D, and GluN3A–B) (**Figure 1**), and the orphan delta iGluRs (GluD1 and GluD2) (Krieger et al. 2015).

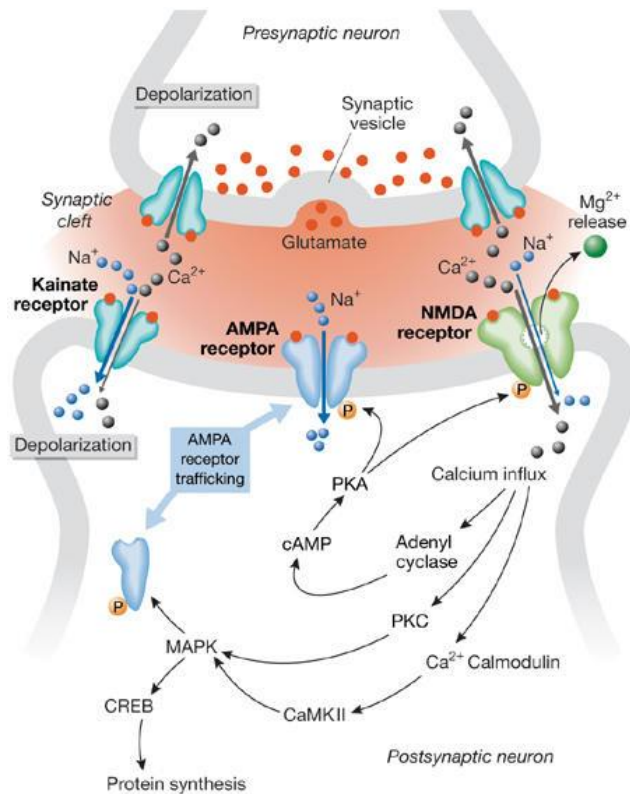


**FIGURE 1 Glutamate receptors and synaptic plasticity.** The arrival of a series of impulses at the presynaptic terminal triggers the release of glutamate, which binds to glutamate receptors at the postsynaptic membrane. On activation, AMPA and kainate receptors conduct sodium ions, which initiate postsynaptic depolarization. Membrane potential changes initiate the release of magnesium ions that block NMDA receptors. Calcium influx through NMDA channels sets off a chain of events that establish long-term potentiation. Kainate receptors at the presynaptic end also seem to facilitate synaptic transmission at specific synapses by augmenting neurotransmitter release. AMPA,  $\alpha$ -amino-3-hydroxy-5-methyl-4-isoxazolepropionate; CaMKII, calcium/calmodulin-dependent kinase II; CREB, cAMP response element binding protein; MAPK, mitogen-activated protein kinase; NMDA, N-methyl-D-aspartate; PKA, protein kinase A; PKC, protein kinase C. (Voglis & Tavernarakis 2006)

## 2.1. Receptors: NMDA

NMDARs are ligand-gated calcium ( $\text{Ca}^{2+}$ ) permeable channels that are involved in synaptic plasticity, including LTP and LTD. As non-selective cation channels tetrameric receptors, they show voltage dependence (Dingledine et al. 1999) and their subunit composition will determine functional properties, like open probability and decay kinetics (Paoletti 2011). Subunits from seven homologous genes have been identified and classified accordingly with their sequence homology: GluN1, GluN2A – GluN2D and GluN3A – GluN3B (Monaghan et al. 2012), with the tetramer being always composed of two GluN1 subunits combined with two regulatory subunits of GluN2 or GluN3 subtype. GluN2A and GluN2B are the most prevalent subunits, and their pairing in heterodimers

or heterotrimers with GluN1 account for the majority of NMDAR subtypes found in the adult brain (Carta et al. 2018), as either GluN1-GluN2A diheteromeric receptors or GluN1-GluN2A-GluN2B triheteromeric receptors (Wyllie et al. 2013).

GluN2A and GluN2B are also the main target of a composition shift during developmental stages, as NMDARs almost exclusively composed by GluN2B are shifted to NMDARs containing a significant GluN2A contribution, with this process taking place usually around postnatal 2-5 weeks in mice (McKay et al. 2018).

GluN1 subunit is ubiquitously expressed in the central nervous system (CNS) whereas GluN2 subunits have different expressions accordingly with the developmental phase and area of the brain. As referred, GluN2A subunit increases gradually after birth, being abundantly expressed in the adult phase while GluN2B peaks around postnatal day (P7-10) and gradually becomes restricted to forebrain areas such as cortex, hippocampus, striatum and olfactory bulb, where its expression will remain high. GluN2C is a late developmental subunit, with an expression mainly restricted to the cerebellum and the olfactory bulb. GluN2D expression decreases after birth, being only expressed in a weakly manner, in the adult, in the brainstem (Paoletti 2011). GluN3A expression is low before birth, peaks at early postnatal stage and then returns to a low expression level as an adult whereas GluN3B acts similarly to GluN2A, starting with a low expression that gradually increases until the adult age, when its universally expressed in the CNS, just as GluN1 – thus indicating a role for GluN3B in the adult NMDAR function (Wee et al. 2008).

The subunits structure is modular, with four semiautonomous domains: the extracellular amino-terminal domain (ATD or NTD), the extracellular ligand-binding domain (LBD), the transmembrane domain (TMD), and an intracellular carboxyl-terminal domain (CTD) (Traynelis et al. 2010). The NTD (first 380 aminoacids) is involved in subunit assembly; the LBD (~300 aminoacids), also called agonist-binding domain, where the binding of glycine in GluN1 and GluN3 and glutamate in GluN2 occurs; and the CTD, that is involved in receptor trafficking, anchoring and coupling to signaling complexes, which is highly variable in length accordingly to the subunit (Paoletti 2011). Particularly, the TMD consists of three transmembrane helices (M1, M3, and M4) and a membrane re-entrant loop (M2) (Sobolevsky et al. 2009). M1, M2, and M3 form a structure that resembles that of an inverted potassium (K<sup>+</sup>)-channel pore, and M4 primarily makes contacts with the TMD of an adjacent subunit (Traynelis et al. 2010).

NMDARs present some characteristic features that distinguish them from other receptors like AMPA or kainate (Dingledine et al. 1999), as for their activation they require the presence of two agonists, glycine and glutamate (**Figure 2**).

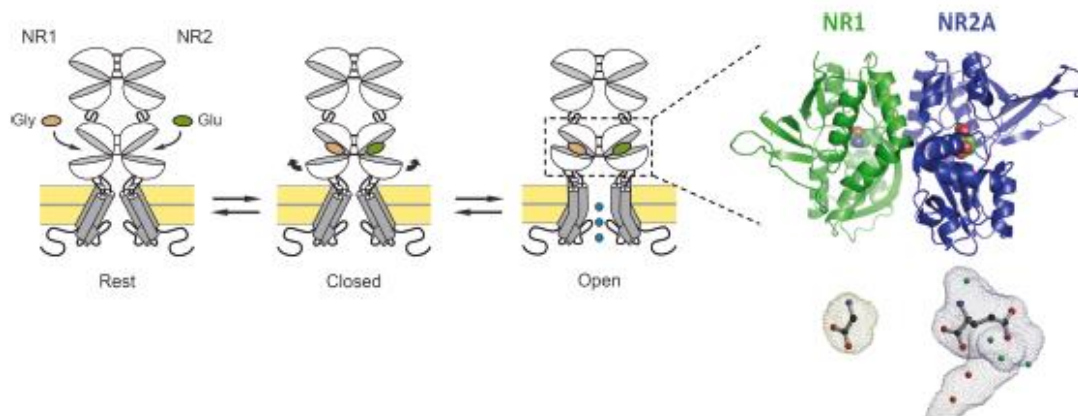


**FIGURE 2 Structural mechanism of NMDAR activation.** Both glycine and glutamate are required for NMDAR channels to open. On the right is shown the X-ray crystal structure of a GluN1 / GluN2A ABD heterodimer with glycine bound to the GluN1 subunit and glutamate to the GluN2A subunit (the size of each agonist binding cavity is also shown). Only a dimer is represented; a full GluN1 / GluN2 receptor is a tetramer made of two such dimers (Paoletti 2011).

NMDA receptor opening needs both glutamate binding and the relief of a magnesium ion ( $Mg^{2+}$ ) block, which involves depolarization of the postsynaptic membrane. This magnesium block turns NMDA currents into voltage dependent currents (Paoletti 2011). As they are highly permeable to  $Ca^{2+}$ , these receptors also participate in both the induction and the maintenance of LTP at postsynaptic hippocampal neurons. The induction of LTP occurs with the opening of NMDA channels to calcium through the removal of the  $Mg^{2+}$  block, although LTP maintenance is achieved by subsequent calcium-induced synapse alterations (Voglis & Tavernarakis 2006).  $Ca^{2+}$  influx through NMDARs is essential for several processes such as synaptogenesis, experience-dependent synaptic remodeling and long-lasting changes in synaptic efficacy such as LTP and LTD, having a very particular effect on calmodulin. Calmodulin is capable of interacting with the C-terminal domain of the GluN1 subunit, reducing the opening and the frequency of the opening of this channel (Ehlers et al. 1996). One of the well-known blockers of NMDA is 5-methyl-10,11-dihydro-5-H-dibenzocyclohepten-5,10-imine maleate, also known as MK-801. This compound is a voltage-dependent blocker of the NMDA receptor ion

channel and has the ability to block this receptor under the depolarized condition (Deshpande et al. 2008). Furthermore, the activity of the NMDARs is modulated by multiple modulations produced by extracellular compounds, usually small molecules or ions, such as hydrogen ( $H^+$ ) and zinc ( $Zn^{2+}$ ), that are endogenously present in the CNS and act as allosteric modulators (Paoletti 2011), as well as phosphorylation. The intracellular domains of NMDAR subunits contain consensus phosphorylation sites for serine/threonine kinases. Protein kinase A (PKA), PKC and several other kinases, including casein kinase II (CK2) and cyclin-dependent kinase 5, have been found to regulate NMDAR function. Moreover, calcium-calmodulin-dependent kinase II (CaMKII) is known to translocate to NMDARs in an activity-dependent manner (Salter et al. 2009). The association of CaMKII with NMDARs is believed to occur following auto-phosphorylation of CaMKII due to  $Ca^{2+}$  entry from activated NMDARs and induction of LTP.

## 2.2. Receptors: AMPA and Kainate

The AMPA receptor (AMPA) is a subtype of the ionotropic glutamate receptor coupled to ion channels that modulate cell excitability by gating the flow of calcium and sodium ions into the cell (Doble 1995). AMPARs are composed by four homologous major core subunits (GluA1-4) that form heteromeric tetrameric complexes (Traynelis et al. 2010) (**Figure 3**). Their subunits differ mostly in their C-terminal sequence, that will determine the type of interaction and with which scaffolding protein. In 1995, Kornau and colleagues discovered that PSD-95 directly interacted with NMDARs (Kornau et al. 1995). PSD-95, as well as other members of the PSD-MAGUKs protein family - PSD-93, SAP102 and SAP97 - bind to the C-terminal of the NMDARs and AMPARs and are involved in the subcellular targeting of their interactors (Huganir & Nicoll 2013). MAGUK proteins are important for AMPAR targeting to synapses, as, for instance, it has been shown that increasing or decreasing the levels of PSD-95 and PSD-93 increase and decrease synaptic AMPARs, respectively (Béïque et al. 2006; Ehrlich & Malinow 2004; Elias et al. 2006; Schlüter et al. 2006).

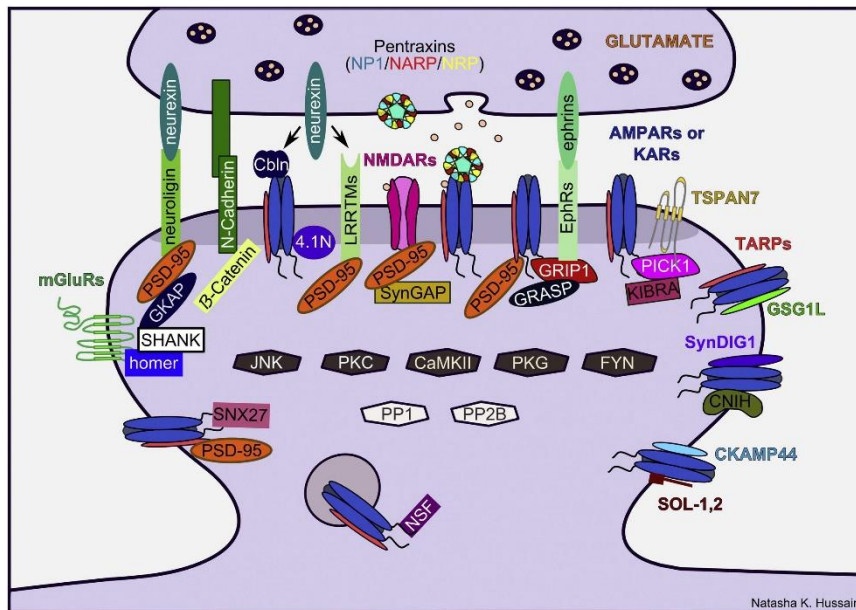


**FIGURE 3 Scaffolding and Trafficking Proteins Involved in AMPAR Membrane Trafficking and Synaptic Plasticity.** Over the last 25 years a molecular machine involved in the structure and function of the excitatory synapse and the regulation of AMPAR membrane trafficking has been revealed. Dozens of proteins have been identified including signaling proteins such as protein kinases (PKA, CaMKII, PKC) and phosphatases (PP2B, PP1) that regulate receptor trafficking as well as proteins that directly or indirectly interact with receptors to immobilize them within the PSD. Central to this PSD structural complex are the MAGUKs, PSD-95, PSD-93, SAP97, and SAP102, which interact with many other proteins to modulate the structure and function of the synapse. Additional proteins, such as NSF, GRIP1/2, and PICK, can couple receptors to the endocytic or exocytic machinery to regulate exocytosis or endocytosis or help escort them through endosomal pathways. Recently, several transsynaptic proteins such as neuroligins, neurexins, and the LRR TMs have been linked not only to synapse formation but also to AMPAR trafficking and synaptic plasticity (Huganir & Nicoll 2013).

GluA1 is one of the most abundant subunits of AMPAR, capable of binding to SAP97 through the PDZ domain and can undergo protein kinase C (PKC) phosphorylation, that has been shown to be required for the expression of long term potentiation (LTP) (Lin et al. 2009). GluA2 and GluA3 were found to bind through their C-terminal PDZ ligands to GRIP1 and 2 (Dong et al. 1997; Dong et al. 1999; Srivastava & Ziff 1999) and PICK1 (Xia et al. 1999), while only GluA2 was shown to bind to the NSF protein, that is involved in the regulation of membrane trafficking (Nishimune et al. 1998). On its turn, it was shown that when the disruption between the binding of GluA2 to PICK1 occurs, there is an inhibition of long term depression (LTD), both in the hippocampus and in the cerebellum (Kim et al. 2001; Seidenman et al. 2003; Chung et al. 2000), while the total knockout (KO) of PICK1 results in deficits in LTP and LTD specifically in the hippocampus (Volk et al. 2010). Most

of the AMPAR that contain the GluN2 subunit are calcium-impermeable (Huganir & Nicoll 2013).

While the roles of GluA1 and GluA2 in hippocampal synaptic plasticity are well established, the role of GluA3 has yet to be fully uncovered. It was shown experimentally that hippocampal neurons lacking GluA3 do not suffer alterations neither in LTP nor in LTD (Humeau et al. 2007; Reinders et al. 2016), and that GluA3 KO does not display any memory deficits (Humeau et al. 2007) thus concluding that GluA3 does not play a role in plasticity related to memory formation. In the other hand, GluA3 has been shown to be required for amyloid-beta ( $A\beta$ ) to mediate synaptic and memory deficits (Reinders et al. 2016). The GluA4 subunit is mainly expressed in pyramidal cells and known to be necessary and sufficient to alter the signaling requirements of LTP (Luchkina et al. 2014; Yasuda et al. 2002). It was also shown that AMPA transmission is less prone to change its intrinsic activity in GluA4 absence (Huupponen et al. 2016).

Some of the commonly known glutamate receptor antagonists include 6-cyano-7-nitro-quinoline-2,3-dione (CNQX) and 2,3-dihydroxy-6-nitro-7-sulfamoylbenzo[f]quinoline-2,3-dione (NBQX). CNQX blocks AMPA/kainate but it is also an antagonist at the glycine site in NMDAR, thus is a non-selective blocker, whereas NBQX is a potent blocker of the AMPA receptors, effective in micromolar concentrations ( $\sim 10$ – $20 \mu\text{M}$ ) and blocks kainate receptors. In experiments, it is used to counter glutamate excitotoxicity (Pitt et al. 2000).

Kainate receptors (KARs) are members of the ionotropic glutamatergic receptor family, just like AMPA and NMDA receptors. Identical to AMPA receptors, KARs are tetramers formed from four subunits: GluK1-3 and GluK4-5. The first present low affinity for kainic acid (KA) and form homomeric receptors in heterologous systems whereas the latter have a higher affinity for KA and must be associated with GluK1-3 in order to form functional receptors. It has been demonstrated that KARs are key players in the glutamatergic synaptic transmission in the hippocampus and that such transmission is different from the one mediated by AMPA in several aspects, such as time course, amplitude, and cellular and synaptic specificity (Epsztein et al. 2017).

## 2.3. Receptors: Metabotropic

The metabotropic glutamate receptors (mGluRs) are members of the G-protein-coupled receptor (GPCR) superfamily. This family includes several subgroupings (with the most commonly expressed being called rhodopsin-like GPCRs), and based on their sequence homology, 8 receptors have been discovered and classified: Group I is composed by mGluRs 1 and 5, Group II has mGluRs 2 and 3 and Group III includes mGluRs 4, 6, 7 and 8 (Figure 4).

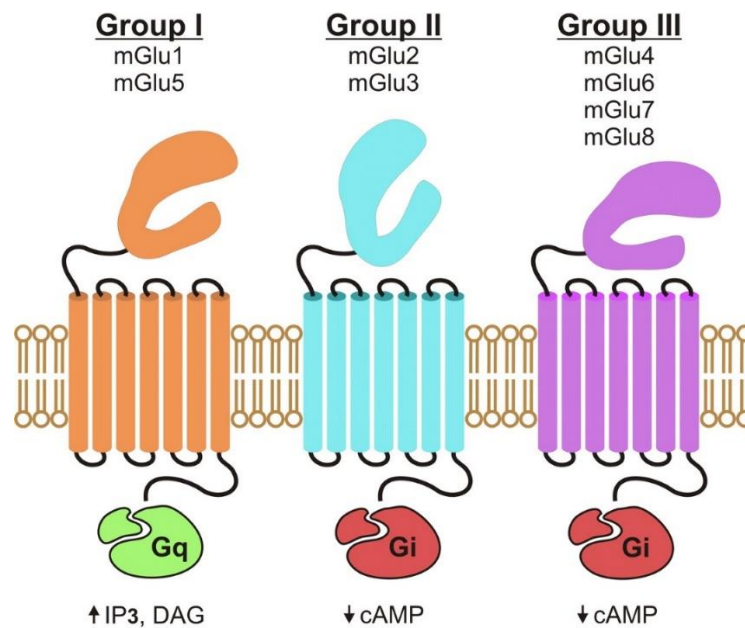


**FIGURE 4 mGlu receptor families.** mGlu receptors are classified into three families: group I, group II, and group III. In the CNS, activation of mGlu receptors from group I induces phosphoinositide hydrolysis with formation of inositol 1,4,5-triphosphate and diacylglycerol, whereas activation of receptors from groups II and III induce a decrease on the intracellular levels of cAMP (Julio-Pieper et al. 2011).

Briefly, Group I mGluRs can be mostly found postsynaptically, with their activation often leading to cell depolarization and an increase in neuronal excitability whereas group II and III mGluRs are more often localized presynaptically or in preterminal axons where they inhibit neurotransmitter release (Niswender & Conn 2010). In more detail, studies show that mGluR1 is capable of inducing hyperpolarization of some neuronal populations such as midbrain dopamine neurons (Valenti et al. 2002) and to lead to somatic calcium transients and neuronal depolarization in CA1 pyramidal cells specifically, whereas the other receptor of the Group I, mGluR5, has been shown to potentiate NMDAR currents

(Mannaioni et al. 2001), as well as exert a possible role in Fragile X syndrome, as the mutation that causes to this disorder leads to an increase signaling of this receptor (Bear et al. 2004).

Group II mGluR2 and mGluR3 are involved in neurotransmitter release inhibition and also in the regulation of the synaptic plasticity, by inducing LTD in the excitatory synaptic activity (Nicoletti et al. 2011) and they are also shown to be involved in the activation of different pathways, such as the phosphoinositide 3-kinase (PI3K) and the mitogen-activated protein kinase (MAPK) pathways (Nicoletti et al. 2011; Muguruza et al. 2016).

Concerning the members of the Group III, they have a broad range of action: mGluR6 was shown to interact and integrate a pathway involving Go protein (Dhingra et al. 2000); mGluR4 is strongly expressed in the cerebellum, where it was demonstrated to be involved in cerebellar synaptic plasticity, in learning motor tasks and in spatial memory performance (Pekhletski et al. 1996; Gerlai et al. 1998); mGluR7 acts as a transient receptor, only becoming active when glutamate levels are very high, thus serving as a brake for glutamate overstimulation and mGluR8 has been suggested to be involved in anxiety, with KO mice for this receptor displaying enhanced anxiety and weight gain in comparison with controls (Linden et al. 2002; Duvoisin et al. 2005; Robbins et al. 2007).

### 3. Synapse-to-nucleus communication pathways

As mentioned before, NMDARs play an important role in synaptic plasticity and memory formation, as well as in cell death and survival. Many aspects of these diverse functions require the regulation of gene expression and synapse-to-nucleus communication. Along the years, the most described and important mechanisms known for the transferring of information along neurons were membrane depolarization and calcium influx (Adams & Dudek 2005; Bading 2013). In the current literature, 5 major routes are widely studied:

- a. Electrochemical signaling: “action potential model”
- b. Regenerative endoplasmic reticulum (ER) calcium waves
- c. Signaling endosomes
- d. Diffusion/facilitated diffusion of signaling proteins
- e. Active transport of soluble proteins (Ch’ng & Martin 2011) (**Figure 5**)

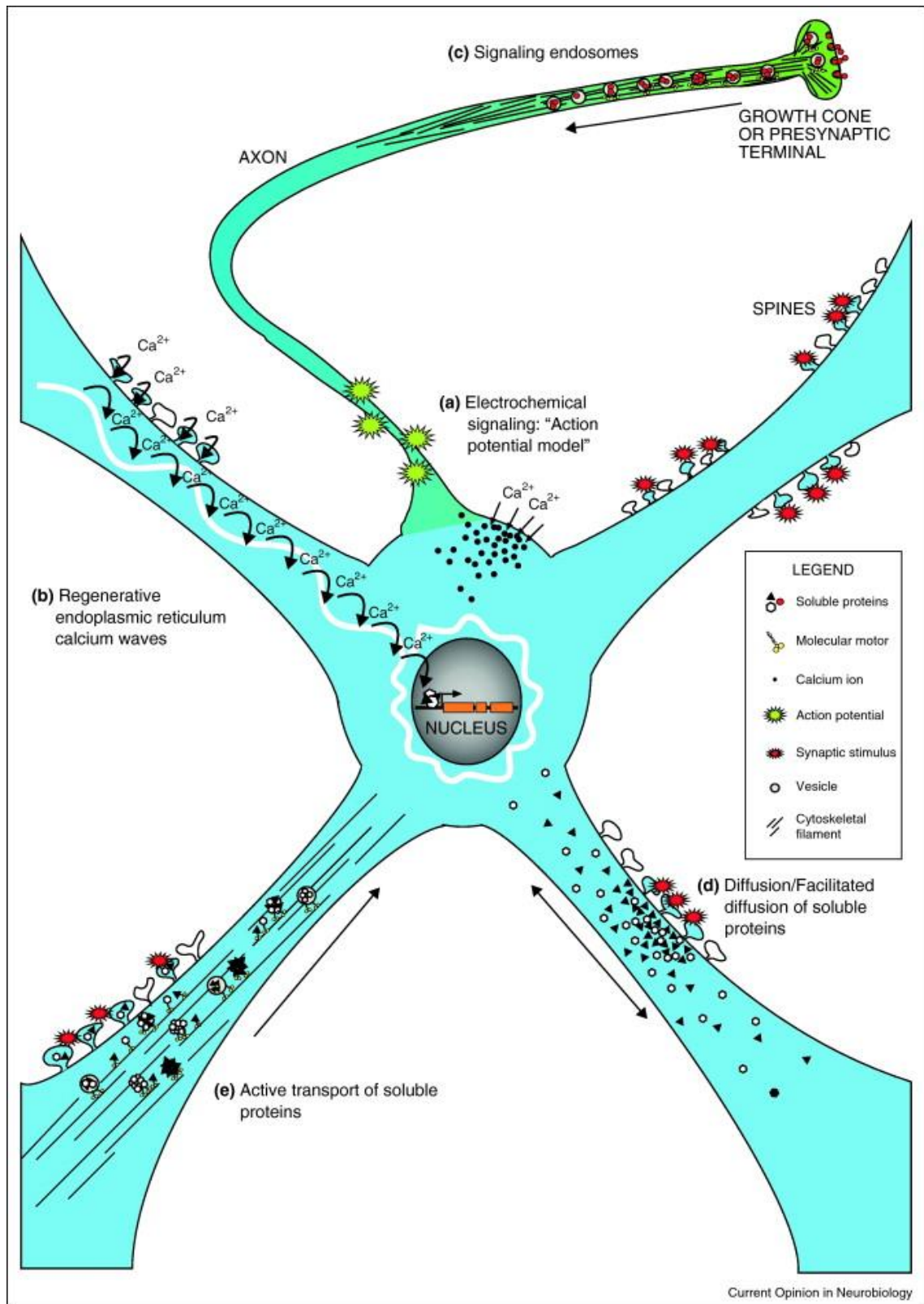


**FIGURE 5 The different mechanisms of synapse-to-nucleus signaling.** Signals generated in distal compartments (axons and dendrites) in neurons are transmitted to the nucleus by multiple mechanisms. Electrochemical signaling (a) and regenerative calcium waves in the endoplasmic reticulum (b) allow for extremely rapid signaling. Signals received at growth cones and axon terminals can be internalized into signaling endosomes that are transported back to the nucleus by molecular motors (c). Soluble proteins can be physically transported from distal sites to the nucleus by passive or facilitated diffusion (d) or by active motor-driven

transport (e). All black arrows indicate the net movement of proteins, vesicles or ions in neurons following stimulation. All solid black lines indicate cytoskeletal filaments (Ch'ng & Martin 2011).

#### a. Electrochemical signaling

In between the different mechanisms that neurons can use to communicate within distance, the electrochemical signaling allows a rapid transmission that trigger fast responses in the cell body and the nucleus, hence activating and changing gene expression in a matter of minutes. Ions such as calcium can form waves upon the generation of dendritic action potentials, coupled with the NMDA receptors. The synaptic and nuclear  $Ca^{2+}$  waves link is not fully understood yet, nevertheless it is known that an activity-dependent increase in nuclear calcium can activate transcription factors both directly and indirectly. One example of a direct activation is the downstream regulatory element antagonist modulator (DREAM), as by decreasing the intracellular concentration of  $Ca^{2+}$  increases the affinity to which DREAM binds to the downstream regulatory elements (DRE), leading to the transcriptional repression of the target genes (Tiruppathi et al. 2014). As far as an indirect activation, the example of the activation of cAMP response element binding protein (CREB) via the regulatory kinase  $Ca^{2+}$ /calmodulin-dependent kinase IV (CaMKIV) (Deisseroth et al. 2003) can be observed.

#### b. Regenerative ER calcium waves

The calcium-dependent nuclear signaling compiles several methods, being one the involvement of regenerative calcium waves that propagate along the ER (Berridge 1993). The endoplasmic reticulum, an organ composed by tubules and flattened sacs, has its major function in the production, processing and transport of proteins and lipids. It mainly produces transmembrane proteins and lipids for its membrane, among other cell components such as lysosomes, secretory vesicles, the Golgi apparatus and the cell membrane. In the neuronal path, the ER is capable of internally store calcium, as it presents two calcium-sensitive calcium channels at the surface: the inositol triphosphate receptor ( $InsP_3R$ ) and the ryanodine receptor (RZR) (Berridge 1998). Specifically,  $InsP_3Rs$  are present in Purkinje cells and spiny striated neurons, including spines and synaptic ending, whereas RZR are primarily located in the soma of neurons.

Within the last several years, one of the most studied models for synapse to nucleus signaling comprises specific signaling molecules and proteins that have been uncovered as synaptonuclear messengers. Involving signaling endosomes (c), diffusion/facilitated diffusion of soluble proteins (d) or active transport of soluble proteins – synapse-to-nucleus messengers (e), this transport is slower than the ones already described, but is significantly longer in duration and effectiveness.

#### c. Signaling endosomes

Neurotrophins are a family of small proteins factors that regulate many aspects of neuronal functions, including neuronal survival, differentiation, migration and synaptic plasticity (Chao et al. 1998; Neet & Campenot 2001; Campenot & MacInnis 2004). Within the family of these trophic factors, one can find nerve growth factor (NGF) and brain-derived neurotrophic factor (BDNF), each binding to the p75 neurotrophin receptor (p75), as well as to another specific member of the surface tyrosine receptor kinases (Trks), acting through them: in the case, NGF binds to TrkA and BDNF to TrkB (Wu et al. 2009). Specifically, the NGF-bound activated TrkA receptor is endocytosed into a signaling endosome and sequentially trafficked to the cell body via microtubules, where it interacts with several intermediates such as MAPK, PI3K and phospholipase C gamma (PLC $\gamma$ ) (Grimes et al. 1996), thus activating transcription factors (such as CREB) that will trigger gene expression in the nucleus as a result. Even though this model has plenty of experimental evidence to support itself, over the last years other supporting models have been proven as an alternative fashion for endosomes, such as the wave model or the signaling effector model, to explain how the transport to axon terminals is done (Wu et al. 2009).

#### d. Diffusion/facilitated diffusion of soluble proteins

Diffusion is a common mechanism in most of all the biological beings, and the diffusive motion of macromolecules and their binding-dissociation reactions with cellular organelles is a crucial component of cell function (Kühn et al. 2011). However, considering the distances that proteins must travel from the distal synapses to the nucleus, it is hard to find evidences that this would be an effective mechanism for this purpose. Despite the

odds, Wiegert and colleagues have demonstrated that stimulus-induced extracellular signal-regulated kinase 1/2 (ERK1/2) nuclear translocation is mediated by facilitated diffusion (Wiegert et al. 2007). ERK1/2 is part of the MAPK cascade, being ubiquitously expressed as an hydrophilic non-receptor protein (Wortzel & Seger 2011). The MAPK cascade has been reported to participate in several distinctive processes such as cell adhesion, migration, survival, differentiation, metabolism, proliferation and transcription, as well as playing a part in cell cycle progression. In summary, ERK2 can be phosphorylated, turning into a tiny molecule (4.0 nm x 4.4 nm x 7.0 nm), being this size reported as capable of diffusing through the nuclear pore complex without the help of additional mechanisms (Roskoski Jr 2012).

#### e. Synapse to nucleus messengers

Since the early years that scientists wonder how macromolecular signals are transported from the axon and synapse back to the cell body, and it wasn't until Ambron and colleagues (1992) discovered the importance of the nuclear localization signal (NLS) that some light was shed in the subject. Briefly, Ambron microinjected a rhodamine-labelled construct of nuclear import signal peptide of the SV-40 T antigen of *Aplysia californica* coupled to the human serum albumin protein and discovered that the NLS alone was enough for the protein translocation to the nucleus (Ambron et al. 1992). This implicated a role for the classical nuclear import pathway, that comprises the binding of the importin  $\alpha/\beta$  complex to the NLS-bearing cargo site, in long-distance retrograde transport from distal sites to the soma. Importin  $\alpha$  mediates the import of proteins that carry a classical NLS, and performs as the actual NLS receptor, by binding both cargo and importin  $\beta$  in the cytoplasm (Görllich & Kutay 1999). They have been localized in distal synapses and accumulate in the nucleus in response to stimuli in hippocampal neurons. Furthermore, importin  $\alpha$  has been shown to bind to a NLS encoded by exon 21 in the NR1-1a subunit of the NMDA receptors, being regulated by a mechanism where the stimuli that induced the transcription triggered PKC phosphorylation within the NLS, breaking the ligation of the importin and leaving it free to bind to other cargo (Jeffrey et al. 2009).

In recent years, a number of potential synaptonuclear protein messengers such as Abelson interacting protein-1 (Abi-1), Amyloid precursor protein intracellular domain-associated protein-1 (AIDA-1D), cAMP responsive element binding protein-2 (CREB2), juxtasyntaptic attractor of Caldendrin on dendritic buttons (Jacob), Nuclear factor kappa of light chain enhancer of activated B-cells (Nf- $\kappa$ B), CREB regulated transcriptional coactivator-1 (CRTC1) and RING Finger Protein 10 (RNF10) have been identified (Jordan & Kreutz 2009; Budnik & Salinas 2011; Marcello et al. 2018) (**Figure 6**).

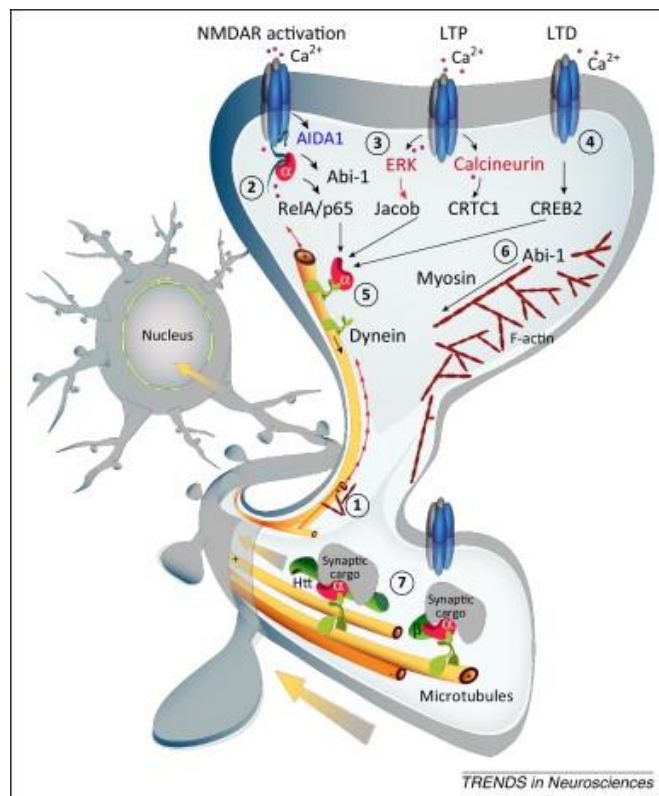


**FIGURE 6 Long-distance transport from synapse to nucleus. (1)** Dynamic microtubules can transiently invade a subset of spine synapses following NMDAR activation in a strictly Ca<sup>2+</sup>-dependent manner. **(2)** Neuronal importins can associate with several synapto-nuclear messengers at synaptic sites, but it is currently unclear how this interaction might be regulated. **(3,4)** Signaling downstream of NMDAR that eventually elicits nuclear transport might also encode that type of NMDAR activation. **(3)** Ca<sup>2+</sup>-dependent (Jacob and CRTC1) and independent (AIDA1, blue) dissociation of protein messengers from NMDAR has been reported and local phosphorylation via ERK in the case of Jacob or dephosphorylation via calcineurin in the case of CRTC1 is required to exit the synapse. **(4)** Interestingly, NMDAR-dependent LTP but not LTD induces nuclear translocation of Jacob, while the reverse occurs for CREB2. **(5)** For many proteins binding to a dynein motor, likely via association with an importin  $\alpha$ , is a prerequisite for long-distance transport. Whether this transport requires microtubule invasion of dendritic spines is presently unclear. **(6)** Alternatively, proteins like Abi-1 might leave the synapse utilizing a myosin motor. **(7)** At present it is also unknown whether the macromolecular transport complex is assembled in spines or in the dendritic shaft below the synapse (Panayotis et al. 2015).

### 3.1. Abelson interacting protein-1 (Abi-1)

Abi-1 is a substrate for the nonreceptor tyrosine kinase c-Abl and is a binding partner for the postsynaptic density protein ProSAP2/Shank3. As a part of several micromolar complexes, Abi-1 interacts with Eps8 and Sos-1, forming a trimeric signaling complex. Other functions include the control of Rac activity, and the formation and activation of the WAVE2 signaling complex (Proepper et al. 2007). During development, Abi-1 takes part in regulating the growth of dendrites and helps to determine the morphology and number of synaptic contacts (Ito et al. 2010; Proepper et al. 2007), while in mature neurons Abi-1 can be found in the dendrites, playing a pivotal role in phosphorylation (Tani et al. 2003), localization of protein complexes to cellular subcompartments and in actin reorganization, especially through the regulation of Rac-dependent pathways (Stradal et al. 2001; Leng et al. 2005). The nuclear translocation of this protein was proven experimentally by adding NMDA to cultured neurons, after which the protein translocates from the dendrites to the nucleus, depending on an active microtubule network to do so. Recently, it has been reported that Abi-1, like c-Abl, also shuttles to the nucleus in NIH 3T3 fibroblasts, providing a dual function of the protein in distinct cellular compartments (Echarri et al. 2004).

### 3.2. Amyloid precursor protein intracellular domain-associated protein-1 (AIDA-1d)

AIDA-1d was identified as a synaptically localized protein, and thus as a potential synapse-to-nucleus messenger by mass spectrometry analysis of PSD fractions (Jordan et al. 2004). Despite the fact that AIDA-1d is highly enriched in the synaptic junction, the NMDA receptor stimulation determines a fast redistribution into the nucleus, Cajal bodies and nucleoli (Jordan et al. 2007). Furthermore, the nuclear accumulation is reversible, with NLS requirement, thus indicating shuttling capabilities, which indeed have been shown, as the translocation of this protein is related with the activation of NMDA receptors that elicit proteolysis, releasing AIDA-1d from the N-terminal fragment of the PSD-95 cytosolic anchor (Jordan & Kreutz 2009).

### 3.3. cAMP responsive element binding protein-2 (CREB2)

CREB2, also known as activating transcription factor 4 (ATF4), is a transcription factor with distinct functions of CREB and that has been shown to localize in synapses and distant dendrites. Lai and colleagues (2008) have demonstrated that this transcription factor is capable of translocate from distal neuronal processes to the nucleus during LTD of rodent hippocampal neurons, and phenylalanine-methionine-arginine-phenylalanine-amide (FMRFamide)-induced LTD in *Aplysia californica* sensory-motor synapses. Furthermore, their studies also showed that the binding of CREB2/ATF4 is specific to importin  $\alpha$ 1 and  $\alpha$ 6, thus allowing the shuttling between cytoplasm and the nucleus. Interestingly, it was also demonstrated that the nuclear translocation of CREB2 depends on the stimulation protocol, as NMDA and glycine combined successfully triggered the translocation, whereas glycine alone had no effect on this (Lai et al. 2008).

### 3.4. Juxtapositional attractor of Caldendrin on dendritic buttons (Jacob)

Jacob is a recently identified plasticity-related protein that couples NMDAR activity to nuclear gene expression. Jacob has been shown to be present exclusively in the brain, more specifically the cortex and limbic system. It has a predominant dendritic localization in the hippocampus, being the 3'-untranslated region of Jacob mRNA the responsible for this.

In mouse brain, it has been demonstrated that Jacob transcripts are linked with the fragile X mental retardation protein and with the kinesin family member 5C motor complex. The first regulates dendritic mRNA targeting and translation, whereas the second mediates the dendritic mRNA transport. Jacob can be rapidly degraded in a  $\text{Ca}^{2+}$ - and Calpain-dependent manner, being Calpain-mediated clipping of the N-terminus of Jacob required for its nuclear translocation following NMDAR activation (Kindler et al. 2009).

This NMDA activation and the sequential calcium influx trigger the dissociation of Jacob from caldendrin, unmasking the NLS where importin  $\alpha$  will bind, thus allowing the nuclear import to happen (Dieterich et al. 2008).

Dieterich and colleagues have experimentally demonstrated this nuclear import, first with the stimulation of hippocampal primary neuron cultures with NMDA for 3 minutes and sequential quantification of the endogenous Jacob by signal intensity of the

fluorescent propidium iodide-counterstained neuronal nuclei. They accessed that Jacob's presence in the neuronal nuclei increased within 30 minutes of the NMDA receptor activation, reaching its peak in 2 hours, and returning to its control levels in a 4h period. Using a time-lapse experiment (**Figure 7**), and transfecting the cultures with *WT-Jacob-GFP* or the  $\Delta$ *NLS* mutant, they proved the essential role of the NLS in Jacob translocation, as *WT-Jacob-GFP* cultures resulted in an increase of green fluorescent protein (GFP) fluorescence in a time course similar to the endogenous protein one (**Figure 7A-7D**), while the neurons transfected with the  $\Delta$ *NLS* did not present a nuclear accumulation (**Figure 7E and 7F**), giving a strong evidence of the need for a binding site for importin  $\alpha$  for the accumulation of Jacob. Interestingly, GFP fluorescence decreased in proximal and distal dendrites in accordance with the nuclear accumulation of *WT Jacob* (**Figure 7C**), an effect not observed in the  $\Delta$ *NLS* neurons, thus indicating that the presence of the NLS and its interaction with importin  $\alpha$  are crucial to the import of Jacob to the nucleus (Dieterich et al. 2008).

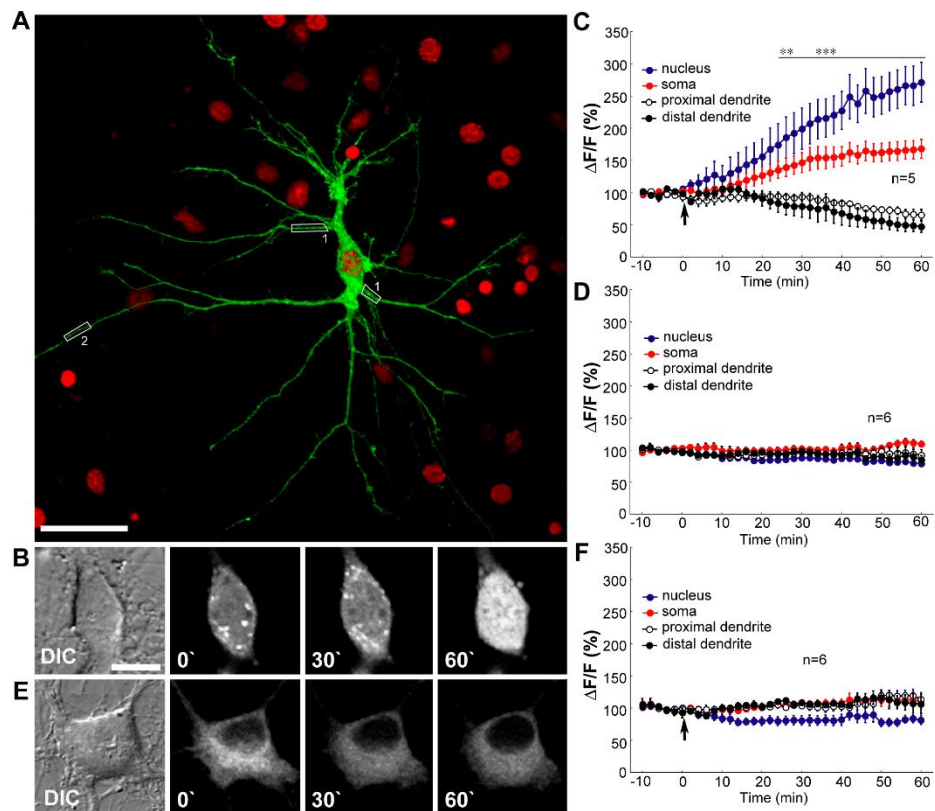


**FIGURE 7 Time-Lapse Imaging of Jacob's Nuclear Translocation.** (A) Confocal maximal intensity image of a living hippocampal primary cultured neuron (DIV10) overexpressing WT-Jacob-GFP (green channel) and merged with a nuclear stain (DAPI) obtained after the experiment (red channel). (B) Representative selective video frames obtained from a WT-Jacob-GFP overexpressing neuron before (0) and after (from left to right) glutamate stimulation at time points indicated. DIC, difference interference contrast image of the neuronal soma. (C) Averaged temporal dynamics of the changes in WT-Jacob-GFP fluorescence intensity, quantified using ImageJ software in distinct regions of interest before and after stimulation with glutamate (50  $\mu$ M). The arrow indicates the time point of glutamate application. The increase in WT-Jacob-GFP fluorescence in the soma and nuclei is accompanied by a reduction of fluorescence intensity in the dendrites. Statistically significant differences in GFP fluorescence in neuronal nuclei, somata and dendrites after stimulation in comparison to baseline fluorescence are indicated; double asterisks (\*\*) indicate  $p < 0.01$ ; and triple asterisks (\*\*\*) indicate  $p < 0.001$ . (D) Without glutamate stimulation, no significant changes in WT-Jacob-GFP fluorescence in the nucleus as well as in soma and dendrites were observed. (E) Overexpression of the deletion mutant  $\Delta$ NLS-Jacob-GFP leads to an extranuclear localization of the mutant protein. Representative selective video frames obtained from  $\Delta$ NLS-Jacob-GFP overexpressing neuron before (0) and after (from left to right) glutamate stimulation at time points indicated. DIC, difference interference contrast image of the neuronal soma. (F) Application of glutamate in  $\Delta$ NLS-Jacob-GFP-transfected neurons do not change the GFP fluorescence levels in dendrites, soma, and nucleus. Scale bars indicate 40  $\mu$ m in (A) and 25  $\mu$ m in (B) and (E) (Dieterich et al. 2008).

### 3.5. Nuclear factor kappa of light chain enhancer of activated B-cells (Nf- $\kappa$ B)

Nf- $\kappa$ B belongs to a family of dimeric transcription factors, with five DNA-binding subunits already described: p50, p52, RelA (p65), c-Rel and RelB, of which the p50:p65

dimer is the most commonly found in neurons (Meffert et al. 2003). To complete its structure, it also contains an inhibitory subunit: I $\kappa$ B $\alpha$ , I $\kappa$ B $\beta$ , I $\kappa$ B $\gamma$  (p105), I $\kappa$ B $\delta$  (p100) and I $\kappa$ B $\epsilon$ . The interaction with the I $\kappa$ B $\alpha$  inhibitory subunit allows the complex to anchor to the cytoplasm (Kaltschmidt et al. 1993), permitting also the physical blockage of the NLS on the RelA subunit, preventing the transport of the complex to the nucleus. Furthermore, the degradation of this subunit results in the activation of NF- $\kappa$ B by exposing the NLS, thus activating its transport to the nucleus where it will exert its function as a transcription factor, after being specifically post-translationally regulated. Besides that, when in the nucleus, NF- $\kappa$ B can function as a molecular switch for turning on gene expression, and as an immediate retrograde signal transducer, which unifies signal perception at distant sites (dendrites, axons, and synapses) (Wellmann et al. 2001).

### 3.6. CREB-regulated transcriptional coactivator-1 (CRTC1)

CREB-regulated transcriptional coactivator-1, CRTC1, also known as the transducer of regulated CREB – TORC, has been identified as a protein with a synapse-to-nucleus messenger role. CRTC has three known isoforms (CRTC1-3) and while CRTC2 and CRTC3 are abundantly expressed in the lungs and in muscles (Wu et al. 2006), CRTC1 is highly expressed in the brain, particularly in the hippocampus, and has demonstrated to be essential in long-term synaptic plasticity and development (Xue et al. 2015). CRTC enhances CREB-mediated gene transcription by associating with the bZIP binding/dimerization domain of CREB instead of using the phosphorylation route, via phospho-Ser133, and potentiates the activity of CREB (Conkright et al. 2003). It has been demonstrated that CRTC1 undergoes neuronal activity-induced translocation from cytoplasm to the nucleus, as cytoplasmic CRTC1 dephosphorylation by calcium at Ser151 activates the nuclear translocation and activation (Bittinger et al. 2004; Sreaton et al. 2004; Altarejos et al. 2008).

### 3.7. RING Finger Protein 10 (RNF10)

As demonstrated earlier, Jacob is a binding partner of the GluN2B-containing NMDAR. In the search for binding partners for GluN2A, our laboratory has identified RNF10 protein as a possible interactor. RNF10 is a member of the RING (Really Interesting New Gene) finger family, classified in general as ubiquitin protein ligases, with a range of functions

such as transcriptional regulation, DNA repair, site-specific recombination, and signal transduction (Seki et al. 2000). Some specific proteins of this family, including RNF10, were recently reported to be involved in neuronal differentiation, development and differentiation processes (Malik et al. 2013). This protein, with a size of 804 aminoacids (aa) (approximately 90 kDa), contains a binding sequence for the Mesenchyme Homeobox 2 (Meox2) transcription factor (Lin et al. 2005), a Ringer Finger Domain (RFD, aa 225–270) and two putative nuclear localization sequences (NLS1, aa 591–599 and NLS2, aa 784–791) (Figure 8).

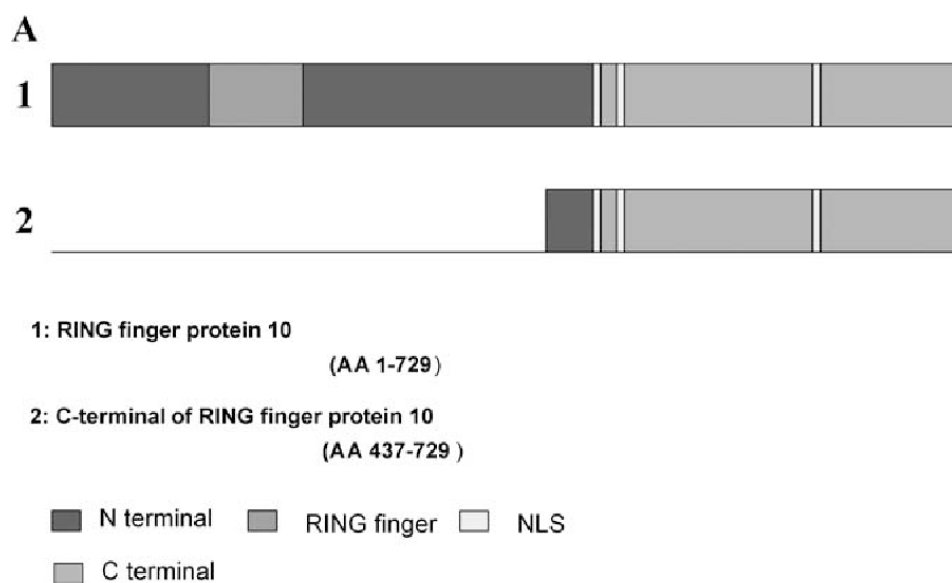


**FIGURE 8 Characterizing the RNF10 binding region of MEOX2.** (A) The full-length RNF10 protein contains one RING finger motif and three putative nuclear localization signals. The carboxyl terminal region of RNF10 isolated by the yeast two-hybrid screen does not contain the RING figure motif (Lin et al. 2005).

Indeed, RNF10 is present at the nucleus, where it is known to associate with Meox-2 transcription factor. Lin and colleagues (2005) demonstrated this connection, by screening a human heart cDNA library using a MEOX2ΔHQ bait as a transcription factor (Lin et al. 2005). Based on positive interactions of the initial yeast-two hybrid screen and the rescue after re-transformation of the isolated cDNAs, they found RNF10 as a very strong candidate. Undeniably, RNF10 had been previously showed to be ubiquitously expressed and isolated from heart cDNA libraries (Seki et al. 2000). Furthermore, not only they demonstrated that all Meox-2 domains (except the C-terminal) were sufficient to bind RNF10, as they also showed that Meox-2 binds RNF10 in a pull-down assay, co-

immunoprecipitates with this protein and also that RNF10 potentiates Meox-2 transcriptional activation (Lin et al. 2005).

In our lab, Dinamarca and colleagues (2016) have recently identified RNF10 as a novel synaptonuclear protein messenger, highly enriched at the excitatory synapse, where it associates specifically with the GluN2A subunit of the NMDARs. Localized at the PSD, RNF10 is activated by  $Ca^{2+}$  signals at the postsynaptic compartment and elicits discrete changes at the transcriptional level. The activation of the synaptic NMDARs and the induction of LTP lead to the translocation of RNF10 from the dendritic spines to the nucleus.

To demonstrate all of this, studies using a yeast two-hybrid screening were used. The first, using the C-terminal domain of GluN2A as a bait, was demonstrated RNF10 to be a positive clone. Using a glial fibrillary acidic protein (GFAP) glia-specific marker and a microtubule-associated protein 2 (MAP2) neuron-specific marker, it was confirmed that RNF10 is expressed in both glia and neurons, with RNF10 in neurons showing more nuclear and somatodendritic distribution (Dinamarca et al. 2016). Furthermore, transfected GFP-RNF10 presented a significant co-localization with PSD-95 and GluN2A at the dendritic spines in the hippocampus. As an interesting fact, the silencing of GluN2A in primary hippocampal neurons severely decreased RNF10 synaptic levels, but with no modifications in the nuclear level. By co-immunoprecipitation, it was shown that the interaction between RNF10 and the NMDARs is specific to GluN2A but not GluN2B, and these results were confirmed using cell lysates from COS7 cells, and by proximity ligase assay (PLA).

To understand the neuronal function of RNF10, the protein was silenced using a short hairpin (sh) RNF10 knock-down, with a scramble sequence as control in hippocampal cultures. It was observed that RNF10 silencing induced a significant reduction in dendritic spine density, without affecting the dendritic spine length nor the dendritic spine head width. After spine categorization, no effect was observed in the proportion of the dendritic subtypes. In a parallel experiment, it was demonstrated that RNF10 silencing resulted in a significant decrease in GluN2A, PSD-95 and GluA1.

To further access the effect of RNF10 in gene expression, a microarray analysis of organotypic hippocampal slices infected with pLKO-shRNF10 lentivirus was performed, being observed that RNF10 can interfere with genes involved in excitatory synaptic

transmission and dendritic spine morphology, such as oligophrenin 1 (Ophn1), Rho GTPase activating protein 4 (ArhGap4) and Rho guanine nucleotide exchange factor 6 (ArhGef6).

To validate the hypothesis of RNF10 being a synaptonuclear protein messenger, the excitatory synaptic activity was enhanced using the gamma-aminobutyric acid A (GABA-A) receptor antagonist Bicuculline and the K<sup>+</sup> channels were blocked with 4-aminopyridine (4-AP). This enhanced excitatory activity significantly decreased RNF10 immunoreactivity in dendrites, without affecting PSD-95, and increased the nuclear staining of the protein. Furthermore, the transport of RNF10 was confirmed by performing a time-lapse experiment using a photoconvertible tandem dimer protein, tdEOS. In other experiments, RNF10 displayed a prominent co-localization with importin  $\alpha$ 1 and surface GluN2A along dendrites, leading to the conclusion that excitatory synaptic activity leads to the dissociation of RNF10 from the cytoplasmic tail of GluN2A at postsynaptic sites, presenting also a very close interaction with the neuronal importin, and an association with the transcription factor Meox2. Moreover, it was confirmed that RNF10 nuclear translocation is mediated by LTP induction, using a potentiation electrophysiology assay, and also that the downregulation of RNF10 expression prevents cLTP expression.

In addition, it was demonstrated that the translocation of RNF10 to the nucleus leads to its binding to Meox2, which stimulates the expression of target genes such as p21<sup>WAF1/cip1</sup> and Ophn1 (Dinamarca et al. 2016). Taken these results all together, RNF10 was successfully confirmed as a synaptonuclear protein, with a very clear mechanism described.

Other functions have been associated with this protein, including an interaction in metabolic syndrome and in myelin-associated glycoprotein (MAG).

Yu and colleagues (2018) have demonstrated that RNF10 is implicated with metabolic syndrome (MetS) (Yu et al. 2018). MetS is defined as multiple metabolic abnormalities, including insulin resistance, glucose intolerance, dyslipidaemia, hypertension, and obesity (Houshyar et al. 2012). The ubiquitin-proteasome system is activated in injured vascular intima under insulin resistance (Herrmann et al. 2004), and one important member of this system is RNF10. In sum, it was demonstrated that the overexpression of

RNF10 suppresses hyperplasia in MetS rats, as well as an increase in apoptosis via Bcl-2 protein inhibition.

On their turn, Hoshikawa and colleagues (2008) have established the connection between RNF10 and myelination by demonstrating that RNF10 interacts with the *cis*-acting element region of the *MAG* promotor, directly activating it in Schwann cells. In addition, RNF10 displayed a negative regulation in Schwann cell proliferation and when RNF10 is knockdown, it is capable of inhibiting myelin formation (Hoshikawa et al. 2008).

## 4. Synaptopathies

As previously mentioned, synapses are the most abundant and distinguished feature of the brain, as a complex system with a multitude of interactors. Over the last years, it has become more prominent that disruptions and defects in the synapses could result in diseases – defined by the term *synaptopathies* – that cross the traditional boundaries of neurology and psychiatry, mostly affecting cognition, emotion, and synaptic plasticity (Figure 9) (Grant 2012; Sala & Segal 2014).

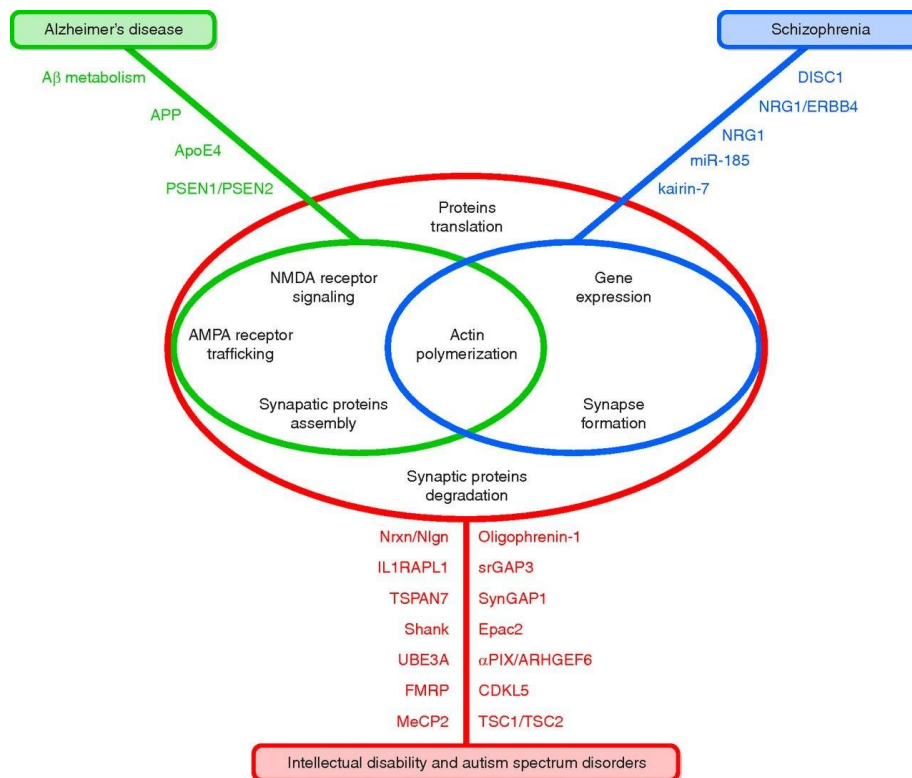


**FIGURE 9 Disease proteins dysregulating spine morphology.** The diagram shows the list of major proteins, codified by genes mutated in the indicated neurological diseases (Alzheimer's disease in green, schizophrenia in blue, and intellectual disability and autism spectrum disorders in red), which are involved in altering spine morphologies through different molecular mechanisms listed in the center of the figure (Sala & Segal 2014).

#### 4.1. Alzheimer's disease

AD is an age-related neurodegenerative disorder that was first described by Alois Alzheimer in 1906. Today, AD is the most common form of dementia in the population over 65 years (~7-10%), affecting more than 30 million people worldwide while this number is predicted to be increased to 115 million by 2050 (1 in 85 persons) (Prince et al. 2013) raising the number of caregivers at 216 million (Brookmeyer et al. 2007), with the financial reports showing that more than 105 billion Euros per year were spent on dementia in Europe in 2010 (DiLuca & Olesen 2014). A better appreciation of the detrimental influence of this world health problem on community derives from the compounding societal impact of longevity which increases the risk of AD, especially in Europe whose population is aging faster than that of any other continent (Parliament 2011).

The disease is clinically characterized by memory deficits, impaired learning and judging abilities, apathy, severe mood oscillations and personality changes. In latter stages of the disease, these symptoms are aggravated, with psychosis, agitation, extreme disorientation and impossibility of exerting motor coordinated tasks and some patients also describe seizures. Over the last decades, worldwide research efforts have been increasingly focusing on understanding the cellular pathways and molecular mechanisms that characterized AD and contribute to its development. The main histopathological features of AD are the neurofibrillary tangles (NFTs) and senile plaques (Sisodia & Tanzi 2007; Perl 2010; Drummond et al. 2018) (**Figure 10a**). Specifically, NFTs are intracellular fibrillar structures composed of aggregations of paired helical filaments (PHFs) which are made up with abnormally phosphorylated forms of the microtubule-associated protein Tau (Grundke-iqbal, Iqbal, Tung, Zaidi, et al. 1986; Grundke-iqbal, Iqbal, Tung, Quinlan, et al. 1986). Abnormal Tau hyperphosphorylation results to detachment of Tau from microtubules that in turn leads to their depolymerization while the free, unbound Tau

aggregates in oligomers and polymers that give rise to the formation of NFTs (Wang et al. 2013) (Figure 10b).

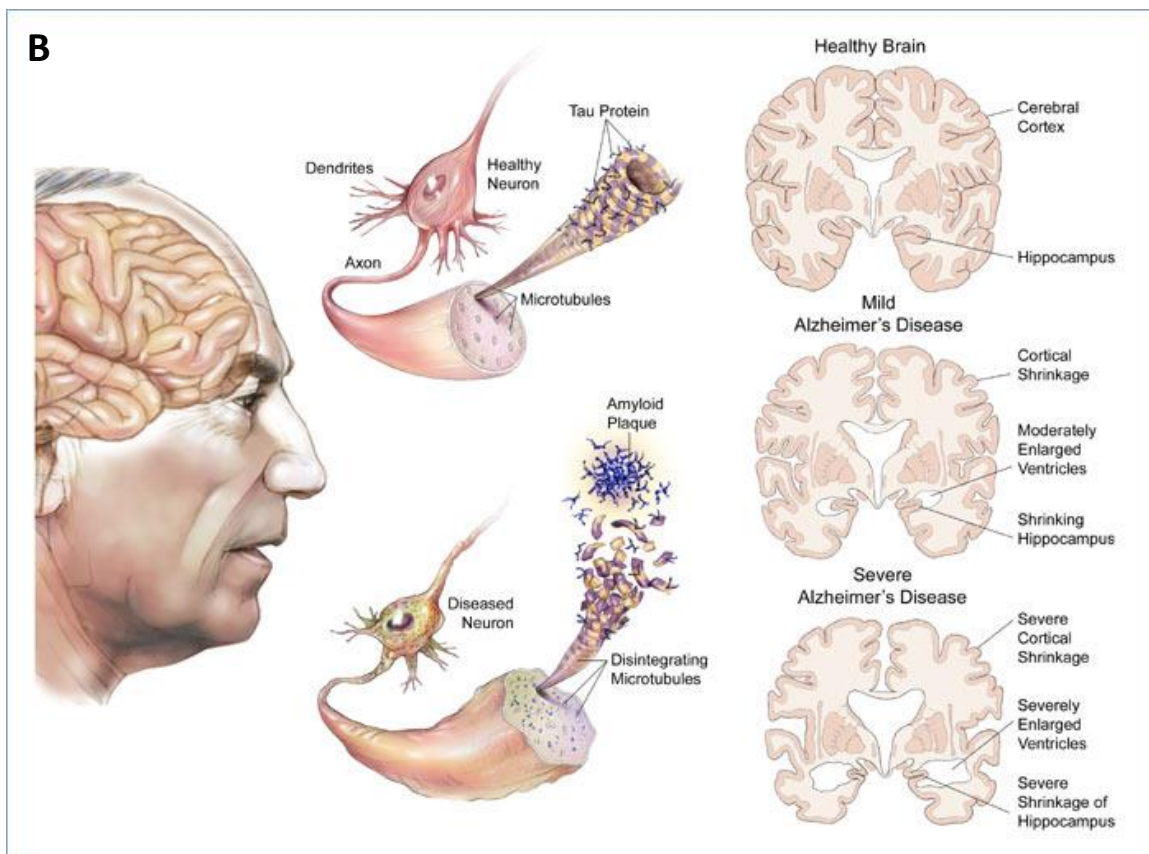
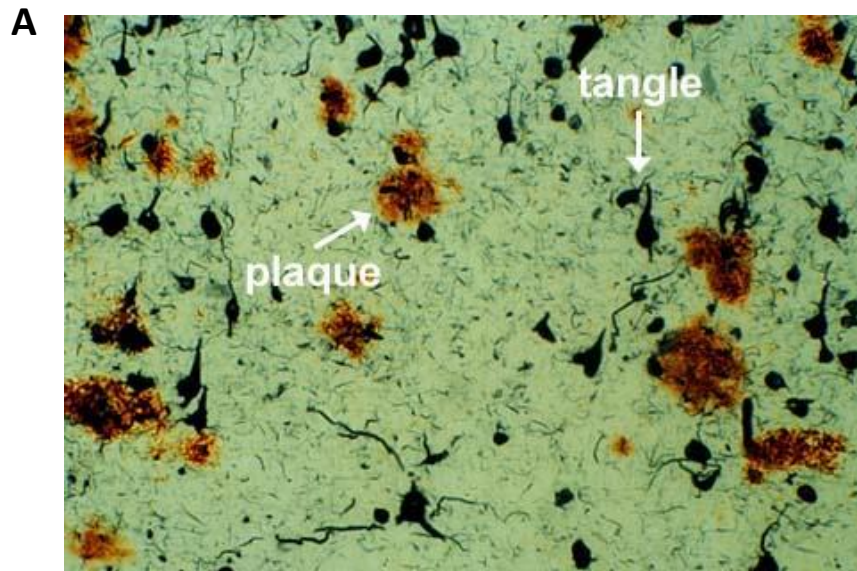


**FIGURE 10 Alzheimer's disease: histopathology, mechanisms and progression. A)** AD is characterized by senile plaques and neurofibrillary tangles (Eastman 2012). **B)** During the progression of AD, amyloid-beta ( $A\beta$ ) and its aggregates trigger Tau hyperphosphorylation and aggregation which results in microtubule destabilization and progressive neuronal and brain area atrophy that characterized the disease (Halzmyth 2012).

While tau hyperphosphorylation is a critical event in AD neurodegenerative pathways, the upstream triggering parameter is the neurotoxic peptide A $\beta$  which is a protein fragment of a larger protein called amyloid precursor protein (APP) (Takashima et al. 1998; Zhang et al. 2011).

APP is a type-I transmembrane protein and it is abundant in the CNS (Menéndez-González et al. 2005). It is also expressed in other body parts, such as epithelium and blood cells (Di Luca et al. 2000). Although including other proteins in its protein family, the A $\beta$  domain is exclusive to the APP protein.

APP is the target of many investigations, but its physiological function remains partially unknown. There is a suggestion in which the APP has an important role in neurite outgrowth and synaptogenesis as well as in neuronal protein trafficking, transmembrane signal transduction, cell bonding and calcium metabolism, among others (Zheng & Koo 2011). Furthermore, APP was found to be an important part in herpes simplex viral particles and possibly it mediates fast anterograde transport of these particles (Satpute-Krishnan et al. 2003; Satpute-Krishnan et al. 2006). With these facts, there is a suggestion that APP mostly plays an important role in the regulation of protein transport.

The metabolism of APP is fundamentally linked to neuronal function and survival. APP is synthesized in the ER and then transported across the Golgi apparatus to the trans-Golgi-network (TGN) where the highest concentration of APP is found and where A $\beta$  can also be made (Xu et al. 1997; Hartmann et al. 1997; Greenfield et al. 1999). From the TGN, APP can be translocated in secretory vesicles to the cell surface where it is either cleaved (Sisodia 1992), or re-internalized via an endosomal/lysosomal degradation pathway (Nordstedt et al. 1993; Caporaso et al. 1994). APP is sequentially processed by at least three proteases termed  $\alpha$ -,  $\beta$ - and  $\gamma$ -secretases (Zheng & Koo 2011) following two different pathways: the non-amyloidogenic pathway and the amyloidogenic pathway (**Figure 11**).

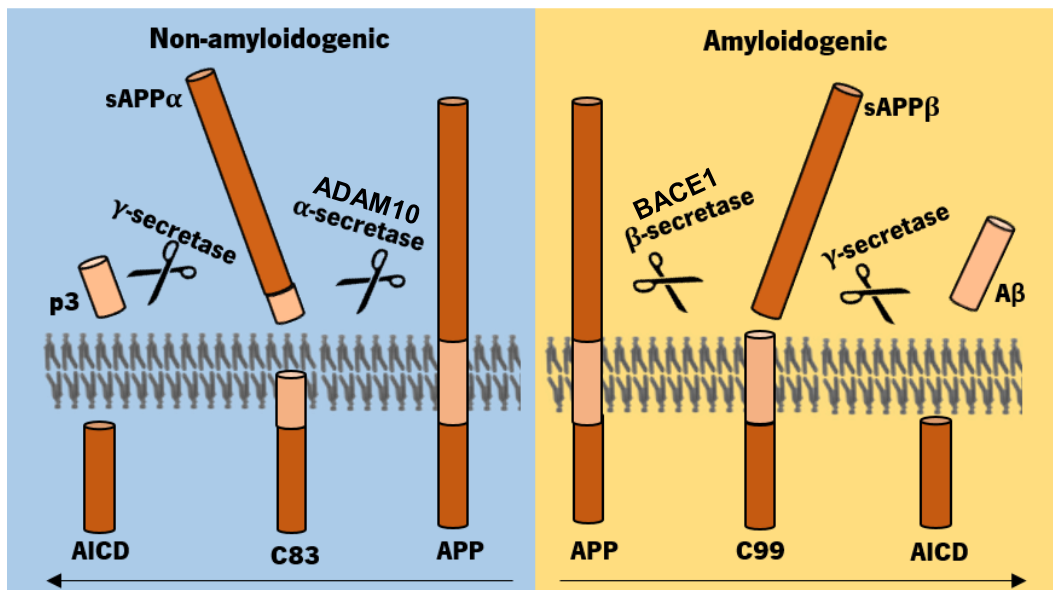


**FIGURE 11 APP processing pathways.** APP is sequentially cleaved by three different enzymes: alfa ( $\alpha$ )-secretase, beta ( $\beta$ )-secretase and gamma ( $\gamma$ )-secretase, in two distinct pathways (the non-amyloidogenic (left) and amyloidogenic (right) pathway). In AD, the amyloidogenic pathway is more active resulting the overproduction of A $\beta$  that will aggregate into senile plaques (drawn by Ribeiro, A) (based on (LaFerla et al. 2007)).

In non-amyloidogenic pathway, APP is first cleaved by  $\alpha$ -secretase (ADAM10) within the luminal domain, resulting in the detaching of nearly the whole ectodomain and generation of  $\alpha$ -C-terminal fragments (CTFs) (Sisodia & Tanzi 2007). The APP-CTFs are then cleaved by  $\gamma$ -secretase to produce a 3 kDa fragment (p3, from APP-CTFa), and the APP intracellular domain (AICD) (Zheng & Koo 2011).

The amyloidogenic pathway begins with APP being cleaved by  $\beta$ -secretase (also called BACE1). BACE1 cleaves APP inside the ectodomain, creating the N-terminus of A $\beta$  (Vassar 2004), soluble sAPP $\beta$ , which is released from the membrane, and a C-terminal fragment (C99) that rests related in the membrane (Small et al. 2010). C99 is again cleaved, this time by  $\gamma$ -secretase in its transmembrane domain and results in creation of A $\beta$  that deposits into senile plaques.

While APP is cleaved following both pathways, the amyloidogenic one is the most preferential in AD; interestingly, recent evidence suggest that little amount of A $\beta$  are also produced under normal, pathology-free conditions (Kamenetz et al. 2003) while the non-amyloidogenic pathway is the preferential one.

In this non-amyloidogenic pathway, the main player is  $\alpha$ -secretase, that was proposed to be a membrane bound endoprotease that cleaves APP mainly at the plasma membrane

(Sisodia 1992). Using proteinase inhibitor profiling, it was revealed that  $\alpha$ -secretase is a zinc metalloproteinase (Roberts et al. 1994). There is  $\alpha$ -secretase-like activity in some members of the ADAM family (which are metalloproteinases and disintegrinases) and three of them have been pointed to act as  $\alpha$ -secretase: ADAM9, ADAM10 and ADAM17, which are type-I transmembrane proteins just like APP. ADAM9 can influence sAPP $\alpha$  concentrations while ADAM17, in complex with tumor necrosis factor A-converting enzyme (TACE) is co-localized with senile plaques and NFT's in hippocampus and cortex of AD patients (Buxbaum 1998). ADAM10 and ADAM17 are primarily responsible for the  $\alpha$ -secretase activity: ADAM17 is thought to be responsible for the inducible  $\alpha$ -secretase activity while ADAM10 is accountable for the constitutive activity and may also contribute to the inducible activity (Adeniji et al. 2017). During embryonic development ADAM10 seems to be vital for at least neuronal differentiation as it has been demonstrated that ADAM10 is implicated in the regulation of neuronal differentiation by maintaining precursor cells undifferentiated (Postina & Fahrenholz 2013). Specifically, it was shown that ADAM10 is involved in ephrin-mediated axon guiding via a contact-mediated, axon-repelling mechanism in cultured mouse hippocampal neurons (Hattori et al. 2000), thus demonstrating an ADAM10 contribution in neuronal pattern formation *in vivo*.

As A $\beta$  overproduction is a key pathological characteristic in AD brains and it is known to be upstream of the other AD neurodegenerative mechanism, the Tau hyperphosphorylation, the role of enzymes (secretases) involved in APP misprocessing have received a lot of attention over the last years. The most important neuronal  $\beta$ -secretase is a transmembrane aspartyl protease, labeled BACE1 ( $\beta$ -site APP cleaving enzyme; also called Asp-2 and memapsin-2) (Sinha et al. 1999; Vassar et al. 1999; Yan et al. 1999; Lau et al. 2000; Cai et al. 2001) that is highly expressed in the neurons and in astrocytes, and cleavage by BACE1 creates the N-terminus of A $\beta$ . As BACE1 needs an acidic surrounding for optimal activity, it can be found in early Golgi, late Golgi/early endosomes and can also be found in cell surface (Sinha et al. 1999), yet the regulation mechanisms of BACE1 trafficking and activity have not been yet fully expounded. BACE1 has a BACE2 homolog which is expressed extensively but does not seem to play a role in A $\beta$  generation because it looks to cleave near the  $\alpha$ -secretase site (Solans et al. 2000; Yan et al. 2001).

In contrast to  $\beta$ -secretase,  $\gamma$ -secretase activity resides in a high molecular weight complex with four components: presenilin (PS, PS1 or PS2), Nicastrin, anterior pharynxdefective-1 (APH-1) and presenilin enhancer-2 (PEN-2) (Kimberly et al. 2003; Takasugi et al. 2003). PS is a multitransmembrane protein with an uncertain number of transmembrane domains (Kim & Schekman 2004). It possesses two highly conserved aspartate residues indispensable for  $\gamma$ -secretase activity which are believed to be the crucial catalytic components of this enzyme. Studies have shown that mutations in PSEN1 (the gene that encodes for presenilin) are associated with familial Alzheimer's disease (FAD), and it was suggested that these mutations lead to a toxic gain of function as they are linked with a relative increased production of more hydrophobic A $\beta$  species, that will aggregate early in the course of the disease (Citron et al. 1997; Delacourte et al. 2002), while another study showed that the mutations in PSEN1 cause a loss of  $\gamma$ -secretase activity (Cacquevel et al. 2012).

The other important partner of  $\gamma$ -secretase complex is Nicastrin which is also a type I transmembrane glycoprotein that is considered the scaffolding protein within  $\gamma$ -secretase complex. In addition to secretases, caspases (caspase-3 mainly) can directly cleave APP at position Asp664 releasing a fragment containing the last 31 amino acids of APP, called C31 (Zhang et al. 2011). While APP is cleaved following both pathways, the amyloidogenic one is the most preferential in AD and, together with A $\beta$  overproduction, are suggested to have a central role in AD neurodegenerative processes.

Indeed, many studies demonstrated that both C99 and A $\beta$  are neurotoxic and has cognition-impairing properties arousing synaptic dysfunction and atrophy as well as neuronal death (Selkoe 1998; Shankar & Walsh 2009). There are two main species of A $\beta$ , A $\beta$ 40 and A $\beta$ 42, with the last to be the most hydrophobic and more predisposed to aggregation (Burdick et al. 1992). Studies of familial AD patients show increases in the ratio of A $\beta$ 42/40 (Borchelt et al. 1996; Scheuner et al. 1996) suggesting that elevated levels of A $\beta$ 42 is more critically involved in AD pathogenesis (Jarrett et al. 1993; Iwatsubo et al. 1994).

On the other hand, recent evidence demonstrates that A $\beta$  can also be neurotrophic and has important role in normal synaptic function and plasticity. Indeed, soluble A $\beta$  is a normal, physiological product, detectable in the blood plasma and cerebrospinal fluid of young and old healthy individuals (Seubert et al. 1992) while A $\beta$  is produced during

normal cellular metabolism (Haass et al. 1992). Furthermore, Kamenetz and colleagues showed that activated healthy neurons secrete A $\beta$  which, in turn downregulates excitatory synaptic transmission, thus illustrating that A $\beta$  can serve a homeostatic role in the maintenance of neuronal activity (Kamenetz et al. 2003). A later study by Abramov and colleagues pointed a more specific role for A $\beta$ , as they showed that it can serve as a positive endogenous regulator of vesicle release in the hippocampal synapses, turning A $\beta$  peptides crucial for the preservation of the synaptic vesicle release in a functional range (Abramov et al. 2009).

#### 4.2. Synapse-to-nucleus impact in synaptopathies

In the last few years, more has been uncovered about nuclear translocation of synaptonuclear messengers, its mechanisms, the importance of this model and the diversity of factors involved in it. As more is understood, there are increasing indications of possible roles of the synaptonuclear messengers in several brain diseases (**Table 1**), and despite the efforts being made to comprehend their role, the relevance of synapse-to-nucleus signaling in these pathologies remains largely unknown (**Figure 12**).

**TABLE 1:** Synaptonuclear messengers, related pathologies and their molecular mechanisms. Based on (Marcello et al. 2018; Parra-Damas & Saura 2019).

Messenger	Related pathologies	Molecular mechanism
<i>Synaptonuclear proteins</i>		
<b>RNF10</b>	Fragile X syndrome	Strong deregulation of RNF10 expression in male carriers of the fmr1 premutation and in mouse model of a Fragile X associated Tremor/Ataxia Syndrome.
<b>ProSAP2/Shank3</b>	Autism spectrum disorders, Schizophrenia	Insertion and deletion mutations of the SHANK3 gene in about 0,5% of ASD patients. Two mutations identified in patients with schizophrenia.
<b>Jacob</b>	Kallmann syndrome Alzheimer's disease	KO mice show a profound hippocampal dysplasia. Involved in synaptic depression induced by A $\beta$ oligomers.

<b>AIDA-1</b>	Alzheimer's disease	Reduction of A $\beta$ -production by inhibiting the activity of the $\gamma$ -secretase.
<b>CREB2/ATF4</b>	Alzheimer's disease Parkinson's disease	Upregulated in AD patients and in AD mouse model. Knockdown prevents A $\beta$ induced neurodegeneration. ATF4-parkin signaling limits neuronal death, exerting a protective effect.
<b>CRTC1</b>	Alzheimer's disease Parkinson's disease Huntington's disease	Reduced at Braak III/IV stages. Involved in A $\beta$ -dependent effects on associative learning deficit. Overexpression reverses memory impairment in an AD transgenic model.
<b>MAPK/ERK</b>	Alzheimer's disease Parkinson's disease	ERK1/2 mediates A $\beta$ -induced neurodegeneration; tau is phosphorylated by ERK.
<b>NF-<math>\kappa</math>B</b>	Huntington's disease Alzheimer's disease	A mutated pathogenic Htt impairs the trafficking by Htt/importin $\alpha$ 2. NF- $\kappa$ B mediates aging related neuroinflammation.
<b><i>Cytosol-to-nucleus proteins</i></b>		
<b><math>\gamma</math>CaMKII</b>	Intellectual disability	<i>CAMK2G</i> point mutation associated with severe intellectual disability; mental retardation impairs $\gamma$ CaMKII-mediated CaM nuclear translocation.

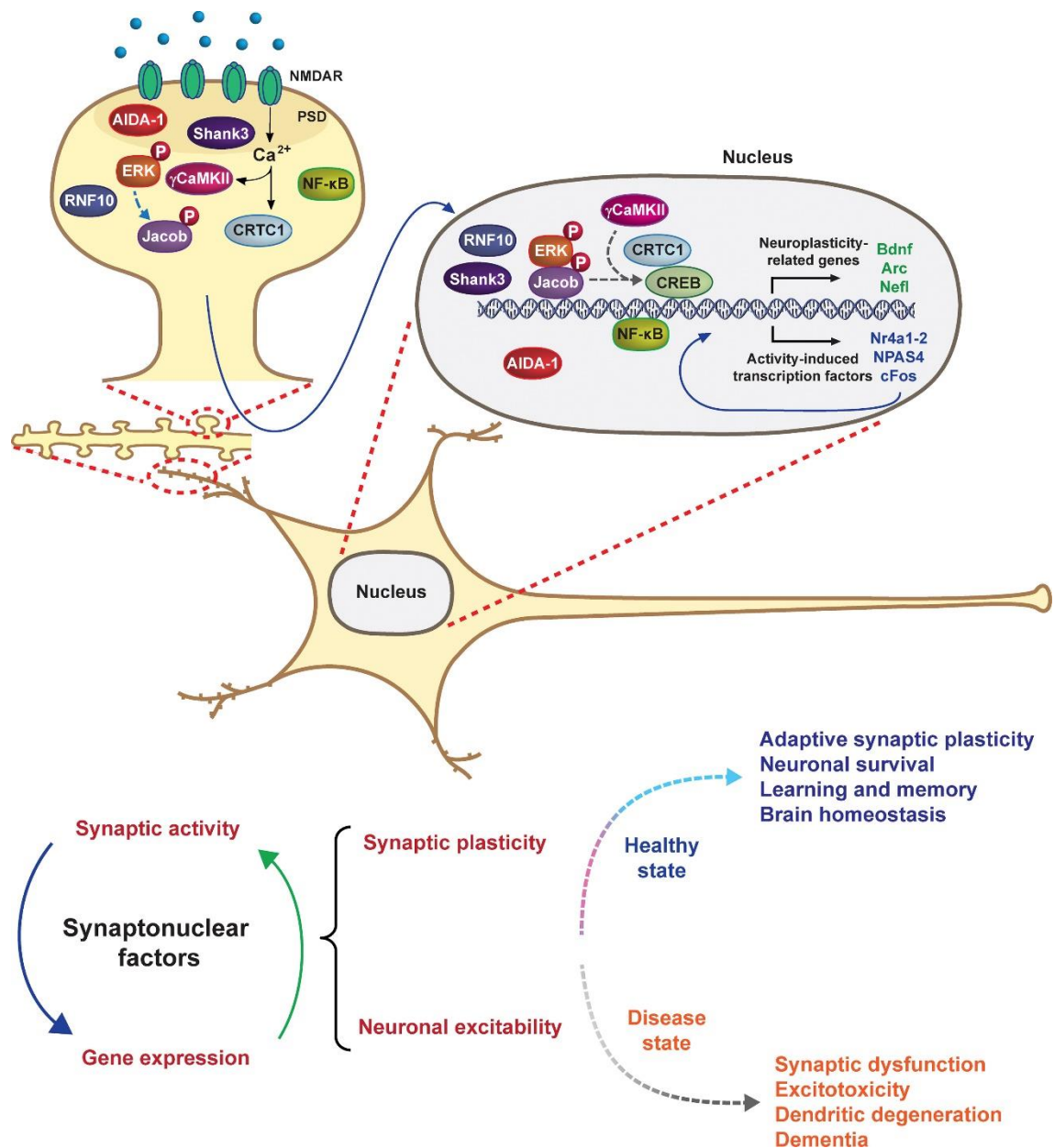


**FIGURE 12 Synapse-to-nucleus signaling regulates neuronal excitability and synapse plasticity.** *Top image:* Several synaptic factors (CRTC1, ERK, Jacob, NF-κB, RNF10, Shank3, γCaMKII...) are activated by synaptic activity at distal dendrites, including synapses, and translocate to the nucleus to regulate CREB-mediated transcription. By contrast, activity-dependent synapses-to-nucleus AIDA-1 translocation does not affect CREB-mediated transcription. Blue lines indicate signals travelling from dendritic spines or dendrites to the nucleus to regulate gene expression. *Bottom image:* Synaptonuclear factors regulate synaptic plasticity and neuronal excitability by affecting gene expression. Imbalance of synaptic plasticity and neuronal excitability can affect health and disease states. Some brain physiological and pathological states that are directly or indirectly regulated by synapse-to-nucleus signaling are indicated on the right (Parra-Damas & Saura 2019).

#### a) RNF10

As previously mentioned, RNF10 is a postsynaptic protein with the capacity to translocate from the dendritic spines to the nucleus after association with importin  $\alpha$  (Dinamarca et al. 2016). It was shown that some of the target genes of this protein are important in the actin cytoskeleton and spine morphology, such as ArhGap4, ArhGef6 and Ophn1, and it was demonstrated that mice lacking these genes develop cognitive deficits (Ramakers et al. 2012; Barresi et al. 2014), being associated with X-linked mental retardation and Fragile X syndrome (Raymond 2006). It was also demonstrated that RNF10 is downregulated in blood samples of male patients that present the fmr1 premutation as well as in brain samples from a mouse model with Fragile X Tremor/Ataxia syndrome (Mateu-Huertas et al. 2014).

#### b) ProSAP2/Shank3

ProSAP/Shank proteins are a family of scaffolding molecules found at excitatory glutamatergic synapses (Grabrucker et al. 2014). They are capable of regulating synapse formation, morphology and function after interacting with other postsynaptic density proteins, such as Abi-1 (Jiang & Ehlers 2013). It was shown that patients with autism spectrum disorders (ASD) present alterations such as insertion and deletion mutations in SHANK3 gene (Durand et al. 2007), impacting mainly synapse morphology and signaling, and exacerbating autistic/maniac behaviors due to Shank3 loss of function (Han et al. 2013). Two specific mutations in this gene – R1117X and R536W – were found to be related to schizophrenia (SCZ): particularly, R1117W was shown to impact synapse to nucleus translocation, as the mutation leads to a nuclear localization independently of the synaptic activity (Grabrucker et al. 2014).

#### c) Jacob

Jacob, as described before, translocates from the synapse to the nucleus after the activation of the GluN2B-containing NMDA receptors (Hardingham et al. 2001a; Hardingham et al. 2001b; Hardingham et al. 2002). Phosphorylated Jacob promotes CREB signaling, whereas its inactivation leads to impaired CREB signaling, as demonstrated in Jacob KO mice, resulting in reduced synapses, simplification of dendrites and deficits in hippocampal-dependent synaptic plasticity and memory (Spilker et al. 2016), thus leading

to the conclusion that the phosphorylation state of a factor can influence and determine its function. Mutations on the gene encoding Jacob have been demonstrated to be linked to Kallmann syndrome, a disease of idiopathic hypogonadotropic hypogonadism with anosmia or hyposmia (Pitteloud et al. 2007). In relation to Alzheimer's disease, it is known that A $\beta$  oligomers cause nuclear accumulation of Jacob, possibly contributing to the cognitive deficits that we observe in patients with this disease (Rönicke et al. 2011).

#### d) AIDA-1

AIDA-1, also known as Ankyrin repeat and sterile alpha motif domain containing 1B (ANKS1B), is a PSD-95/NMDAR binding protein capable of translocating to the nucleus after synaptic activation (Jordan & Kreutz 2009). It was shown that the inactivation of *Anks1b* in mice results in deficits in hippocampal-dependent synaptic transmission, plasticity deficits, prepulse inhibition and increased locomotor activity (Jordan et al. 2007; Tindi et al. 2015). In humans, mutations in this gene have been shown to be related to neuropsychiatric disorders such as SCZ (Fromer et al. 2014; Chang et al. 2018) and ASD (Pinto et al. 2010; Hu et al. 2011). It was also demonstrated that AIDA-1 inhibits A $\beta$  generation by modulating amyloid precursor protein (APP) processing at the level of  $\gamma$ -secretase (Ghersi et al. 2004).

#### e) CREB2/ATF4

ATF4 is a transcriptional CREB repressor, shown as capable of regulating synaptic plasticity and memory, and has a particularly increased expression in response to stress factors (Lai et al. 2008). ATF4 has been shown to be involved with Parkinson's disease (PD), as it is the major effector in the endoplasmic reticulum stress pathway, one of the mechanisms implicated in this disease. ATF4 is also an expression regulator of parkin, that causes early-onset, autosomal recessive PD when mutated, even though recent studies show that ATF4-parkin signaling play a role in limiting neuronal death in the context of this disease, hence having a protective effect against PD (Sun et al. 2013).

In the context of Alzheimer's disease (AD), recent studies show that the axonal ATF4 synthesis is implicated for the retrograde spread of A $\beta$ <sub>1-42</sub>-induced neurodegeneration, and that the axons in brains of AD patients show more frequent localization of ATF4 protein and mRNA (Baleriola et al. 2014). It is also recognized that this protein is

upregulated in the brain of AD patients and mouse models expressing the apolipoprotein E (ApoE)  $\epsilon$ 4 alleles, which is the most prevailing gene risk factor in this disease (Segev et al. 2015).

f) CRTC1

CRTC1 is one of the many messengers involved in the control of the CREB pathway, with a demonstrated role in AD, as CRTC1 levels are reduced in the hippocampus of patients (Parra-Damas et al. 2014). In the presence of intraneuronal A $\beta$ , the nuclear translocation of CRTC1 is reduced, causing severe learning deficits (Wilson et al. 2017) whereas the overexpression of the protein has been shown to successfully rescue amyloid-induced transcriptional and cognitive deficits (Parra-Damas et al. 2014). In Parkinson disease, the low levels of phosphorylated CRTC1 in the substantia nigra of the patients indicate a possible reduction in this protein's function (Won et al. 2016), while in Huntington's disease patients, this protein shows a significant decrease in striatal levels (Chaturvedi et al. 2012).

g) MAPK/ERK

Mitogen-activated protein/extracellular signal-regulated kinase (MAPK/ERK) mediates transcription and excitation in different forms of glutamate-dependent synaptic plasticity. In Alzheimer's disease context, ERK is capable of mediating the phosphorylation of Tau; and one of the components of the MAPK/ERK pathway, c-Jun N-terminal kinase (JNK), is capable to phosphorylate and stabilize APP (Kim & Choi 2010). In PD, the increased activated forms of JNK and ERK correlate with the restricted distribution of neurofibrillary tangles in an  $\alpha$ -synuclein-overexpressing mouse model. Furthermore, reduced activity of ERK1/2 was found in the substantia nigra of a mouse model of dopaminergic neuronal degeneration (Kim & Choi 2015).

h) NF- $\kappa$ B

As mentioned previously, Nf- $\kappa$ B belongs to a family of dimeric transcription factors, activated at the postsynaptic compartments and transported to the nucleus. Recent studies have uncovered that this synapto-nuclear trafficking is mediated by huntingtin (Htt) and importin  $\alpha$ 2, and consequentially impaired when Htt is mutated, leading to the

hypothesis that this altered trafficking might contribute to Huntington's disease (Marcora & Kennedy 2010). Interestingly, NF- $\kappa$ B is also pointed to associate with AD, as recent findings have shown tissue specific brain inflammation provoked by aging is mediated by this factor, being aging one of the most significant risk factor for developing AD (Jones & Kounatidis 2017).

#### i) $\gamma$ CaMKII

Calcium/Calmodulin-dependent protein kinase II (CaMKII), the major post-synaptic protein at excitatory synapses, is a holoenzyme of 12 subunits, each derived from one of four genes ( $\alpha$ ,  $\beta$ ,  $\gamma$  and  $\delta$ ) (Rosenberg et al. 2005), and encoded by *CAMK2G* gene. Even though the subunits  $\alpha$  and  $\beta$  are the most common, recent studies have uncovered some facts about the  $\gamma$  subunit. Briefly, it was demonstrated that depolarization and high frequency stimuli induce  $\gamma$ CaMKII-dependent trafficking of calmodulin (Ma et al. 2014). It was found that a point mutation in *CAMK2G* associated with severe intellectual disability and mental retardation impairs this  $\gamma$ CaMKII trafficking (De Ligt et al. 2013), pointing towards a possible role for this mechanism in this pathology. Interestingly, the  $\alpha$  subunit has also been correlated with diseases such as AD (**Figure 13**). Recent studies have shown that T286-autophosphorylation of  $\alpha$ CaMKII is impaired at synapses in the disease, and since this autophosphorylation is essential for spatial memory formation, it could imply a role in the AD characteristic cognitive impairment. CaMKII has also been appointed as an interactor with tau and its phosphorylation. The increased expression of  $\alpha$ CaMKII in CA1 neurons (McKee et al. 1990; Wang et al. 2005), as well as increased autophosphorylation in CA3 neurons (Reese et al. 2011; Gu et al. 2009) and granule cells in the DG suggest an hyperactivation of  $\alpha$ CaMKII outside the synapses, and as a tau kinase, that hyperactivity can trigger the neurofibrillary tangles' formation (Ghosh & Giese 2015).

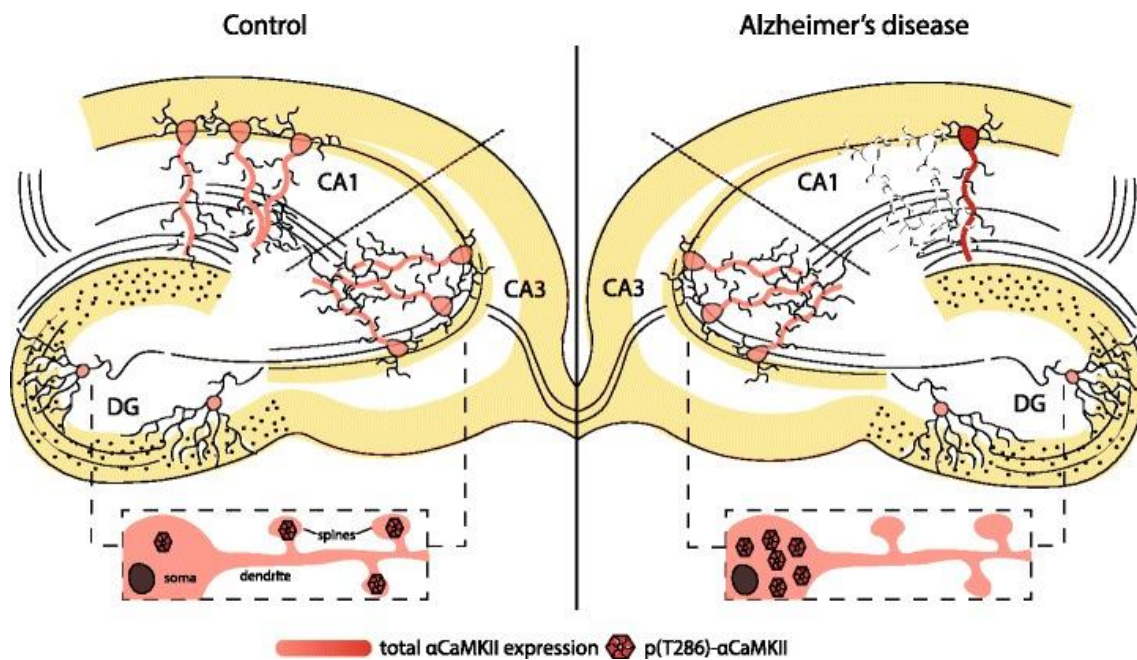


**FIGURE 13  $\alpha$ CaMKII is dysregulated in the Alzheimer's disease hippocampus.**  $\alpha$ CaMKII-expressing neurons are selectively lost in the hippocampal CA1 subfield in AD, a region that shows devastating atrophy when compared to age-matched controls. Remaining pyramidal neurons of this region show increased expression of  $\alpha$ CaMKII. This increased expression may critically contribute to tau hyperphosphorylation and other neurodegenerative processes, such as caspase-3 overactivation, in CA1 pyramidal neurons. On the other hand, CA3 pyramidal neurons and granule cells of the DG do not develop these changes in total  $\alpha$ CaMKII. They do however show a change in subcellular distribution of T286-autophosphorylated  $\alpha$ CaMKII (inset). This change is suggested to shift CaMKII activity from the synapse to soma leading to synaptic deficits, neurodegenerative processes, and impaired memory formation. AD, Alzheimer's disease; CA1/3, Cornu Ammonis areas 1/3;  $\alpha$ CaMKII,  $\alpha$  subunit of calcium/calmodulin-dependent protein kinase II; DG, dentate gyrus (Ghosh & Giese 2015).

**AIMS**

RNF10 is a novel synapse-to-nucleus messenger, therefore with plenty of possibilities yet in the open concerning the effect of this protein messenger in several neuronal functions.

A previous work from our laboratory demonstrated that RNF10 interacts at synapses with the GluN2A subunit of NMDA receptors, shedding some light on the possible mechanisms by which this protein travels from the dendritic spines to the nucleus (Dinamarca et al., 2016). Importantly, RNF10 silencing in cultured neurons was sufficient to induce a dramatic decrease in spine density (Dinamarca et al., 2016). Of relevance, it was also suggested a possible effect of RNF10 in a synaptopathy, a disease that is a major concern in the actual world health panorama: Alzheimer's disease (AD). AD is the most common form of dementia in the population over 65 years (~7-10%), affecting more than 30 million people worldwide while this number is predicted to be increased to 115 million by 2050, with the costs associated with the disease growing every year. Despite having two major and well described hallmarks (the production and aggregation of amyloid-beta and the hyperphosphorylation of Tau protein), so many other proteins are currently associated with the disease, and with many more still underlying undiscovered.

In our working case, the presence of reduced levels of RNF10 in brain samples from patients with AD and the capability of amyloid-beta to induce RNF10 trafficking to the nucleus (Musardo *et al*, unpublished results, see below **Figure 43** and **44**) raised some questions concerning the actual role of this protein in the disease context.

Starting from these considerations and preliminary data, we hypothesized that RNF10 could exert a role in AD, but since much more is unknown about this protein at the moment, as a starting point we aim to unravel the role of RNF10 in cognitive function and plasticity, using the RNF10 KO mice as an experimental model.

Since only few information is available in the literature about the RNF10 KO mouse model, we started the project with the characterization of the experimental model. An extensive characterization is a thorough process, that combines several techniques to achieve a detailed description. Here, we evaluate many different aspects of the animal model, from a general visual characterization, to a more complex level, such as spines and electrophysiology.

# **MATERIALS AND METHODS**

## 1. Animals

The animals used in this project were male and female C57BL6 mice from 2 to 18 months old, lacking the RNF10 gene (KO), wildtype (WT) littermates or heterozygous (HE). Mice were placed with a maximum of five per cage under standard environmental conditions (ambient temperature of  $21 \pm 1$  °C and a relative humidity of 50–60%; 12h light/dark cycle (lights on at 8:00 A.M.; dark at 8:00 P.M.) with *ad libitum* access to food and water unless otherwise required for the experiments. The Institutional Animal Care and Use Committee of the University of Milan and the Italian Ministry of Health (#191/2016) approved the experiments involving RNF10 KO mice. Animal handling and surgical procedures were carried out with care, taken to minimize discomfort and pain, in accordance with the ethical guidelines and regulations of the European Parliament and of the Council on protection of animals used for scientific purposes (Directive of 22 September 2010, 2010/63/EU).

## 2. Genotyping procedures

For animal genotyping, the Polymerase Chain Reaction (PCR) technique was used based on total DNA extracted by tail biopsy. After cutting the tail of the animal, it was incubated in 200  $\mu$ L of sodium hydroxide 60 mM for 17 minutes at 98°C. The sample then rested for 5 minutes at 4°C, and subsequently added 40  $\mu$ L of Tris-HCl 1M pH 8. After a brief vortex, the sample was then centrifuged at 12.000 rpm for 3 minutes. The PCR Master mix uses the following products: WonderTaq buffer 5x, WT primers: CSD-Rnf10-F: GGAGGAAAAGTTTAGGTTTATGACAGG, CSD-Rnf10-ttR: AATCCCAGCACTCAGAAGACAGAGG. Tg primers: CSD-neoF: GGGATCTCATGCTGGAGTTCTTCG, CSD-Rnf10-R: ACACGCCAGACTAGAGAATTAGCCC, WonderTaq polymerase and dH<sub>2</sub>O. The PCR cycle was set as follows: 94°C for 5 minutes; (94°C for 15 seconds, 65°C for 30 seconds, 72°C for 40 seconds – 10 cycles, decrease 1°C per cycle); (94°C for seconds, 55°C for 30 seconds, 72°C for 40 seconds – 30 cycles); 72°C for 5 minutes and 4°C until further processing. The samples were then run in a gel electrophoresis using Safe-Green™, and bands were detected at either 746 bp (transgenic, Tg - KO) or 307 bp (WT), or both (HE).

### 3. Immunohistochemistry

For the immunohistochemistry, we used 100  $\mu\text{m}$  brain slices that were permeabilized in 0,3% Triton for 30 minutes at 4°C and then blocked in a 0,1% Triton solution in PBS, with 10% of normal goat serum. The primary antibodies (RNF10 and MAP-2) were incubated in a solution of 0,1% Triton with 3% of normal goat serum, shaking at 4°C overnight. After washes, the secondary antibody was incubated in the same solution for 1-2h at room temperature, shaking. Afterwards another set of washes, a brief stain with DAPI to stain the nuclei was performed; slices were then mounted in microscope slides and images were acquired in a confocal microscope.

### 4. RNA extraction and Real Time PCR (qPCR)

To prepare the samples and extract the RNA, we used the TRIzol method, using the Direct-zol™ RNA MiniPrep kit (Zymo Research, Irvine, USA), and following the manufacturer's instructions. To evaluate the RNA quality, after extraction samples were measured in a NanoVue™ apparatus (GE Healthcare, Chicago, USA).

Samples from mouse cortex were diluted to 5 $\mu\text{g}/\mu\text{l}$  and used for mRNA quantification. Specific RNA sequences were amplified and quantified by qPCR, using iTaq Universal SYBR Green One-Step Kit for qPCR (Bio-Rad, CA, USA), following the manufacturer's instructions. Experiments were performed with triplicates of each sample. We calculated the target mRNA levels comparing the target gene values with the housekeeping gene values. The qPCR protocol is composed of 40 cycles of amplifications, each consisting of a denaturation step at 95° C for 15 seconds and an annealing/extension step at 60° C for 60 seconds. The oligonucleotides used for qPCR were obtained from Eurofins MWG Operon (Ebersberg, Germany). qPCR primers sequences are reported below:

#### **Housekeeping gene (36B4)**

Forward: AGATGCAGCAGATCCGCAT

Reverse: GTTCTTGCCCATCAGCACC

#### **RNF10**

Forward:

GATCTCCTTCAGGTTGATCTTCTTAGGGTTCAAGAGACCCTAAGAAGATCAACCACAATTTTTG  
GAAG

Reverse:

AGCTCTCCAAAAATTGTGGTTGATCTTCTTAGGGTCTCTTGAACCCTAAGAAGATCAACCTGAA  
GGA

## 5. Food intake, insulin and glucose tolerance tests

For the food intake test, the animals were housed individually, and their body weight was monitored daily for a week. For the same period, food was weighted and the differences between days was calculated.

For the insulin and glucose tolerance tests, the animals were fasted for a minimum of 6 hours, with free access to water only. After this period, each animal had their glucose levels measured as a baseline parameter, after which they were injected with either insulin in a concentration of 0,5 IU/g animal or glucose in a concentration of 2g/kg, depending on the test. Blood drops were collected from the tail and analyzed in a glucometer in the 15, 30, 60, 90 and 120 minutes after injection.

## 6. Purification of triton insoluble postsynaptic fractions and crude nuclear fractions

The Triton Insoluble Fraction (TIF), a fraction highly enriched in all categories of postsynaptic density proteins (i.e., receptor, signaling, scaffolding, and cytoskeletal elements) absent of presynaptic markers, was obtained from mouse half brain (**Figure 14**). Samples were homogenized at 4°C in an ice-cold buffer with protease inhibitors (*Complete™*, GE Healthcare, Mannheim, Germany), phosphatase inhibitors (*PhosSTOP™*, Roche Diagnostics GmbH, Mannheim, Germany), 0.32 M Sucrose, 1 mM HEPES, 1 mM NaF, 0.1 mM PMSF and 1 mM MgCl<sub>2</sub> using a hand-held Teflon-glass. A small amount derived from homogenate (Homo) was immediately frozen and saved for further Western Blot analysis. The HOMO was then centrifuged at 1.000 g for 5 min at 4°C, to remove nuclear contamination and white matter. The supernatant was collected and centrifuged at 13.000 g for 15 min at 4°C. The resulting pellet (crude membrane) was resuspended in hypotonic buffer (1 mM HEPES with protease inhibitors (*Complete™*, GE Healthcare)) and then centrifuged at 100.000 g for 1 h at 4°C. The resulting pellet of this centrifuge was then resuspended in an extraction buffer (1% Triton-X 100, 75 mM KCl and protease inhibitors (*Complete™*, GE Healthcare) and left for 15 min at 4°C for extraction. After that,

the samples were centrifuged at 100.000 g for 1 h at 4°C and the pellet that represents the TIF fraction was resuspended using a glass-glass homogenizer in 20 mM HEPES with protease inhibitors (*Complete™*, GE Healthcare). The protein content of the samples was quantified using a Bio-Rad (Hercules, CA, USA) protein assay.

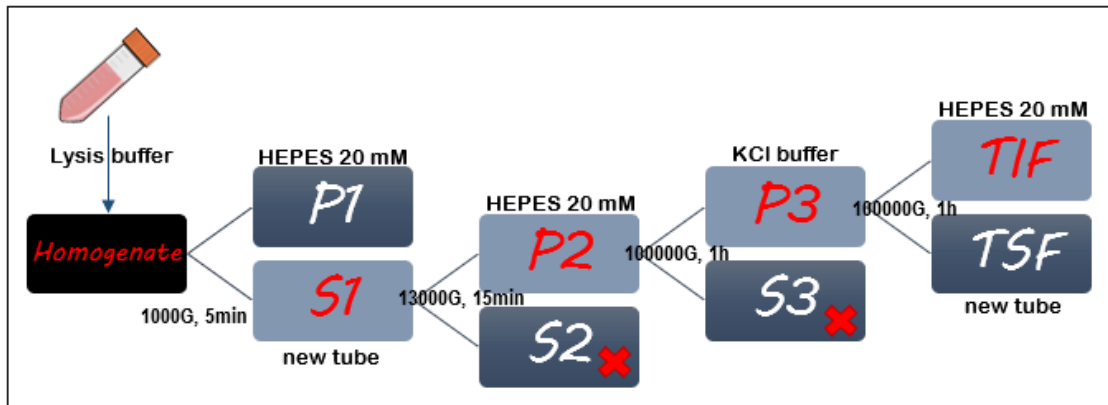


**FIGURE 14 Representative scheme of the fractionation**, with all the steps from half brain to TIF fraction.

## 7. Western Blot

One of the most common methods used to separate macromolecules is using a sodium dodecyl sulfate polyacrylamide gel electrophoresis (SDS-PAGE), where those molecules run in an electric field in a polyacrylamide gel and are denaturated by the SDS, an anionic detergent.

Proteins were separated in an 8% or 12% total acrylamide gels, accordingly to their molecular weight, and were transferred to a nitrocellulose membrane, using a “blotting buffer” (20% Methanol with 1X Blotting buffer (Tris 0,025 M, glycine 0,192 M, MeOH 20%, pH 8.3) for 2 hours at 240 mA.

Once the transference was finished, the presence of proteins was confirmed by Ponceau staining, followed by an incubation with a blocking solution of iBlock-TBS (Invitrogen, T2015) for at least 45 minutes, and then left overnight exposed to the primary antibody, diluted in iBlock-TBS, at 4°C. On the second day, the membranes were washed 3 times, 10 minutes each wash in a horizontal shaker at room temperature, in a Tris-buffered saline/Tween 20 (TBS-T) solution and sequentially incubated with the secondary antibody, coupled with horseradish peroxidase (HRP) for at least 1 hour at room temperature. After a second set of washes, and to reveal the membrane, the trans-

UV (302nm) Chemidoc MP System (Bio-Rad Laboratories) was used, in combination with the substrate Clarity™ Western ECL (Bio-Rad Laboratories).

## 8. Antibodies

The following antibodies were used: ADAM10 (Calbiochem - 422751), actin (20-30) (Sigma – A5060), APP A4 (22C11) (Millipore – MAB348), BACE1 (Sigma – SAB2100200), Cool2/ $\alpha$ Pix (C23D2) (Cell Signaling – 4573), CREB (Millipore – AB3006), ARHGAP4 (Novus Biologicals – NBP1-88527), GluA1/GluR1 (Neuromab – 75-327), GluN2A (Sigma – M264), GluN2B (Neuromab – 75-101), N-cadherin (BD Biosciences – 610920), Oligophrenin-1 (Cell Signaling – 11939), p21 (BD Biosciences – 556430), phospho-CREB (Ser133) (Millipore – 06-519), phospho-GluA1 (Ser845) (Millipore – 04-1073), PSD-95 (Neuromab – 75-028), RNF10 (Proteintech – 16936-1-AP), tubulin (Sigma, T9026). The Peroxidase-conjugated secondary anti-mouse antibody was purchased from Pierce whereas peroxidase-conjugated secondary anti-rabbit antibody was purchased from Bio-Rad.

## 9. Spine analysis procedures

(1,1'-Diocetadecyl-3,3',3',3'-Tetramethylindocarbocyanine Perchlorate ('Dil'; DiI<sub>C18</sub>(3))) (Dil) is a lipophilic membrane stain that diffuses laterally to stain the entire cell. It is weakly fluorescent until incorporated into membranes. This orange-red fluorescent dye, which is spectrally similar to tetramethylrhodamine, is often used as a long-term tracer for neuronal and other cells.

Mice were anesthetized by intraperitoneal (ip) injection, followed by a cardiac perfusion with PB 0.1M at room temperature first, and then with cold 1.5% PFA in PB 0.1M. The brain was collected and post fixed by keeping it for 40 min in 1.5% PFA in PB 0.1M at 4°C. After this time, it was washed twice with PB 0.1M and the brain was cut coronally around region of interest (hippocampus) to make a slice of 2-3 mm, in order to have a nice visibility of the beginning and end of region. Dil crystals were applied using a thin needle by delicately touching the region of interest on both sides of the 2-3 mm coronal slice and Dil was left to diffuse in PB 0.1M for 12-24h in the dark at room temperature. The slice was then fixed with 4% PFA in PB 0.1 M for 45min-1h at 4°C and then 100-150  $\mu$ m coronal slices were prepared in the vibratome in PB 0.1M on ice. Finally,

the slices were mounted on glass slides with Fluoromount mounting medium and sealed with nail polish for confocal imaging.

## 10. Confocal imaging

Immunohistochemistry images were acquired using a 63x objective in a Zeiss LSM510 Meta system (Zeiss, Oberkochen, Germany) confocal microscope or by whole slice imaging in a NanoZoomer S60 (Hamamatsu Photonics, Shizuoka, Japan).

For spine morphology, imaging was done with a 63x objective, using the 543nm laser. Z-stacks of 0.5µm steps were acquired, with a max zoom of 2. The minimum resolution for a successful image is 1024 pixels. To have a clear and easy visible image, speed was adjusted to 3 with a mean scan line of 2-4. Using ImageJ (National Institutes of Health) program, spine density was measured by tracing all spines present in each segment (in this order, **length** of spine – **head width** – **neck width**, as represented in **Figure 15**). After all the spines had been traced, the free-hand line function was used to measure the length of total dendrites. Total spine density per 10 µm was calculated from these values.

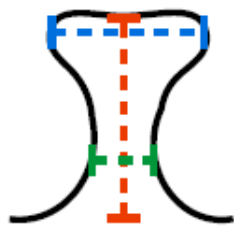


**FIGURE 15 Model used to count dendritic spines.** Each Spine was measured using the following parameters, in this order: **length** of spine – **head width** – **neck width**.

## 11. ELISA

To test insulin and FGF21 levels, we collected blood from the tail of the animal and added EDTA 0,5M to prevent immediate coagulation. We then spinned the samples at 8.000g for 5 minutes and used the obtained plasma in two different ELISA kits. For insulin, we used the Mercodia Ultrasensitive Mouse Insulin ELISA kit (Mercodia AB, Uppsala, Sweden) and for FGF-21 we used the Mouse/Rat FGF-21 ELISA kit (BioVendor, Brno, Czech Republic), following the indicated protocols. Experiments were performed with duplicates of each sample. For the quantification step, the 96-wells plate was read at the indicated absorbance in the spectrophotometer, and relative optical density was measured.

As for A $\beta$  measurements, we used the Amyloid-beta (1-42) (mouse/rat) ELISA kit (IBL International, Hamburg, Germany). After testing the sample for the most adequate dilution, it was determined that WT samples should be used at 1:5 dilution and KO should be used at 1:50 dilution. Therefore, 5  $\mu$ l of KO sample and 50  $\mu$ l of WT were used. The kit was then used following the manufacturer's instructions. As done before, the experiments were performed with duplicates of each sample and for the quantification step, the 96-wells plate was read at 450 nm in the spectrophotometer, and relative optical density was measured.

## 12. Behavioral testing

### 12.1. Rotarod

The rotarod test is used to evaluate the motor skill learning, where the animal is placed in a wheel that moves at a defined speed. The protocol that was used consisted of 2 days of training at a constant speed (20 rpm) for a maximum of 600 s in two trials. On the third day, animals were tested in a constant speed (30 rpm) for a maximum of 600 s in two trials. Latency to fall and gripping were recorded.

After a 1-hour rest period, the animals were subjected to two trials on an acceleration rod (20–40 rpm, 5 min) with a 10–15-long interval between each trial.

### 12.2. Y-Maze

Mice were subjected to a 2-trial test in a Y-shaped maze separated by 30 minutes inter trial interval to assess spatial recognition memory as a form of episodic-like memory. Spatial recognition information could be considered as a form of episodic-like information since the rodent remembers the arms visited during the training session dependently of the inter-session and then preferentially explores the novel arm during the retrieval session.

The 3 identical arms of the maze are randomly designated start arm (S), familiar arm (F) and novel arm (N), with visual cues placed in the top walls of the arms of the maze. In the first trial, mice are positioned in the beginning of the starting arm and allowed to explore only 2 arms (S and F) for 5 minutes. For the retrieve trial, 30 minutes later, the animals are placed back in the starting arm of the maze and can explore for 5 minutes

with free access to all 3 arms. The behavioral videos were analyzed using VLC, in combination with the software Clickr.

### 12.3. Novel Object Recognition Test (NORT)

The Novel Object Recognition (NOR) task is used to evaluate cognition, particularly recognition memory, in rodent model of CNS disorders. This test is based on the spontaneous tendency of rodents to spend more time exploring a novel object than a familiar one. It is useful to assess impaired cognitive ability in transgenic strains of mice and evaluating novel chemical entries for their effect on cognition. The choice to explore the novel object reflects the use of learning and recognition memory. The test was performed in a modified Y-maze protocol.

**Habituation phase:** animals are placed in the center of the arms (hub) and allowed to explore only 2 arms for 10 minutes. Between trials, animals return to their home cages. The habituation phase lasts for at least 4 consecutive days.

**Familiarization:** the animals can explore the 2 open arms during 10 min. Two identical objects are placed in the end of the arms (**Figure 16**). The time spent exploring each object and the discrimination index percentage is recorded.

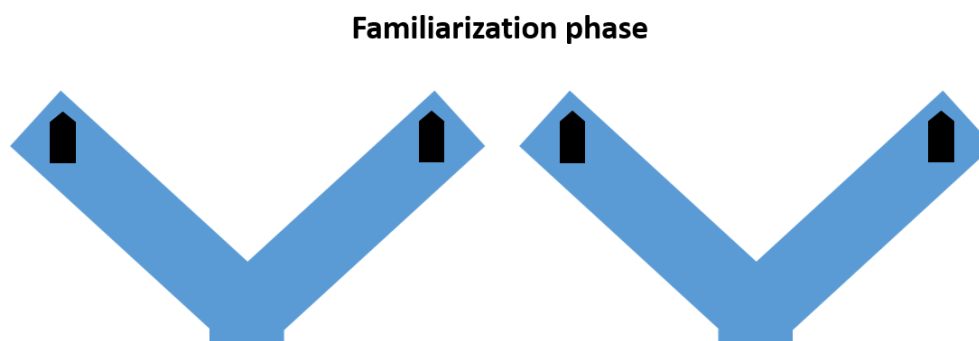


**FIGURE 16** Representative scheme of the maze setup for the familiarization phase of the NORT.

**2h test:** Mice can explore the maze in the presence of the familiar object (that was used in the familiarization) and a novel object (in the other arm) for 10 minutes (**Figure 17**). This test is performed 2h after the familiarization. Again, the time spent exploring each object and the discrimination index percentage is recorded.

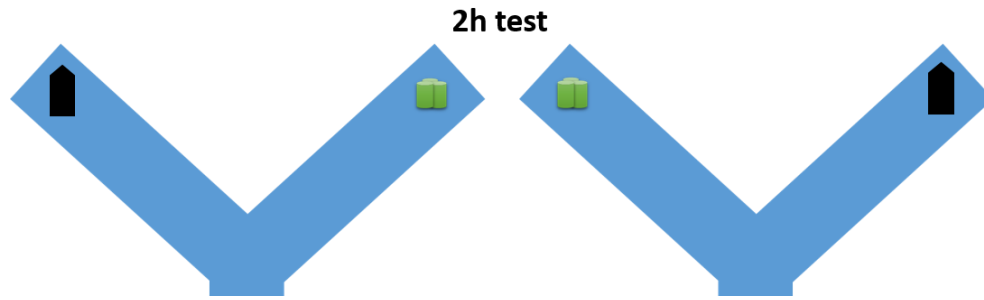


**FIGURE 17** Representative scheme of the maze setup for the 2 hours test of the NORT.

**24h test:** 24 hours after the familiarization test, animals are tested for long-term recognition memory. Mice are placed in the hub of the maze: one arm contains the same familiar object used in the familiarization and the other arm has a new unfamiliar object (different from the object used in both familiarization and the 2h test) for 10 minutes (**Figure 18**). Again, the time spent exploring each object and the discrimination index percentage is recorded.

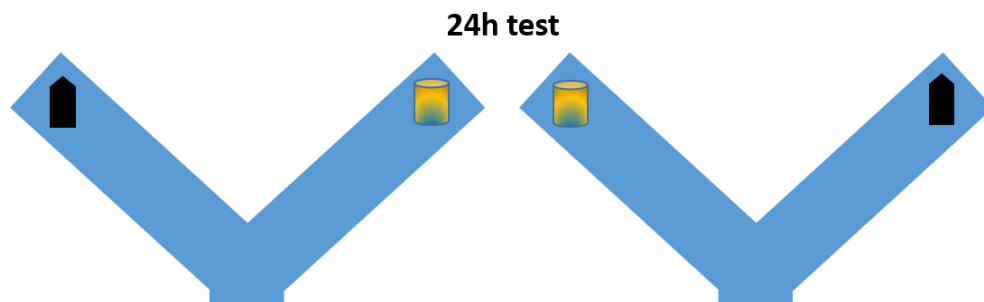


**FIGURE 18** Representative scheme of the maze setup for the 24 hours test of the NORT.

### 13. Electrophysiology

For the first incursion in the electrophysiology field in this animal model, the perforant path to granule cells was assessed. The perforant path provides a route from the entorhinal cortex to all fields of the hippocampus, including dentate gyrus, all CA fields and the subiculum.

Parasagittal hippocampal slices (260  $\mu\text{m}$  thick) were obtained from 21-50 days old RNF10 WT or KO C57Bl/6 mice. From the moment of slicing until the end of recordings, the slices were continuously infused with an oxygenated extracellular medium composed by 120 mM NaCl, 16.5 mM glucose, 1 mM  $\text{MgCl}_2$ , 2 mM  $\text{CaCl}_2$ , 2.5 mM KCl, 1.25 mM

NaH<sub>2</sub>PO<sub>4</sub>, 2.8 mM pyruvic acid, 27 mM NaHCO<sub>3</sub> and 0.5 mM ascorbic acid and supplied with 95% O<sub>2</sub> and 5% CO<sub>2</sub>. To characterize the excitatory inputs to granule cells (GC) of the dentate gyrus, whole-cell recordings were made using borosilicate glass capillaries which had resistance between 4 and 6 MΩ, with the patch pipette containing an intracellular solution supplied with 125 mM CsCH<sub>3</sub>CO<sub>3</sub>, 2mM MgCl<sub>2</sub>, 4 mM NaCl, 10 mM EGTA, 10 mM HEPES, 5 mM phospho-creatinine and 4 mM NaATP, pH 7.3 (**Figure 19**). Bicuculline (10 μM), a GABA-A receptor antagonist, was present throughout all experiments. To record AMPA/NMDA ratios, AMPA-EPSCs were first recorded in the voltage-clamp mode holding the potential at -70 mV, then to record NMDA-EPSCs the membrane potential was changed to +30 mV in the presence of NBQX (10 μM), an AMPA receptor antagonist. The decay time was calculated by measuring the time between 90% and 10% of the amplitude of the EPSC.

Miniature EPSCs (mEPSCs) were recorded in the same area of the hippocampus, and the spontaneous activity of the network was eliminated by adding the voltage-gated sodium channel inhibitor tetrodotoxin (TTX).

We investigated the potency of the Schaffer collateral to CA1 synapses to long-term potentiation (LTP) in response to theta-burst stimulation. The stimulating and recording electrodes were placed in the field of CA1 pyramidal neurons dendrites at equivalent distance from the cell soma and at approximately 500 μm from each other. The stimulation was of 100 μA for 600μs. After the recording of the baseline transmission for 10 minutes (stimulation at 0.1 Hz), theta-burst stimuli (TBS) were applied. These were composed of bursts of 4 pulses at 100 Hz, given 5 times and interspaced 200 milliseconds. This sequence was looped four times with 20 s interval. Then, the transmission was recorded for 60 min (at 0.1Hz).

All the recordings were made using an EPC 9.0 or EPC 8.0 amplifier (HEKA Elektronik, Lambrecht/Pfalz, Germany), filtered at 0.5-1 kHz, digitized at 1-5 kHz and further analyzed with IGOR (IGOR PRO 6.37, WaveMetrics, Lake Oswego, OR, USA).

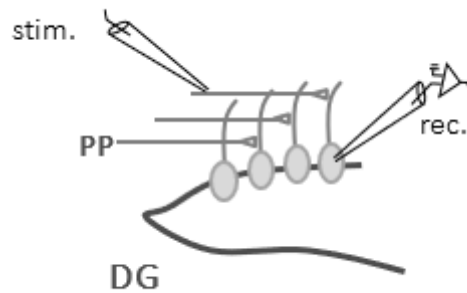


**FIGURE 19** Schematics of the protocol used to record the excitatory inputs from the perforant path to the dentate cells.

#### 14. Statistical Analysis

Quantification of WB analysis was performed by means of computer-assisted imaging (ImageLab, Biorad). The levels of the proteins were expressed as relative optical density (OD) measurements and normalized on actin or tubulin. Levels and values were analyzed using GraphPad Prism 7 software (GraphPad Software, La Jolla, CA, USA) and expressed as mean  $\pm$  standard error of the mean (SEM). Statistical evaluations were performed by Student *t* test or, as appropriate, by one-way ANOVA followed by Bonferroni's as a *post hoc* test.

# RESULTS

## 1. Genotypic confirmation of RNF10

To confirm the genotype of the animals that we received from the Knockout Mouse Project (KOMP) Repository (UC Davis), we first used the commercially available antibodies for RNF10. Unfortunately, all tested antibodies did not work properly in the recognition of RNF10 specific band by western blotting analysis. To overcome this difficulty, we used two approaches: immunocytochemistry and PCR.

In the immunocytochemistry (**Figure 20**), with RNF10 stained in red, we can observe the obvious absence of the expression of this protein in the KO model (right panel) in the CA1 region of the hippocampus of mice brain, in comparison with the presence of the protein in the WT model (left panel).

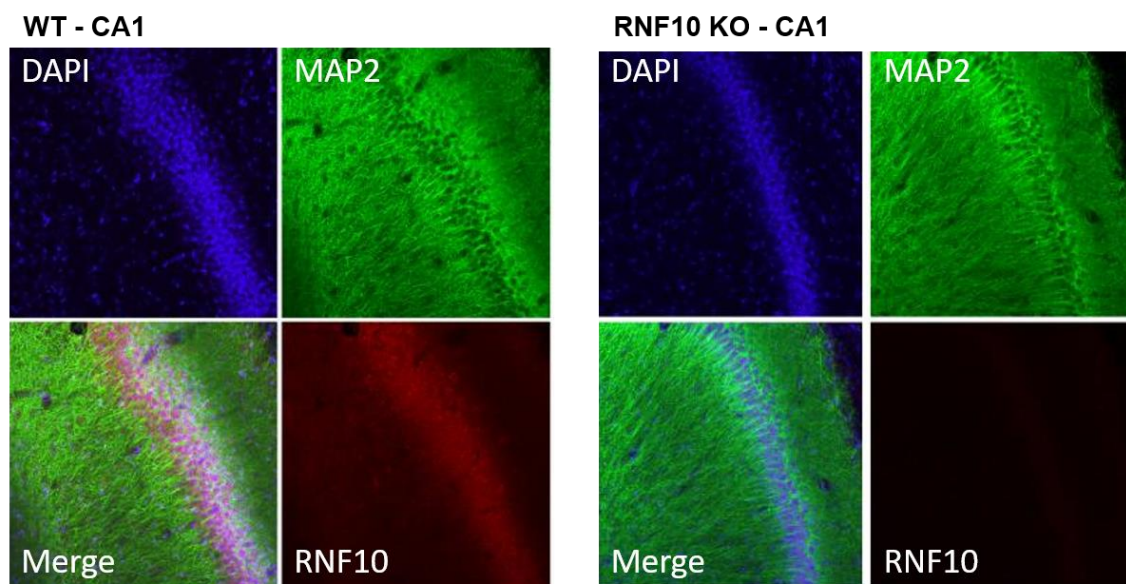


**FIGURE 20** Immunocytochemistry of the CA1 region of the hippocampus in RNF10 KO and WT mice. Observing the lower RNF10 panel, it is possible to see that RNF10 KO mice do not express this protein, in comparison with the WT animals.

Moreover, these results were further confirmed by quantitative PCR technique (**Figure 21A**) used to quantify RNF10 expression. As shown in **Figure 21A**, RNF10-KO animals present close to null expression of the gene, being significantly decreased in comparison with WT animals. In addition, to perform a detailed genotypic assessment after the colony was set in our facilities, we used the PCR technique, in combination with electrophoresis to evaluate whether the animal presented the WT band at 307 bp, the KO band at 746 bp or both, being this way a heterozygous (HE) (**Figure 21B**).

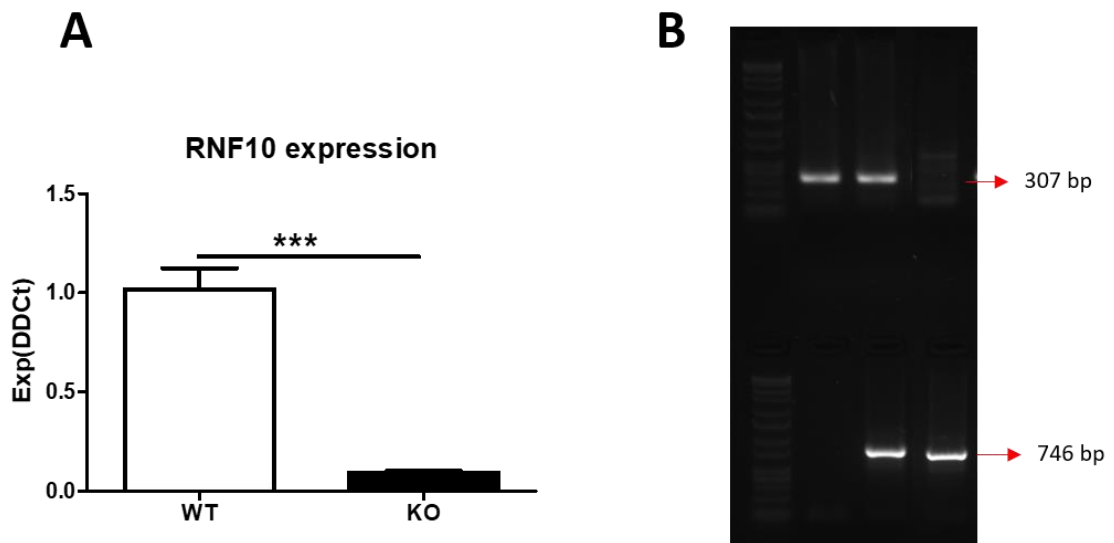


**FIGURE 21 Determination and confirmation of RNF10 genotype.** (A) Quantitative PCR for RNF10 expression. KO animals present a significant decrease in the expression of this protein. (B) An example of the detected bands after the PCR, 307 bp for WT and 746 bp for the transgenic; having both bands represents a heterozygous animal (*t*-test, \*\*\*  $p < 0.001$ ).

## 2. RNF10 KO animals have lower body weight and increased food intake

Proceeding with the characterization of the KO animals, we monitored their body weight. As presented in **Figure 22A**, adult homozygous (KO) animals present significantly reduced body weight in comparison with both WT and heterozygous (HE) animals. Conversely, no alterations were found in HE animals compared to WT. As we can observe in **Figure 22B**, KO are visually smaller and slimmer in comparison with the WT, thus confirming the previous result.

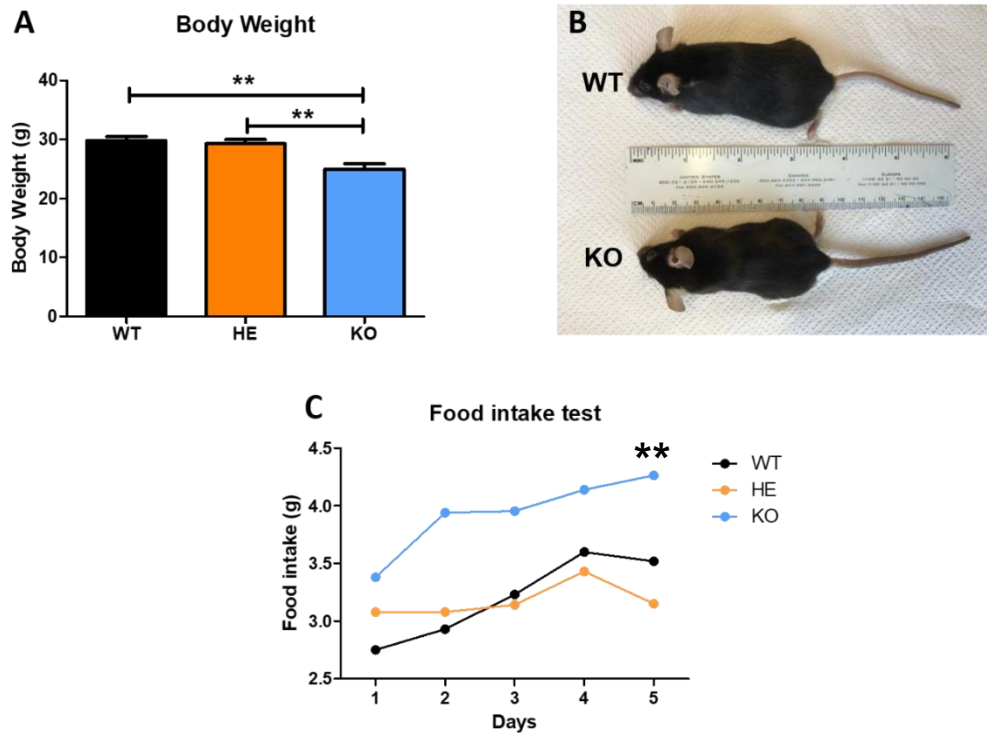


**FIGURE 22 Assessment of body weight and food intake of the animals.** (A) KO animals present a significant decrease in their body weight in comparison with both WT and HE animals, being visually smaller and leaner than the WT (B). (C) KO animals have a higher food intake in comparison with both WT and HE animals (ANOVA, \*\*  $p < 0.01$ ).

### 3. Metabolic studies in RNF10 KO animals

As mentioned in the introduction, a recent paper found a connection between RNF10 and metabolic syndrome (Yu et al. 2018). Accordingly, we hypothesized that the difference in body weight could be present because these animals have a different feeding behavior (**Figure 22C**). Surprisingly, KO animals display a higher food intake behavior in comparison with both WT and HE animals. Again, no significant alterations also of food intake was observed between HE and WT animals. Since HE did not show a significant phenotype in any of the assessed tests, from this point we decided to focus the presentation of the results exclusively in the direct comparison between WT and KO animals.

The results above described led us to consider other possible alterations in metabolism features, such as basal temperature, total glucose, insulin and FGF-21 levels (**Figure 23**). Fibroblast growth factor 21 (FGF-21) is an endocrine hormone, that plays an important role in the regulation of metabolism, being induced in the liver in response to

fasting and other forms of metabolic stress (Sa-nguanmoo et al. 2016; Talukdar et al. 2015).

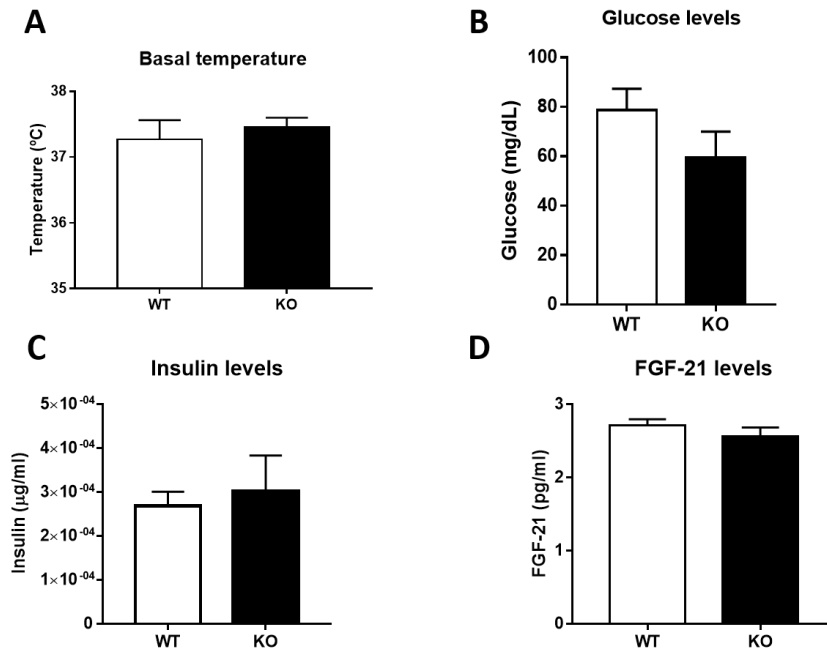


**FIGURE 23** Measurements of basal temperature (A), total glucose levels (B), and insulin (C) and FGF-21 (D) by ELISA. There are no differences in any parameters between WT and KO animals.

As shown in **Figure 23**, there are no differences concerning basal body temperature (A), nor total glucose levels (B) in KO animals compared to WT. Using blood samples from both WT and KO animals, we ran ELISA tests in the insulin and FGF-21 proteins. Observing in **Figure 23C**, there are no significant differences in what concerns the insulin levels, nor differences in the FGF-21 as seen in **Figure 23D**. Although this data could come as conclusive by itself, we took a step further by assessing in more depth the metabolic variations. Starting from the hypothesis that these animals could present differences in glucose or insulin processing and clearance, we tested the animals in both glucose and insulin tolerance tests (**Figure 24**).

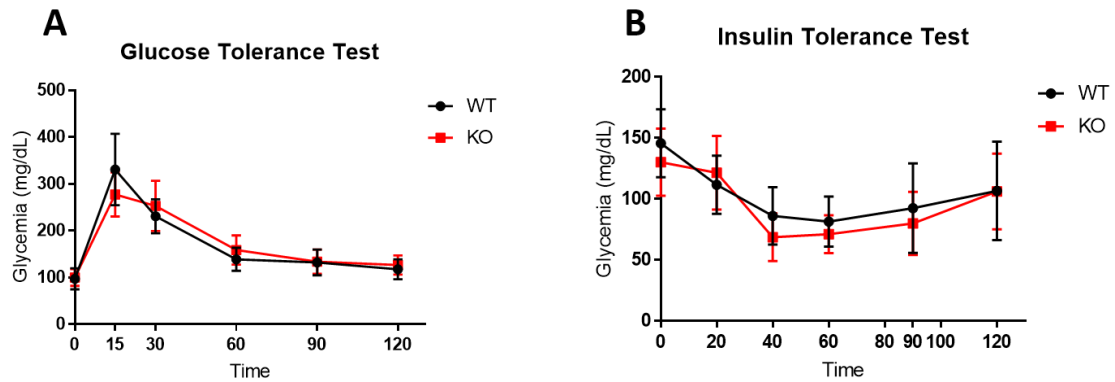


**FIGURE 24 Glucose (A) and Insulin (B) Tolerance tests.** No alterations were observed in either one of these tests, considering both genotypes.

As we can observe in the **Figure 24** above, KO animals do not present any differences concerning to the WT in the two tolerance tests. Put together, these results prove that KO animals do not present main metabolic differences in the periphery, nor on basic metabolic pathways.

#### 4. KO animals show altered spine morphology in the hippocampus

As shown in **Figure 25**, RNF10-KO animals present differences in the volume in several different areas of the brain, particularly in the hippocampus, where the CA1 volume looks significantly reduced in comparison with the WT animals (in collaboration with Binnaz Yalcin, IGBMC, France).

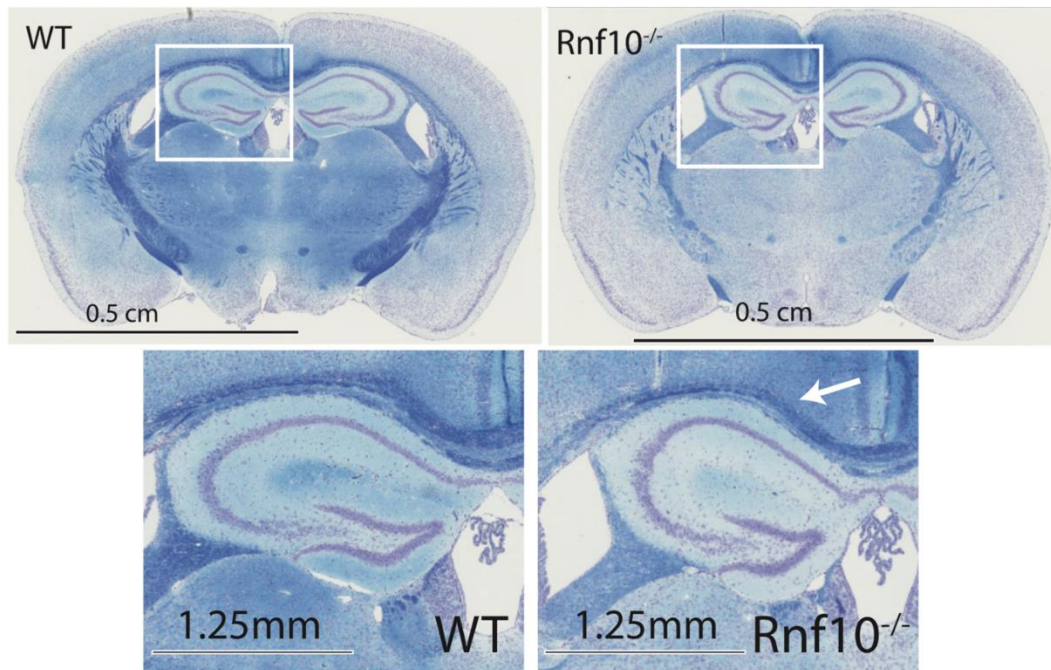


**FIGURE 25 Immunohistochemistry in brain slices of WT and KO animals.** KO animals present differences in several areas of the brain, most notably in the hippocampus, where CA1 seems visibly smaller than in WT animals.

Observing **Figure 25**, KO animals display some evident differences in the morphology of the brain. In addition, our group previously showed that RNF10 plays a fundamental role in regulating dendritic spine density (Dinamarca et al. 2016) in primary hippocampal neurons: it was found that RNF10 silencing in slices produced a significant reduction in dendritic spine density without affecting the dendritic spine morphology. Accordingly, we hypothesized that RNF10 KO mice would also show differences at cellular level once we looked in the hippocampus at the neurons and the spines.

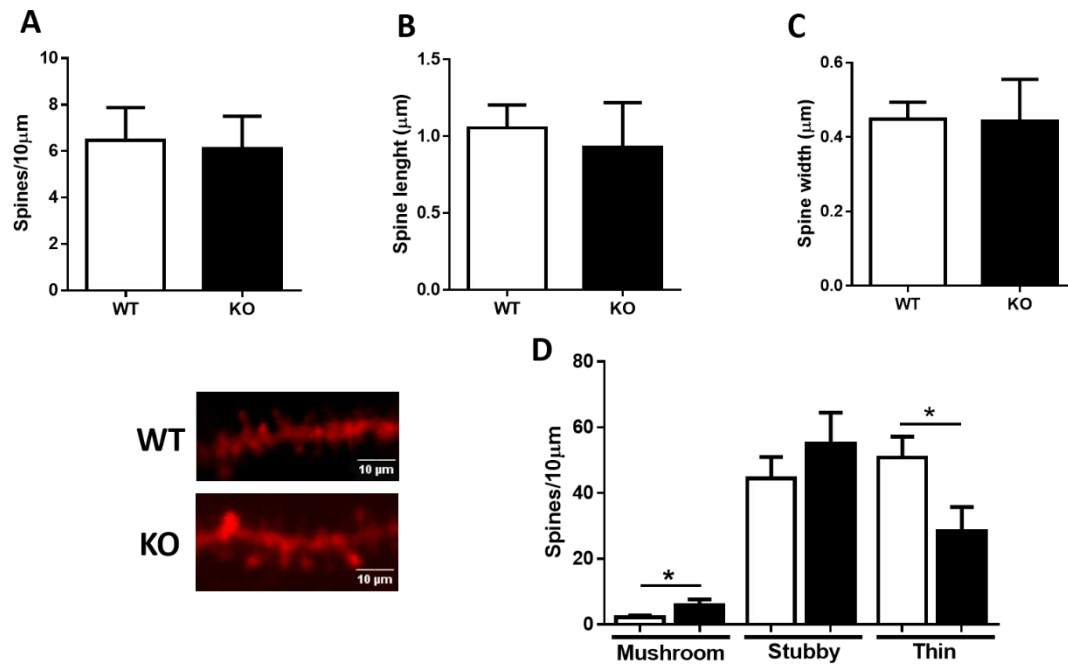


**FIGURE 26 Spine morphology count and categorization results.** RNF10 KO do not show any difference in the total density of spines (A) nor in the spine length (B) or spine head width (C). There is a significant increase in the percentage of mushroom-type spines and a significant decrease in the thin spines in the KO animals (D) in comparison with the WT animals (ANOVA,  $p < 0.05$ ).

As we can see in **Figure 26**, RNF10 KO mice do not show any difference in the total density of spines (**Figure 26A**), nor in the spine length (**26B**) or spine head width (**26C**). However, there is a significant increase in the percentage of mushroom-type spines in knockout animals and a significant decrease in the thin type spines, in comparison with the WT animals (**26D**).

### 5. KO animals display differences in the molecular composition of the synapse

A previous study from our group indicated that RNF10 is enriched at the synapse where it interacts with the NMDA receptor complex (Dinamarca et al. 2016). Moreover RNF10 silencing in cultured hippocampal neurons induced a significant decrease in several key PSD proteins such as PSD-95, the GluN2A subunit of the NMDA receptor and the GluA1 subunit of the AMPA receptor (Dinamarca et al. 2016). Starting from this previous data, we decided to test the levels of main PSD proteins (**Table 2**) in RNF10 KO mice. Moreover, we analyzed the levels of selected RNF10 target genes (Dinamarca et al., 2016) and key proteins involved in APP processing and AD pathogenesis (**Table 2**).

**TABLE 2** All proteins assessed in the molecular characterization, in both total brain and hippocampus.

Synaptic processes	GluN2A	Gene regulation	p21	AD pathogenesis	APP
	GluN2B		Oligophrenin-1		ADAM10
	GluA1		$\alpha$ PIX/ArhGef6		BACE-1
	phospho-GluA1		ArhGap4		phospho-Tau
	PSD-95				

For that, we started with a very broad characterization, collecting brain samples from WT and RNF10-KO young adult mice. After tissue fractionation, a homogenate and a triton insoluble postsynaptic fraction (TIF) were obtained, and subsequently tested by western blotting analysis.

In this broad total brain assessment, all AD-related proteins tested displayed no significant differences besides ADAM10 in the homogenate (Figure 27).

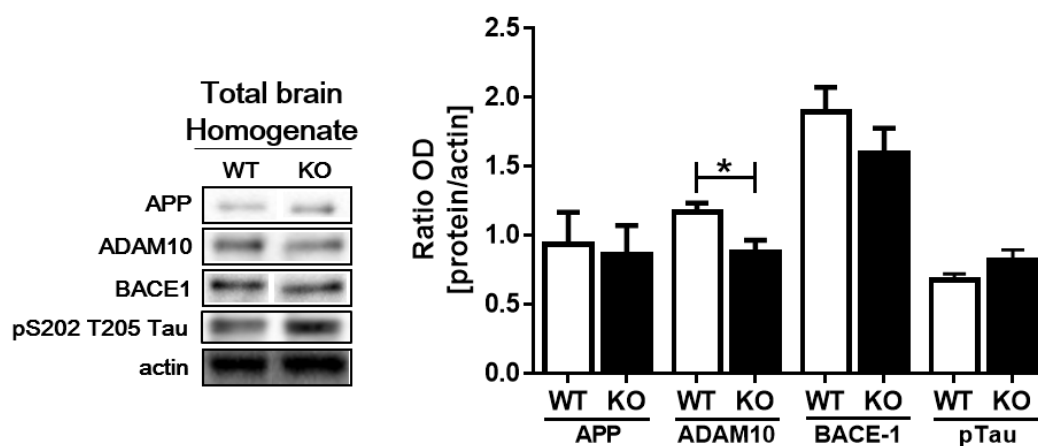


**FIGURE 27** Western Blot assessment in proteins involved in AD pathogenesis. KO animals present a significant decrease in ADAM10 levels in the homogenate in total brain, in comparison with WT animals (ANOVA,  $p < 0.05$ ).

Taking into account that, as shown in Figure 25, one of the most striking morphological differences was found within the hippocampus, we moved to the analysis of the proteins summarized in Table 2, not in total brain but in the hippocampus. Particularly, we evaluated proteins involved in the synaptic processes (Figure 28), RNF10 target genes (Figure 29) and in the A $\beta$  cascade (Figure 30).

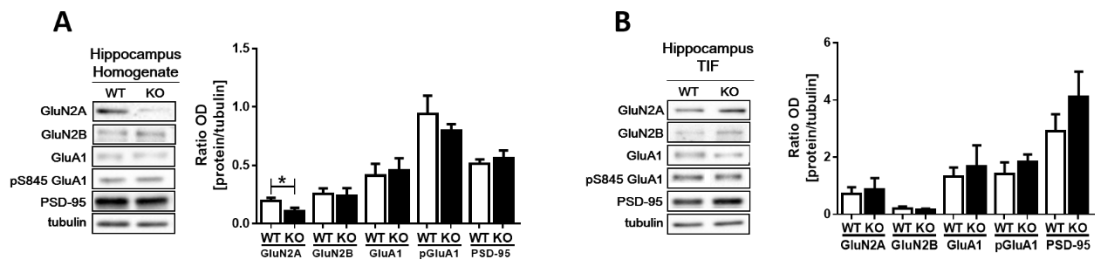


**FIGURE 28 Western Blot analysis of the synaptic proteins in the hippocampus.** Looking at the hippocampus, only GluN2A in the KO animals presents a significant decrease in comparison with WT animals (A) and observing more specifically the TIF fraction (B), there seems to be no significant difference in any of the analyzed proteins (ANOVA,  $p < 0.05$ ).

The quantitative analyses show a significant decrease in the Glu2A in the hippocampal homogenate (Figure 28A), with no alterations in the remaining synaptic proteins. Conversely, no differences in any of the evaluated proteins were observed in the TIF fraction (Figure 28B).

It is known that the RNF10 translocation to the nucleus leads to its binding to Meox2 and it stimulates the expression of the target genes such as  $p21^{WAF1/cip1}$  (Dinamarca et al. 2016), so we looked at the levels of this protein.  $p21^{WAF1/cip1}$  presents a slight tendency to decrease in the KO animals, as observed in Figure 29, but it's not effectively significantly different from the levels in WT animals.

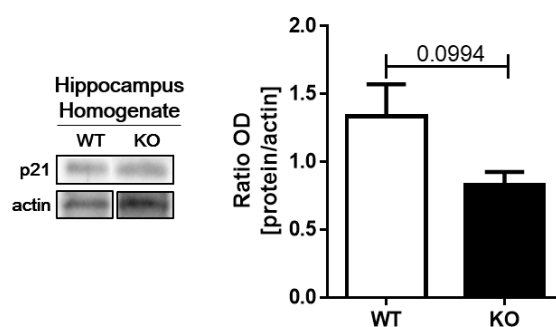


**FIGURE 29 Western Blot on the target gene of RNF10.** There is a tendency to a decrease in the KO animals, even though it's not significant.

As previously mentioned, RNF10 trafficking was found to be regulated by  $A\beta$ , promoting its synapse to nucleus signaling (unpublished observations). Starting from this preliminary data, we checked if RNF10-KO mice present differences in the levels of

proteins involved in A $\beta$  production, as ADAM10, APP and BACE-1 in homogenate (Figure 30A) and TIF (Figure 30B).

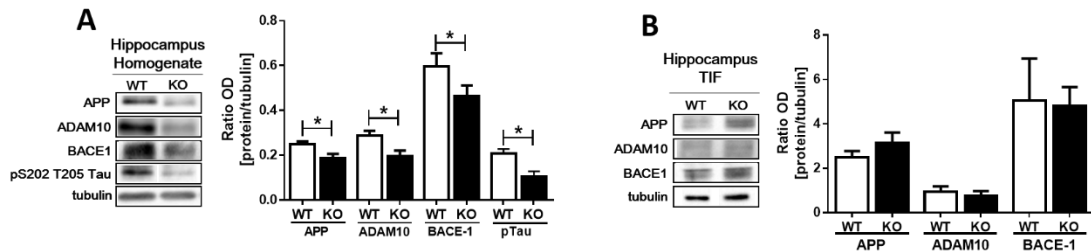


**FIGURE 30 Western Blots in the proteins involved in AD pathogenesis in the hippocampus.** While in the homogenate (A) all proteins are significantly decreased, in the synaptic fraction (B), these differences are not observed any longer (ANOVA,  $p < 0.05$ ).

As we can observe in Figure 30A, all tested proteins involved in the APP processing are significantly reduced in the homogenate from KO mice in comparison with the WT. A significant decrease was also observed in the phosphorylated Tau protein (Figure 30A). No alteration was seen in the synaptic fraction (Figure 30B).

Since we are observing proteins involved in synaptic processes, we also checked CREB in the hippocampus homogenate, which activation and role in long-term forms of synaptic plasticity and formation of long-lasting memories is well known (Benito & Barco 2010) (Figure 31A).

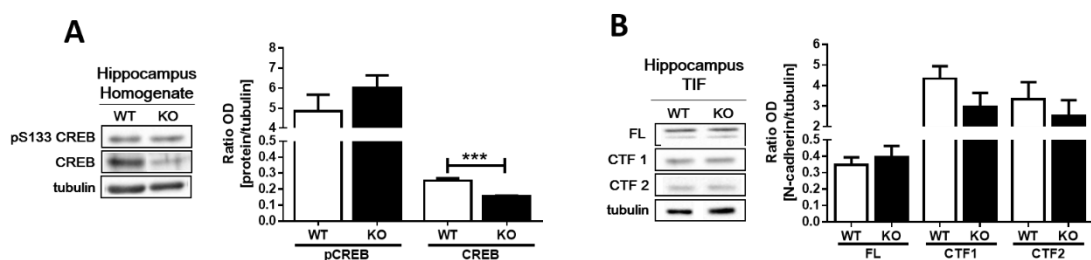


**FIGURE 31 Western Blot in a synaptic plasticity protein and in an adhesion molecule cleaved by ADAM10.** We observe significant differences in the total CREB protein (A), whereas we could not see any differences in N-cadherin full length or soluble fragments (B) (ANOVA,  $p < 0.001$ ).

The significant reduction observed in total CREB observed in Figure 31A can, in firsthand, hypothesize some impairment in synaptic plasticity and function, whereas the phosphorylated form remains unaltered in comparison with the WT animals. We also

tested N-cadherin in the hippocampus synaptic fraction. The full length N-cadherin is cleaved specifically by ADAM10 in its ectodomain, generating a fragment called CTF1, that can be further processed by a  $\gamma$ -secretase into a second fragment termed CTF2 (Reiss et al. 2005). Since we've seen alterations in ADAM10 in **Figure 30**, we hypothesized possible differences in N-cadherin shedding, but although the rationale could be applied, we could not find any differences in N-cadherin neither in full length nor in any of the soluble fragments, as seen in **Figure 31B**.

## 6. KO animals show a decreased level of A $\beta$ in the hippocampus

Considering the results observed in **Figure 30**, showing alterations of the proteins involved in the A $\beta$  cascade, we performed an ELISA test to quantify A $\beta$  in the hippocampus (**Figure 32**).

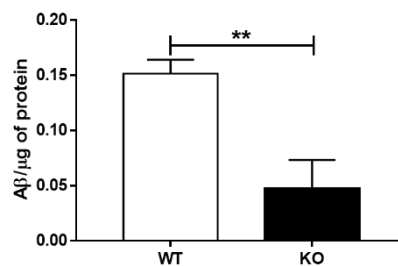


**FIGURE 32 ELISA performed to detect amyloid-beta in the hippocampus.** We observed a significant decrease of A $\beta$  in the KO animals in comparison with the WT animals (*t*-test,  $p < 0.01$ ).

As we can see in **Figure 32**, and in agreement with the results presented in **Figure 30A**, A $\beta$  is significantly reduced in the hippocampus of KO mice compared with the WT animals, reinforcing the possible role for RNF10 in Alzheimer's disease, as previously hypothesized.

## 7. KO animals do not present any difference in the locomotion

We performed a general behavioral characterization of the model, assessing several parameters as locomotion, cognition and memory. Taking into account the above-described preliminary results about a possible role of RNF10 in AD, which onset appears in the later stages in age, we used adult (6-months old) and aged (18-months old) mice in the tests.

We started by evaluating the locomotion using the Rotarod and the Accelerated Rotarod in the adult animals (**Figure 33**) and in the aged animals (**Figure 34**).

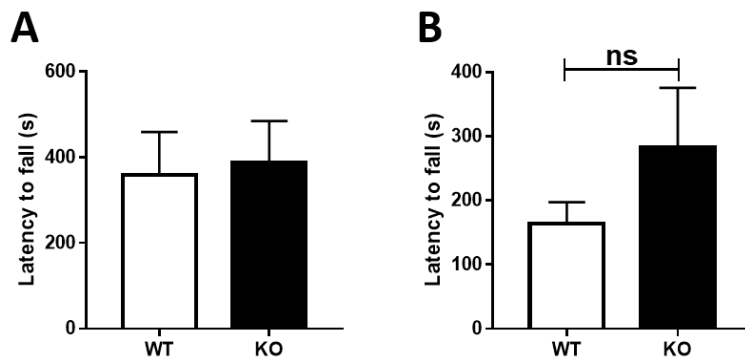


**FIGURE 33 Rotarod and Accelerated Rotarod testing in adult 6-months old animals. (A)** There are no differences between WT and KO animals in rotarod test, nor in the accelerated test **(B)**.

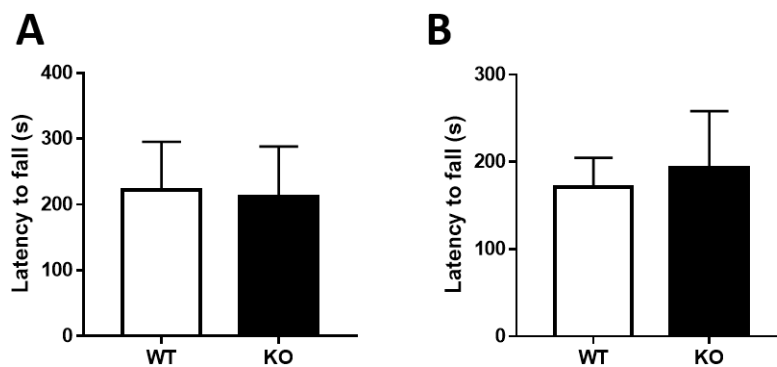


**FIGURE 34 Rotarod and Accelerated Rotarod testing in aged 18-months old animals. (A)** There are no differences between WT and KO animals in rotarod test, nor in the accelerated test **(B)**.

As we can see in **Figures 33** and **34**, WT and KO animals present no differences concerning the normal, steady speed rotarod test (**A panels**). As for the accelerated rotarod (**B**), even though there is a high variability in the KO animals at 6-months old, in comparison with the WT, these animals also do not present any significant differences. At 18-months old animals, the results do not show any differences, leading us to conclude that RNF10 KO animals present a normal locomotion.

## 8. [KO animals display slightly altered exploratory behavior](#)

To evaluate the exploration and cognitive performance of these animals, we performed a Y-Maze test in both ages (**Figure 35**). This behavior test measures the

willingness of rodents to explore new environments, as they will typically prefer to visit and explore a new arm of the maze instead of returning to the previously visited ones, a task that involves several areas of the brain, including the hippocampus.

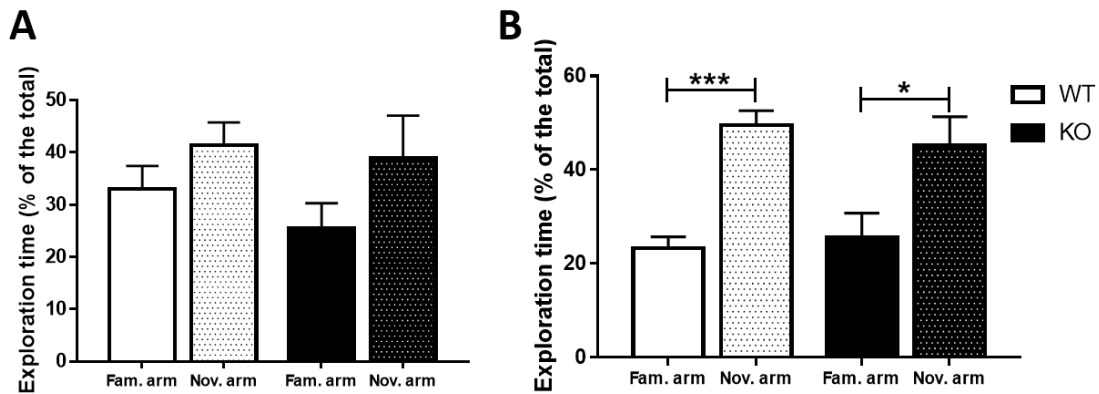


**FIGURE 35 Testing the exploratory activity in a Y-Maze test. (A)** In adult animals, there are no significant differences between the exploration of the familiar and novel arm, nor in between genotypes while in **(B)**, aged animals explore significantly more the novel arm than the familiar, with KO animals showing a slightly less tendency to explore the novel arm when compared to the WT animals (ANOVA, \*  $p < 0.05$ ; \*\*\*  $p < 0.001$ ).

As observed in **Figure 35A**, in adult mice both WT and KO animals explore more the novel arm than the familiar, as expected, even though this exploration is not significantly different between both arms, nor when comparing one genotype to the other (between both arms  $p = 0.3541$ ; between WT familiar and KO familiar  $p = 0.7862$ , between WT novel and KO novel  $p = 0.9908$ ). In **Figure 35B**, we observe that in aged animals the difference between the exploration of the familiar arm and the novel arm turns significant both in WT and KO animals, with an increase in the percentage of time exploring the novel arm for both genotypes. When this is compared between both genotypes, even though they are both effective, the significance in the KO is slightly lower than in WT animals.

### 9. [KO animals display impaired long memory functionality](#)

To further confirm and explore the results seen in the Y-Maze, we tested the same animals in another memory-associated test, the novel object recognition test (NORT) (**Figure 36** and **37**). As mentioned previously, this test is based in the innate preference of the animal to explore the novel object in detriment of the familiar one, specifically evaluating cognition and the recognition memory.

First, the animals were presented with two equal objects, in the familiarization phase of the test, in which their exploration was equally distributed in both objects, in both WT and KO animals (data not shown). After 2 hours, one of the objects was changed to a novel object and the animals were tested again (Figure 36).

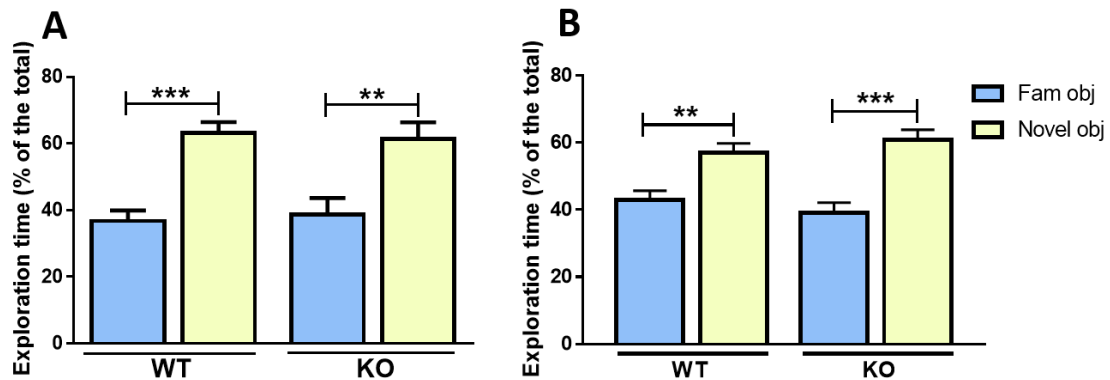


**FIGURE 36 NORT 2 hours after familiarization in adult and aged WT and RNF10 KO mice. (A)** In adult stages, both WT and KO animals favor the novel object towards the familiar object, and the same behavior is observed in aged animals (B) (ANOVA, \*\*  $p < 0.01$ ; \*\*\*  $p < 0.001$ ).

In Figure 36A, we can observe that 2h after familiarization, both WT and KO adult animals have a significantly higher percentage of exploration time in the novel object in detriment of the familiar object. Accordingly, we do not see any differences between genotype. The same is true in the aged animals (B), with KO animals performing slightly better in comparison with the WT animals. This protocol was used as means to assess a “short term” type of memory, with us concluding that these animals do not show problems in this parameter.

We then proceeded to the “long term” memory assessment, where 24h after the familiarization we change the novel object into another novel object, different than the previous, and test the animals on their preferences (Figure 37).

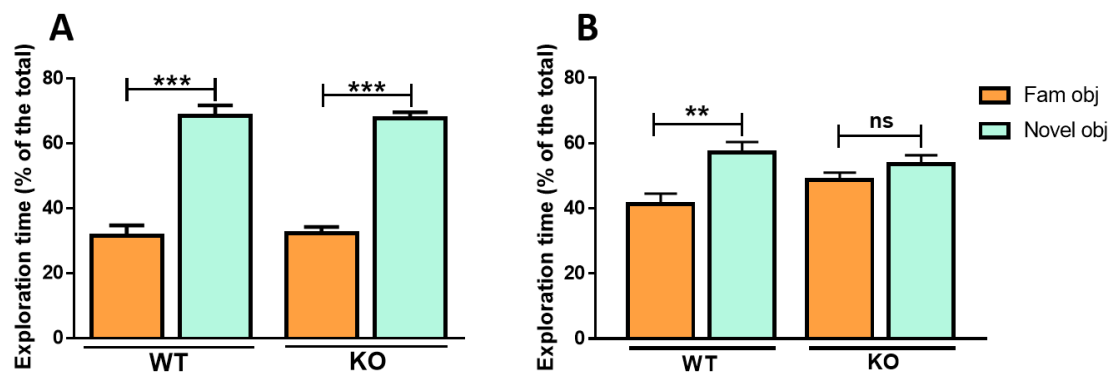


**FIGURE 37 NORT 24 hours after familiarization in adult and aged WT and RNF10 KO mice. (A)** In adult stages, both WT and KO animals favor the novel object towards the familiar object just as observed in the previous figure, but in aged animals **(B)**, only WT animals maintain the same preference, while KO animals lose this phenotype (ANOVA, \*\*  $p < 0.01$ ; \*\*\*  $p < 0.001$ ).

Looking at the **Figure 37** above, panel **A** show us that in adult animals, both WT and KO are still capable of recognizing the familiar object and thus prefer to explore the novel object instead. However, observing panel **B**, in aged animals, KO animals do not display any significant difference in the preference between the familiar object and the novel object, unlike WT animals, hence suggesting that these animals might have some cognitive impairment.

#### 10. KO animals present normal basal synaptic transmission

We characterized excitatory inputs to GC of the dentate gyrus in hippocampal slices from 21 to 50 days-old mice using the whole-cell recording technique (**Figure 38A**). Electrical stimulation of the perforant path evoked in GC short latency excitatory post-synaptic currents (EPSCs) that were composed of both N-methyl-D-aspartate (NMDA) and alpha-amino-3-hydroxy-5-methyl-4-isoxazole-propionate (AMPA) currents (**Figure 38B**). To isolate the recordings of NMDA, recorded at +30 mV, we used NBQX (2,3-dihydroxy-6-nitro-7-sulfamoyl-benzo[f]quinoxaline), an AMPA receptor antagonist.

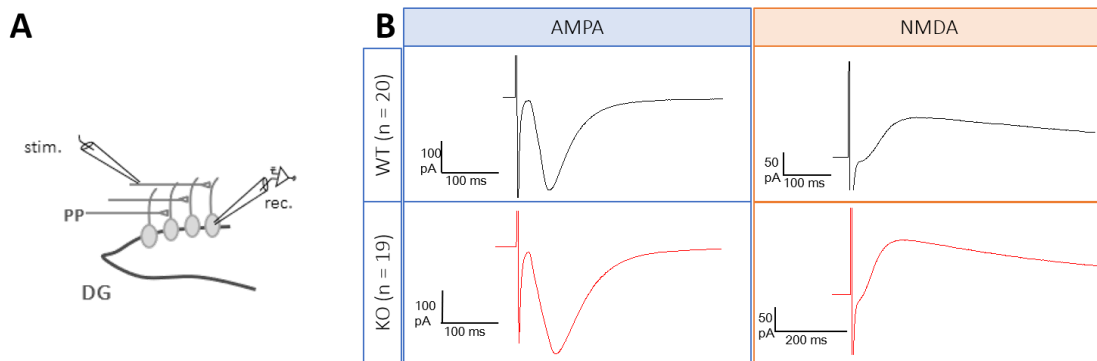


**FIGURE 38 Electrophysiology model used to record EPSCs.** (A) We recorded currents placing the stimulating electrode in the projections from the medial entorhinal cortex and the recording electrode in the granule cells in the dentate gyrus. (B) Example of an AMPA (left) and NMDA (right) current, in WT (upper) and KO (lower) animals: average traces representing EPSCs recorded while holding cells at negative (-70 mV) and positive (+30 mV) membrane potentials.

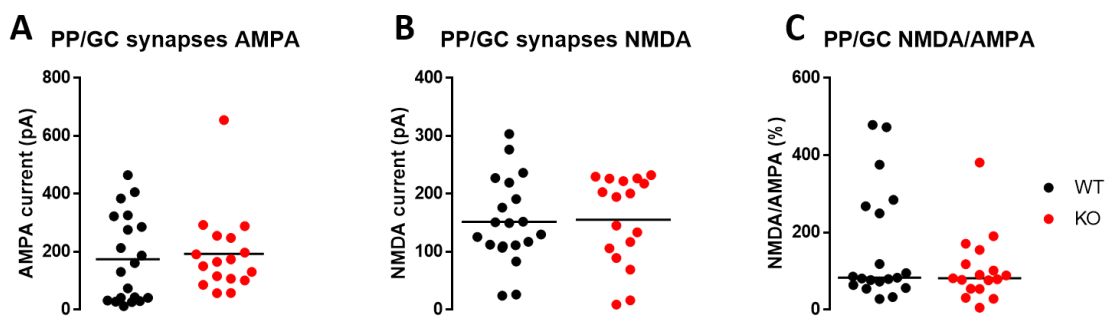


**FIGURE 39 Results of the electrophysiological studies.** First graph (A) corresponds to the AMPA current measurements, second (B) to the NMDA current measurements and (C) represents the ratio NMDA/AMPA. No alterations were observed in any of the graphs.

As seen in **Figure 39**, RNF10-KO and WT animals have very similar AMPA (A) and NMDA (B) currents and, consistently, an identical ratio NMDA/AMPA (C). This means that the relative contribution of AMPA and NMDA in this synapse is not altered in basal condition. We also assessed the kinetics of the currents, by measuring the decay time (**Figure 40**) in patch-clamp experiment. The decay time usually refers to the inactivation of excitatory or inhibitory post-synaptic currents or potentials under voltage- or current-clamp, respectively. In this case, as mentioned before, we look at excitatory post-synaptic currents.

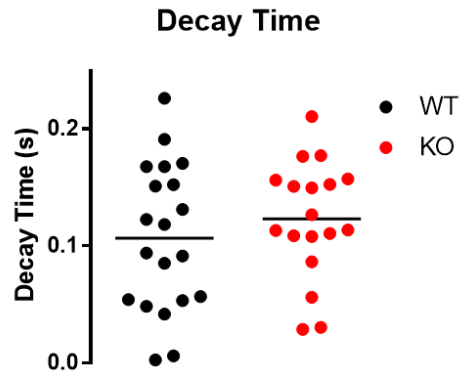


**FIGURE 40 Decay Time Measures in WT and KO in NMDAR currents.** We observe no differences in decay time between WT and KO animals.

As we can observe in **Figure 40**, there are no differences in the decay time of NMDA currents between WT and KO animals, indicating that the interval between the peak and 90% of the decaying phase is no different between genotypes.

We then analyzed the miniature EPSCs in both genotypes, assessing different parameters as the frequency and the amplitude of the currents (**Figure 41**). To eliminate the spontaneous activity of the network, tetrodotoxin (TTX) was added to the circulating ACSF. There are several reasons why the frequency of the mEPSCs could be altered: an increase/decrease in the total number of synapses, an increase/decrease in the size of the readily releasable pool of synaptic vesicles or an increase/decrease of neurotransmitter release. A change in the presynaptic release mechanisms is manifested as an increase in the frequency, while a change in the postsynaptic receptor expression or function would display an increase in the amplitude.

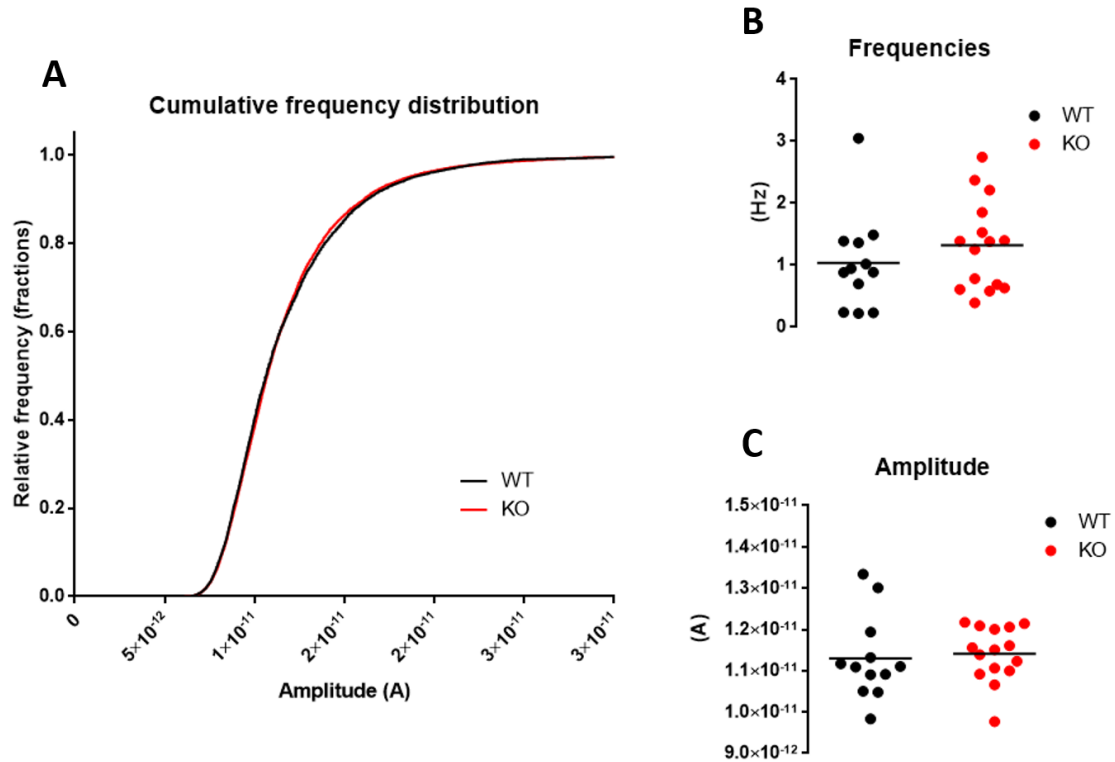


**FIGURE 41 Miniature EPSCs measurements.** We do not see any difference concerning the cumulative frequency (**A**) of the currents, nor in the frequency (**B**) or amplitude (**C**) between WT and KO animals.

As shown in **Figure 41**, none of the referred parameters is altered between WT and KO animals: there are no differences between the frequency of the mEPSCs (**B**) nor in the amplitude of the same (**C**). Given our results, we can conclude that the postsynaptic response to spontaneous fusion of a single synaptic vesicle is not different between WT and KO animals.

We then performed field LTP recording in the CA1 area of the hippocampus, stimulating the Schaffer collateral projections from the CA3 area and recording in the CA1 dendrites, using the theta burst stimulation (TBS) protocol. This protocol is an effective stimulus as the induction of LTP in field CA1 by high frequency stimulation bursts resemble the burst discharges (complex-spikes) of hippocampal pyramidal neurons (**Figure 42**).

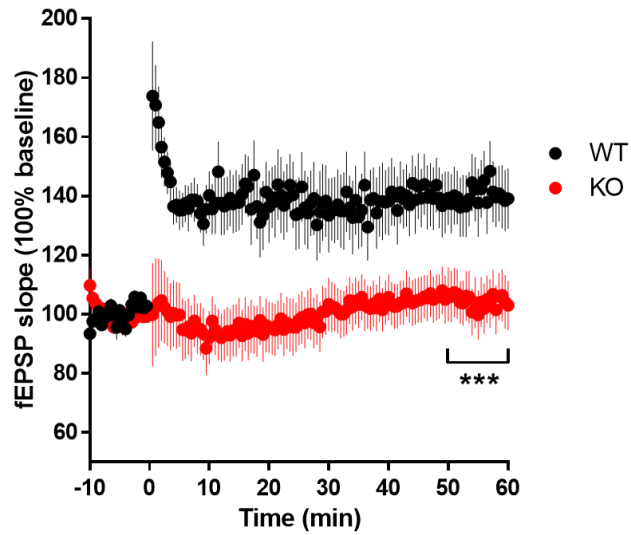


**FIGURE 42 Induction of LTP by theta burst stimulation the CA1 area of the hippocampus.** As we can observe, KO animals display a complete abolition of the LTP in this area of the brain, in comparison with the WT animals.

In **Figure 42**, we can observe that KO animals not respond to the stimulation, displaying a complete abolition of the LTP in the CA1 area of the hippocampus.

# DISCUSSION

Understanding how fast events at synapses are converted into long-lasting changes of neuronal activity is a very important query in neuroscience. Several recent studies demonstrated that synapses and nuclei are linked by bidirectional communication routes that enable the efficient transfer of information and regulate the long-term structural changes of neuronal function.

Over the last years, synapse-to-nucleus proteins have been gaining more relevance, as their mechanisms and roles are more understood, while their associations and implications with several diseases are brought to light. In particular, recent studies indicate a possible direct involvement of synaptonuclear messengers in several diseases, as well as the probable implications that the disturbance of their communication routes have in neurodegenerative diseases, such as Alzheimer's or Parkinson's disease. As mentioned before, synaptonuclear messengers such as Jacob, AIDA-1 or CRTC1 have recently been shown to have implications in these diseases (for further, see **Introduction pages 31 to 38**).

RNF10 has been recently associated with Fragile X syndrome, where there is a strong deregulation of RNF10 expression in male carriers of the *fmr1* premutation and in a mouse model of a Fragile X associated Tremor/Ataxia Syndrome (Mateu-Huertas et al. 2014).

The putative role of RNF10 in a neurodegenerative disease was firstly suggested from preliminary data of our laboratory showing that amyloid-beta promotes the translocation of RNF10 from the dendritic spines to the nucleus (**Figure 43**) and that RNF10 shows to be significantly reduced in patients with AD in confirmed Braak IV and V stages, in comparison with healthy controls (**Figure 44**).

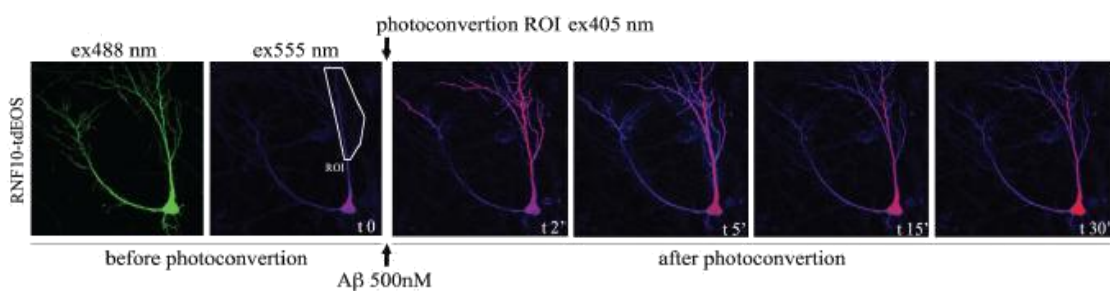


**FIGURE 43** A $\beta$ 42 treatment induces RNF10-tdEOS translocation from distal dendrites to the nucleus in hippocampal neurons. **2 left panels:** Baseline confocal image of RNF10-tdEOS expressing hippocampal neuron illuminated sequentially with 488nm and 555nm laser excitation wavelengths showing no emitted signal in the red spectra. Distal dendrite (ROI)

selected for photoconversion was illuminated with UV laser (405nm wavelengths) repetitively through the image z-stack. **Right panels:** confocal max intensity projection images at respective time points in control after A $\beta$ 42 treatment neurons. (Musardo S, Doctoral thesis, unpublished data).

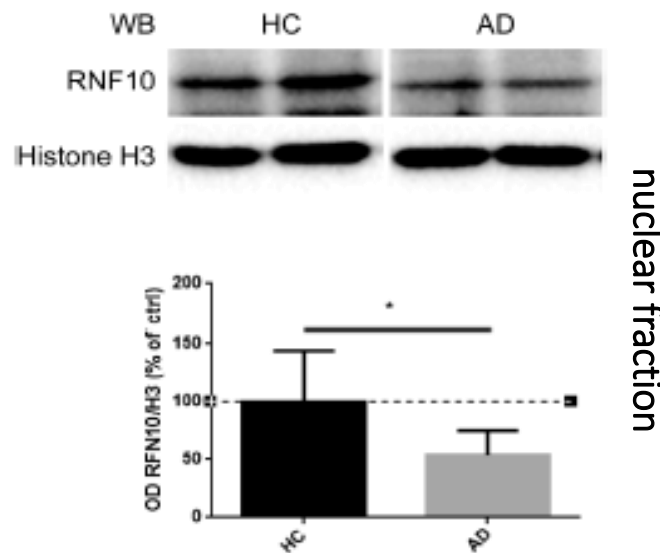


**FIGURE 44 RNF10 expression and localization are affected in AD patients.** Representative immunoblot of nuclear fraction of autaptic specimens of hippocampi obtained from 6 AD patients, fulfilling Braak 4 and 5 stage, and 6 aged-matched healthy control (HC). Quantitative analysis reveals that in AD patients there is a significant decrease of nuclear localization (HC 100%±17.87, AD 54.11%±8.505% \* $p$ <0.05) (Musardo S, Doctoral thesis, unpublished data).

From the results presented in this thesis, we can observe an interesting phenotype in the RNF10 KO mice, with a significative relevance within different fields. RNF10 KO mice present a decrease in body weight and body size in comparison with WT animals, while displaying an increase in food intake, suggesting a possible role for this protein in the metabolism. Indeed, RNF10 has been reported to have an unknown role in weight regulating pathways, and to be associated with adiposity and nominally increased risk for type 2 diabetes (Huang et al. 2014). Despite this relation, the absence of any significant alteration in the glucose levels and tolerance test, as well as insulin levels and tolerance, suggest a more restrained and yet to identify role in a more specific pathway. Our effort to correlate metabolic alterations in this mouse model also led us to look at FGF-21, a hormone that is associated with the preference for sweet foods via signaling through the receptors in the hypothalamus (Talukdar et al. 2015). Despite our results not indicating

any differences concerning this hormone, the complexity of the network and pathways that are involved (Figure 45) could possibly lead us to extend our studies to a more broaden field. Overall, performing additional behavioral tests such as a sucrose preference test would address this question to a better extent, and possibly provide us some additional information in the matter.

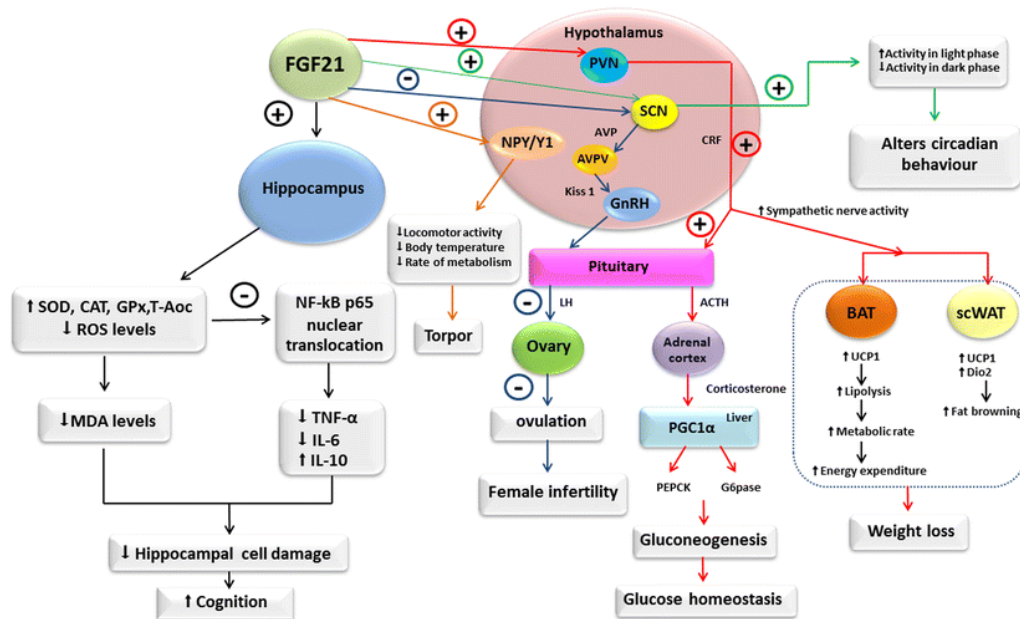


**FIGURE 45** Represents the effects of FGF21 on the brain. The *red arrow* suggests that the direct activation of FGF21 in the paraventricular nucleus (PVN) leads to increased levels of corticotrophin releasing factor (CRF) and increased sympathetic activity to brown and white adipose tissues, resulting to body weight loss. In addition, an increase in CRF activates the pituitary gland, leading to increase hepatic gluconeogenesis during prolonged fasting to prevent hypoglycemia. The *green arrow* suggests that the direct activation of FGF21 in the suprachiasmatic nucleus (SCN) subsequently alters circadian behavior. The *blue arrow* suggests that the direct inhibition of FGF21 in the SCN subsequently inhibits luteinizing hormone (LH) surge and ovulation, resulting in female infertility. The *orange arrow* suggests that the direct activation of FGF21 in the hypothalamus leads to increased neuropeptide Y (NPY) levels and NPY activates Y1 receptors in the hypothalamus resulting in torpor condition. The *black arrow* proposes the underlying mechanism of the effect of FGF21 on hippocampus possibly by increased anti-oxidant enzyme, decreased reactive oxygen species (ROS) levels and malondialdehyde (MDA) levels, inhibited nuclear factor kappa B (NF-κB) p65 translocation to the nucleus, decreased inflammatory markers and increased anti-inflammatory markers, which in turn decreases brain cell damage and improves cognition. +: activation; -: inhibition (Sa-nguanmoo et al. 2016).

RNF10 KO mice are also characterized by the almost complete absence of adipose tissue, and it is known the association between FGF-21 and adiponectin: adiponectin is, in fact, a downstream effector of FGF21 and FGF21 induces expression and secretion of adiponectin in adipocytes (Lin et al. 2013). One can hypothesize that the absence of the

adipose tissue could have an important role in the metabolic function of this animal model, but further studies are necessary to clear this parameter.

It is also important to mention the connection between FGF-21 and Klotho, a transmembrane protein involved in the sensitivity of the organism to insulin, that is also involved in aging (Kuro-o 2009). Being aging one of the risk factors for AD, possible alterations in this protein in RNF10 KO mice could possibly make RNF10 the bridge between AD and some reported metabolic alterations.

Analyzing the brain architecture and its properties in RNF10 KO mice revealed the presence of a significant difference in several areas of the brain, namely in the hippocampus and what appears to be a very strong shrinkage in the CA1 area of the hippocampus, as seen in **Figure 25**. Being the CA1 a very remarkable area in the brain circuitry, due to its importance as part of the trisynaptic loop (the axons from the pyramidal cells perforate the subiculum to project mainly to the granular layer in the dentate gyrus. The dentate granule cell axons (mossy fibers) pass on the information to the dendrites of CA3 pyramidal cells, and from there, CA3 axons (Schaffer collaterals) leave the deep part of the cell body, looping up to the apical dendrites and extending to the CA1. On their turn, the axons from CA1 project back to the entorhinal cortex, completing the circuit (Purves et al. 2018)), any changes to this area can impact the normal functioning of the brain.

It is known that dendritic spines are the primary site of excitatory input on neurons, and long-lasting changes in synaptic activity can modify spines shape, size and number. Reports have been correlating the types of spines and their “functionality”: mushroom spines, more stable and with a higher concentration of AMPAR in their surface (Matsuzaki et al. 2001), have been suggested as “memory spines”, whereas thin spines are more responsive to alterations in synaptic activity and thus suggested as “learning spines”. Spines tend to stabilize accordingly with brain maturation, nonetheless, one small portion continues to interchange even in more mature brains, being these the thin spines. In between some possible mechanisms for this, one that can turn the thin “learning spines” into mushroom “memory spines” is activity-dependent synaptic plasticity, namely LTP (Bourne & Harris 2007). Morphological analysis of hippocampal neurons in RNF10 KO

mice did not show any alterations concerning spine density, spine width or spine length, but once we categorize the type of spines, we interestingly saw a significant increase in mushroom-type spines and a decrease in thin-type spines compared to WT mice, meaning an increase in the mature spines (**Figure 26**). This increase in mushroom spines can have several different explanations: one recent work demonstrated the correlation between the increase in these spines with the successful memorization and acquisition of tasks, involving spatial and working memory (Mahmmoud et al. 2015), whereas other possibility comes from a previous work from our laboratory, involving the inhibition of ADAM10 activity, that induces an significant increase in spine head width in small-immature spines and in large-mature spines (Malinverno et al. 2010).

Indeed, when we look at the results obtained when assessing a molecular analysis of the total brain, we do observe a significant decrease in ADAM10 protein levels in the KO mice (**Figure 27**), that is also verified in the hippocampus (**Figure 30**). Notably, a similar alteration was found in all the proteins involved in the amyloid-beta production cascade. This result also correlates with the ELISA performed to measure amyloid-beta in the hippocampus, that was found to be significantly decreased in the KO mice (**Figure 32**). Taken together, these results put forward a possible involvement of RNF10 at molecular and morphological level in the context of AD.

Molecular analysis of the glutamatergic synapse in RNF10 KO mice shows a significative decrease in GluN2A (**Figure 28**) and CREB (**Figure 31**) levels in the hippocampus homogenate compared to WT animals. GluN2A is the specific NMDA receptor subunit to which RNF10 binds, as demonstrated in our previous work and it is known to be implicated in synaptic plasticity induction, as well as being required in learning and memory formation. Specifically, the rising of hippocampal GluN2A-containing NMDA receptors appears to be a general feature after novel “spatial/discrimination” memory (Cercato et al. 2017). Taken together with the fact that the activation of CREB and, subsequently, the gene expression that it leads to is a crucial step in the cascade that leads to the formation of long-lasting memories (Benito & Barco 2010), it is possible to hypothesize that, due to the significant decrease of both these proteins in these animals, they will present a distinct memory impairment.

Indeed, when looking at the results of the novel object recognition test (NORT), while both WT and KO animals present a higher preference for the novel object in both adult and aged stages in the “short-memory” 2h test (**Figure 36**), in the “long-memory” 24h test, aged KO animals lose this preference in comparison with the WT (**Figure 37**). This indicates that the animals cannot remember the previous interactions they had with the familiar object, hence exploring randomly both objects as if they were both new. This represents a very good indication of memory impairment in these animals.

Using another related behavioral test, the Y-Maze, we tested these animals on their memory and exploratory behavior. As we can observe in **Figure 35**, aged KO animals present a slightly reduced exploratory behavior when in comparison with the WT. Due to the results presented previously on their memory, we can now suggest that this difference is due to a memory impairment, but other possibility would be an exploratory difference due to locomotory issues. As tested in **Figure 33** and **34**, both WT and KO adult and aged mice do not present any differences concerning the locomotion parameter, thus clearing out the effect seen in the Y-Maze as a memory impairment effect.

We then looked at the brain circuitry, choosing to perform a patch clamp experiment in the perforant path. The perforant pathway is a large neuronal projection that arises from layers II and III of the entorhinal cortex of the parahippocampal gyrus. It is the principal source of cortical input to the hippocampal formation (Hyman et al. 1986). Being such an important circuit in the brain, it has been reported that changes, such as synaptic loss, in this system can also be correlated with cognitive impairment in several diseases, as it is the case of AD (Robinson et al. 2014).

Looking at the results obtained in **Figure 39**, we do not observe any differences in AMPA or NMDA currents in this area of the brain, nor when we analyze the kinetics of the curve by calculating the decay time (**Figure 40**), hence concluding that both WT and KO animals present a normal basic synaptic functioning in this area. The same is observed when we look at the miniature EPSCs (**Figure 41**), where we do not see any differences between WT and KO animals, thus leading to the observation that, possibly, the total number of synapses, the size of the readily releasable pool of synaptic vesicles and the neurotransmitter release is not altered in these animals in this specific synapse. However, since our animals presented a strong impairment in memory, and the most related area

of the hippocampus connected to memory functioning is CA1, we assessed the whole field LTP in this area. Looking at **Figure 42** and in accordance with the results previously seen concerning both molecular and behavior, KO animals present a complete abolition of the LTP in CA1, thus providing a functional explanation to the memory impairment in this animal model.

In conclusion, RNF10 KO animals present an interesting array of alterations: i) a potential metabolic phenotype, even though we did not find differences in the tests we performed; ii) an aberrant architecture of the brain, with a clear altered volumetric area particularly in the hippocampus; iii) different molecular composition of the synapses; iv) reduced A $\beta$  cascade counterparts and A $\beta$  *per se* and v) a strong memory impairment and a complete impairment in the LTP in the CA1 area in the hippocampus. While some of them interconnect and explain the differences found in one another, a lot more is still to be characterized and cleared in the mechanistic part in this animal model, leaving a challenge open for the future plans.

# REFERENCES

- Abramov, E. et al., 2009. Amyloid-beta as a positive endogenous regulator of release probability at hippocampal synapses. *Nature neuroscience*, 12(12), pp.1567–76.
- Adams, J.P. & Dudek, S.M., 2005. Late-phase long-term potentiation: Getting to the nucleus. *Nature Reviews Neuroscience*, 6(9), pp.737–743.
- Adeniji, A.O., Adams, P.W. & Mody, V. V., 2017. Chapter 7 - Amyloid  $\beta$  Hypothesis in the Development of Therapeutic Agents for Alzheimer's Disease. In A. B. T.-D. D. A. for the T. of N. D. Adejare, ed. Academic Press, pp. 109–143.
- Altarejos, J.Y. et al., 2008. The Creb1 coactivator Crtc1 is required for energy balance and fertility. *Nature Medicine*, 14(10), pp.1112–1117.
- Ambron, R.T. et al., 1992. A signal sequence mediates the retrograde transport of proteins from the axon periphery to the cell body and then into the nucleus. *The Journal of neuroscience : the official journal of the Society for Neuroscience*, 12(7), pp.2813–8.
- Bading, H., 2013. Nuclear calcium signalling in the regulation of brain function. *Nature Publishing Group*, 14(9), pp.593–608.
- Baleriola, J. et al., 2014. Axonally Synthesized ATF4 Transmits a Neurodegenerative Signal across Brain Regions. *Cell*, 158(5), pp.1159–1172.
- Barresi, S. et al., 2014. Oligophrenin-1 (OPHN1), a gene involved in X-linked intellectual disability, undergoes RNA editing and alternative splicing during human brain development. *PLoS ONE*, 9(3), pp.1–12.
- Bear, M.F., Huber, K.M. & Warren, S.T., 2004. The mGluR theory of fragile X mental retardation. *Trends in Neurosciences*, 27(7), pp.370–377.
- Béïque, J.-C. et al., 2006. Synapse-specific regulation of AMPA receptor function by PSD-95. *Proceedings of the National Academy of Sciences*, 103(51), pp.19535–19540.
- Benito, E. & Barco, A., 2010. CREB's control of intrinsic and synaptic plasticity: implications for CREB-dependent memory models. *Trends in Neurosciences*, 33(5), pp.230–240.
- Berridge, M.J., 1993. Inositol triphosphate and calcium signalling. *Nature*, 361, pp.315–325.
- Berridge, M.J., 1998. Neuronal Calcium Signaling. *Neuron*, 21(1), pp.13–26.
- Bittinger, M.A. et al., 2004. Activation of cAMP Response Element-Mediated Gene Expression by Regulated Nuclear Transport of TORC Proteins. *Current Biology*, 14(23), pp.2156–2161.
- Boeckers, T.M., 2006. The postsynaptic density. *Cell and Tissue Research*, 326(2), pp.409–422.
- Borchelt, D.R. et al., 1996. Familial Alzheimer's Disease – Linked Presenilin 1 Variants Elevate A $\beta$  1 – 42 / 1 – 40 Ratio In Vitro and In Vivo. *Neuron*, 17(43), pp.1005–1013.
- Bourne, J. & Harris, K.M., 2007. Do thin spines learn to be mushroom spines that remember? *Current Opinion in Neurobiology*, 17(3), pp.381–386.
- Bourne, J.N. & Harris, K.M., 2008. Balancing Structure and Function at Hippocampal Dendritic

- Spines. *Brain*, 1135(May 2006), pp.47–67.
- Brookmeyer, R. et al., 2007. Forecasting the global burden of Alzheimer's disease. *Alzheimer's & dementia : the journal of the Alzheimer's Association*, 3(3), pp.186–191.
- Budnik, V. & Salinas, P.C., 2011. Wnt signaling during synaptic development and plasticity. *Current Opinion in Neurobiology*, 21(1), pp.151–159.
- Burdick, D. et al., 1992. Assembly and Aggregation Properties of Synthetic Alzheimer ' s A4 / $\beta$  Amyloid Peptide Analogs \*. *The Journal of biological chemistry*, 267(1), pp.546–554.
- Buxbaum, J.D., 1998. Evidence That Tumor Necrosis Factor alpha Converting Enzyme Is Involved in Regulated alpha -Secretase Cleavage of the Alzheimer Amyloid Protein Precursor. *Journal of Biological Chemistry*, 273(43), pp.27765–27767.
- Cacquevel, M. et al., 2012. Alzheimer's disease-linked mutations in presenilin-1 result in a drastic loss of activity in purified  $\gamma$ -secretase complexes. *PLoS one*, 7(4), p.e35133.
- Cai, H. et al., 2001. BACE1 is the major beta-secretase for generation of Abeta peptides by neurons. *Nature neuroscience*, 4(3), pp.233–4.
- Cajal, S.R., 1954. *Neuron theory or reticular theory?: Objective evidence of the anatomical unity of nerve cells*, Consejo Superior de Investigaciones Científicas, Instituto Ramón y Cajal.
- Campenot, R.B. & MacInnis, B.L., 2004. Retrograde Transport of Neurotrophins: Fact and Function. *Journal of Neurobiology*, 58(2), pp.217–229.
- Caporaso, L. et al., 1994. Morphologic and Biochemical Analysis of the Intracellular Trafficking of the Alzheimer b/ A4 Amyloid Precursor Protein. *The Journal of Neuroscience*, 74(May), pp.3122–3138.
- Carta, M. et al., 2018. Activity-dependent control of NMDA receptor subunit composition at hippocampal mossy fibre synapses. *Journal of Physiology*, 596(4), pp.703–716.
- Cercato, M.C. et al., 2017. GluN1 and GluN2A NMDA Receptor Subunits Increase in the Hippocampus during Memory Consolidation in the Rat. *Frontiers in Behavioral Neuroscience*, 10(January), pp.1–14.
- Ch'ng, T.H. & Martin, K.C., 2011. Synapse-to-nucleus signaling. *Current Opinion in Neurobiology*, 21(2), pp.345–352.
- Chang, X. et al., 2018. Common and Rare Genetic Risk Factors Converge in Protein Interaction Networks Underlying Schizophrenia. *Frontiers in Genetics*, 9(4), pp.319–326.
- Chao, M. et al., 1998. Neurotrophin receptors: Mediators of life and death. *Brain Research Reviews*, 26(2–3), pp.295–301.
- Chaturvedi, R.K. et al., 2012. Transducer of regulated CREB-binding proteins (TORCs) transcription and function is impaired in Huntington's disease. *Human Molecular Genetics*, 21(15), pp.3474–3488.

- Chung, H.J. et al., 2000. Phosphorylation of the AMPA receptor subunit GluR2 differentially regulates its interaction with PDZ domain-containing proteins. *The Journal of Neuroscience*, 20(19), pp.7258–67.
- Citron, M. et al., 1997. Mutant presenilins of Alzheimer's disease increase production of 42-residue amyloid  $\beta$ -protein in both transfected cells and transgenic mice. *Nature Medicine*, 3(1), pp.67–72.
- Cohen, R.S., 2016. The Postsynaptic Density. In *Neuroscience in the 21st Century*. New York, NY: Springer New York, pp. 475–509.
- Collingridge, G.L. et al., 2009. A nomenclature for ligand-gated ion channels. *Neuropharmacology*, 56(1), pp.2–5.
- Conkright, M.D. et al., 2003. TORCs: Transducers of regulated CREB activity. *Molecular Cell*, 12(2), pp.413–423.
- Deisseroth, K. et al., 2003. Signaling from synapse to nucleus: The logic behind the mechanisms. *Current Opinion in Neurobiology*, 13(3), pp.354–365.
- Delacourte, A. et al., 2002. Nonoverlapping but synergetic tau and APP pathologies in sporadic Alzheimer's disease. *Neurology*, 422, pp.398–407.
- Deshpande, L.S. et al., 2008. Time course and mechanism of hippocampal neuronal death in an in vitro model of status epilepticus: Role of NMDA receptor activation and NMDA dependent calcium entry. *European Journal of Pharmacology*, 583, pp.73–83.
- Dhingra, A. et al., 2000. The Light Response of ON Bipolar Neurons Requires G alpha o. *Journal of Neuroscience*, 20(24), pp.9053–9058.
- Dieterich, D.C. et al., 2008. Caldendrin-Jacob: A protein liaison that couples NMDA receptor signalling to the nucleus. *PLoS Biology*, 6(2), pp.0286–0306.
- DiLuca, M. & Olesen, J., 2014. The cost of brain diseases: A burden or a challenge? *Neuron*, 82(6), pp.1205–1208.
- Dinamarca, M.C. et al., 2016. Ring finger protein 10 is a novel synaptonuclear messenger encoding activation of NMDA receptors in hippocampus. *eLife*, 5, pp.1–28.
- Dingledine, R. et al., 1999. The glutamate receptor ion channels. *Pharmacol.Rev.*, 51(1), pp.7–62.
- Doble, A., 1995. Excitatory amino acid receptors and neurodegeneration. *Therapie*, 50(4), pp.319–37.
- Dong, H. et al., 1999. Characterization of the glutamate receptor-interacting proteins GRIP1 and GRIP2. *The Journal of neuroscience*, 19(16), pp.6930–6941.
- Dong, H. et al., 1997. GRIP: a synaptic PDZ domain-containing protein that interacts with AMPA receptors. *Nature*, 386, p.279.
- Drummond, E. et al., 2018. Isolation of Amyloid Plaques and Neurofibrillary Tangles from Archived

- Alzheimer's Disease Tissue Using Laser-Capture Microdissection for Downstream Proteomics. In *Molecular Diagnostics: For the Clinical Laboratorian*. pp. 319–334.
- Durand, C.M. et al., 2007. Mutations in the gene encoding the synaptic scaffolding protein SHANK3 are associated with autism spectrum disorders. *Nature Genetics*, 39(1), pp.25–27.
- Duvoisin, R.M. et al., 2005. Increased measures of anxiety and weight gain in mice lacking the group III metabotropic glutamate receptor. *European Journal of Neuroscience*, 22(February), pp.425–436.
- Eastman, Q., 2012. Tanglep up with tau. *Lab Land - The Emory Health Sciences Research Blog*. Available at: <http://www.emoryhealthsciblog.com/tangled-up-with-tau/>.
- Echarri, A. et al., 2004. Abl Interactor 1 (Abi-1) Wave-Binding and SNARE Domains Regulate Its Nucleocytoplasmic Shuttling, Lamellipodium Localization, and Wave-1 Levels. *Molecular and Cellular Biology*, 24(11), pp.4979–4993.
- Ehlers, M.D. et al., 1996. Inactivation of NMDA receptors by direct interaction of calmodulin with the NR1 subunit. *Cell*, 84(5), pp.745–755.
- Ehrlich, I. & Malinow, R., 2004. Postsynaptic Density 95 controls AMPA Receptor Incorporation during Long-Term Potentiation and Experience-Driven Synaptic Plasticity. *Journal of Neuroscience*, 24(4), pp.916–927.
- Elias, G.M. et al., 2006. Synapse-Specific and Developmentally Regulated Targeting of AMPA Receptors by a Family of MAGUK Scaffolding Proteins. *Neuron*, 52(2), pp.307–320.
- Epsztein, J., Represa, A. & Crépel, V., 2017. *Role of Kainate Receptors in Glutamatergic Synaptic Transmission: Implications for Acute and Chronic Seizure Generation* ☆, Elsevier.
- Foster, M. & Sherrington, C., 1897. *A Text Book of Physiology*,
- Fromer, M. et al., 2014. De novo mutations in schizophrenia implicate synaptic networks. *Nature*, 506(7487), pp.179–184.
- Gerlai, R., Roder, J.C. & Hampson, D.R., 1998. Altered spatial learning and memory in mice lacking the mGluR4 subtype of metabotropic glutamate receptor. *Behavioral Neuroscience*, 112(3), pp.525–532.
- Ghersi, E., Noviello, C. & D'Adamio, L., 2004. Amyloid- $\beta$  Protein Precursor (A $\beta$ PP) intracellular domain-associated protein-1 proteins bind to A $\beta$ PP and modulate its processing in an isoform-specific manner. *Journal of Biological Chemistry*, 279(47), pp.49105–49112.
- Ghosh, A. & Giese, K.P., 2015. Calcium/calmodulin-dependent kinase II and Alzheimer's disease. *Molecular Brain*, 8(1), pp.1–7.
- Görlich, D. & Kutay, U., 1999. Transport Between the Cell Nucleus and the Cytoplasm. *Annual Review of Cell and Developmental Biology*, 15(1), pp.607–660.
- Grabrucker, S. et al., 2014. The PSD protein ProSAP2/Shank3 displays synapto-nuclear shuttling

- which is deregulated in a schizophrenia-associated mutation. *Experimental Neurology*, 253, pp.126–137.
- Grant, S.G.N., 2012. Synaptopathies: Diseases of the synaptome. *Current Opinion in Neurobiology*, 22(3), pp.522–529.
- Greenfield, J. et al., 1999. Endoplasmic reticulum and trans-Golgi network generate distinct populations of Alzheimer  $\beta$ -amyloid peptides. *Proceedings of the National Academy of Sciences of the United States of America*, 96(January), pp.742–747.
- Grimes, M.L. et al., 1996. Endocytosis of Activated TrkA: Evidence that Nerve Growth Factor Induces Formation of Signaling Endosomes. *Journal of Neuroscience*, 16(24), pp.7950–7964.
- Grundke-iqbal, I., Iqbal, K., Tung, Y., Quinlan, M., et al., 1986. Abnormal phosphorylation of the microtubule-associated protein X ( tau ) in Alzheimer cytoskeletal pathology. *Proceedings of the National Academy of Sciences of the United States of America*, 83(July), pp.4913–4917.
- Grundke-iqbal, I., Iqbal, K., Tung, Y., Zaidi, M.S., et al., 1986. Microtubule-associated Protein Tau. *The Journal of biological chemistry*, 4(23), pp.6084–6089.
- Gu, Z., Liu, W. & Yan, Z., 2009. B-amyloid impairs AMPA receptor trafficking and function by reducing Ca<sup>2+</sup>/calmodulin-dependent protein kinase II synaptic distribution. *Journal of Biological Chemistry*, 284(16), pp.10639–10649.
- Haass, C. et al., 1992. Amyloid  $\beta$ -peptide is produced by cultured cells during normal metabolism. *Nature*, 359, pp.322–325.
- Halzmyth, M., 2012. What is Alzheimer's? Available at: <http://honeymans.blogspot.pt/2012/10/what-is-alzheimers.html>.
- Han, K. et al., 2013. SHANK3 overexpression causes manic-like behaviour with unique pharmacogenetic properties. *Nature*, 503(7474), pp.72–77.
- Hardingham, G.E., Arnold, F.J.L. & Bading, H., 2001a. A calcium microdomain near NMDA receptors: On switch for ERK-dependent synapse-to-nucleus communication. *Nature Neuroscience*, 4(6), pp.565–566.
- Hardingham, G.E., Arnold, F.J.L. & Bading, H., 2001b. Nuclear calcium signaling controls CREB-mediated gene expression triggered by synaptic activity. *Nature Neuroscience*, 4(3), pp.261–267.
- Hardingham, G.E., Fukunaga, Y. & Bading, H., 2002. Extrasynaptic NMDARs oppose synaptic NMDARs by triggering CREB shut-off and cell death pathways. *Nature Neuroscience*, 5(5), pp.405–414.
- Hartmann, T. et al., 1997. Distinct sites of intracellular production for Alzheimer's disease A $\beta$ 40/42 amyloid peptides. *Nature medicine*, 3, pp.1016–1020.
- Hattori, M., Osterfield, M. & Flanagan, J.G., 2000. Regulated Cleavage of a Contact-Mediated Axon

- Repellent. *Science*, 289(August), pp.1360–1365.
- Herrmann, J. et al., 2004. The ubiquitin-proteasome system in cardiovascular diseases - A hypothesis extended. *Cardiovascular Research*, 61(1), pp.11–21.
- Hoshikawa, S. et al., 2008. A novel function of RING finger protein 10 in transcriptional regulation of the myelin-associated glycoprotein gene and myelin formation in Schwann cells. *PLoS ONE*, 3(10).
- Houshyar, K.S. et al., 2012. Effects of phlebotomy-induced reduction of body iron stores on metabolic syndrome: results from a randomized clinical trial. *BMC Medicine*, 10(1), p.54.
- Hu, V.W., Addington, A. & Hyman, A., 2011. Novel autism subtype-dependent genetic variants are revealed by quantitative trait and subphenotype association analyses of Published GWAS Data. *PLoS ONE*, 6(4).
- Huang, K. et al., 2014. Whole exome sequencing identifies variation in CYB5A and RNF10 associated with adiposity and type 2 diabetes. *Obesity*, 22(4), pp.984–988.
- Huganir, R.L. & Nicoll, R.A., 2013. AMPARs and synaptic plasticity: The last 25 years. *Neuron*, 80(3), pp.704–717.
- Humeau, Y. et al., 2007. A Pathway-Specific Function for Different AMPA Receptor Subunits in Amygdala Long-Term Potentiation and Fear Conditioning. *Journal of Neuroscience*, 27(41), pp.10947–10956.
- Huupponen, J. et al., 2016. GluA4 subunit of AMPA receptors mediates the early synaptic response to altered network activity in the developing hippocampus. *Journal of neurophysiology*, 115(6), pp.2989–2996.
- Hyman, B.T. et al., 1986. Perforant Pathway Changes and the Memory Impairment of Alzheimer's Disease. *Annals of neurology*, 20(4), pp.472–481.
- Ito, H. et al., 2010. Dysbindin-1, WAVE2 and Abi-1 form a complex that regulates dendritic spine formation. *Molecular Psychiatry*, 15(10), pp.976–986.
- Iwatsubo, T. et al., 1994. Visualization of A $\beta$ 42 (43) and A $\beta$ 40 in Senile Plaques with End-Specific A $\beta$  Monoclonals : Evidence That an Initially Deposited Species Is A $\beta$ 42 (43). *Neuron*, 13(43), pp.45–53.
- Jarrett, J.T., Berger, E.P. & Lansbury, P.T., 1993. The carboxy terminus of the  $\beta$  amyloid protein is critical for the seeding of amyloid formation: Implications for the pathogenesis of Alzheimer's disease. *Biochemistry*, 32(18), pp.4693–4697.
- Jeffrey, R.A. et al., 2009. Activity-Dependent Anchoring of Importin  $\alpha$  at the Synapse Involves Regulated Binding to the Cytoplasmic Tail of the NR1-1a Subunit of the NMDA Receptor. *Journal of Neuroscience*, 29(50), pp.15613–15620.
- Jiang, Y. & Ehlers, M.D., 2013. Modeling Autism by SHANK Gene Mutations in Mice. *Neuron*, 78(1),

pp.8–27.

- Jones, S.V. & Kounatidis, I., 2017. Nuclear factor-kappa B and Alzheimer disease, unifying genetic and environmental risk factors from cell to humans. *Frontiers in Immunology*, 8(DEC).
- Jordan, B.A. et al., 2007. Activity-dependent AIDA-1 nuclear signaling regulates nucleolar numbers and protein synthesis in neurons. *Nature Neuroscience*, 10(4), pp.427–435.
- Jordan, B.A. et al., 2004. Identification and Verification of Novel Rodent Postsynaptic Density Proteins. *Molecular & Cellular Proteomics*, 3(9), pp.857–871.
- Jordan, B.A. & Kreutz, M.R., 2009. Nucleocytoplasmic protein shuttling: the direct route in synapse-to-nucleus signaling. *Trends in Neurosciences*, 32(7), pp.392–401.
- Julio-Pieper, M. et al., 2011. Exciting Times beyond the Brain : Metabotropic Glutamate Receptors in Peripheral and Non-Neural Tissues. *Pharmacological Reviews*, 63(1), pp.35–58.
- Kaltschmidt, C., Kaltschmidt, B. & Baeuerle, P.A., 1993. Brain synapses contain inducible forms of the transcription factor NF- $\kappa$ B. *Mechanisms of Development*, 43(2–3), pp.135–147.
- Kamenetz, F. et al., 2003. APP Processing and Synaptic Function State University of New York at Stony Brook. *Neuron*, 37, pp.925–937.
- Kim, C.-H. et al., 2001. Interaction of the AMPA receptor subunit GluR2/3 with PDZ domains regulates hippocampal long-term depression. *Proceedings of the National Academy of Sciences*, 98(20), pp.11725–11730.
- Kim, E.K. & Choi, E.J., 2015. Compromised MAPK signaling in human diseases: an update. *Archives of Toxicology*, 89(6), pp.867–882.
- Kim, E.K. & Choi, E.J., 2010. Pathological roles of MAPK signaling pathways in human diseases. *Biochimica et Biophysica Acta - Molecular Basis of Disease*, 1802(4), pp.396–405.
- Kim, J. & Schekman, R., 2004. The ins and outs of presenilin 1 membrane topology. *Proceedings of the National Academy of Sciences of the United States of America*, 101(4), pp.905–906.
- Kimberly, W.T. et al., 2003.  $\gamma$ -Secretase is a membrane protein complex comprised of presenilin , nicastrin , aph-1 , and pen-2. *Proceedings of the National Academy of Sciences of the United States of America*, 100(11), pp.6382–6387.
- Kindler, S. et al., 2009. Dendritic mRNA Targeting of Jacob and N -Methyl-d-aspartate-induced Nuclear Translocation after Calpain-mediated Proteolysis. *Journal of Biological Chemistry*, 284(37), pp.25431–25440.
- Kornau, H.-C. et al., 1995. Domain Interaction Between NMDA Receptor Subunits and the Postsynaptic Density Protein PSD-95. *Science*, 269, pp.1737–1740.
- Krieger, J., Bahar, I. & Greger, I.H., 2015. Structure, Dynamics, and Allosteric Potential of Ionotropic Glutamate Receptor N-Terminal Domains. *Biophysical Journal*, 109(6), pp.1136–1148.

- Kühn, T. et al., 2011. Protein Diffusion in Mammalian Cell Cytoplasm. *PLoS ONE*, 6(8), p.12.
- Kuro-o, M., 2009. Klotho and aging. *Biochimica et Biophysica Acta (BBA) - General Subjects*, 1790(10), pp.1049–1058.
- LaFerla, F.M., Green, K.N. & Oddo, S., 2007. Intracellular amyloid-beta in Alzheimer's disease. *Nature reviews. Neuroscience*, 8(7), pp.499–509.
- Lai, K.-O. et al., 2008. Importin-mediated retrograde transport of CREB2 from distal processes to the nucleus in neurons. *Proceedings of the National Academy of Sciences*, 105(44), pp.17175–17180.
- Lau, K.-F. et al., 2000. X11 $\alpha$  and X11 $\beta$  Interact with Presenilin-1 via Their PDZ Domains. *Molecular and Cellular Neuroscience*, 16(5), pp.557–565.
- Leng, Y. et al., 2005. Abelson-interactor-1 promotes WAVE2 membrane translocation and Abelson-mediated tyrosine phosphorylation required for WAVE2 activation. *Proceedings of the National Academy of Sciences*, 102(4), pp.1098–1103.
- De Ligt, J. et al., 2013. Diagnostic exome sequencing in persons with severe intellectual disability. *Obstetrical and Gynecological Survey*, 68(3), pp.191–193.
- Lin, D.-T. et al., 2009. Regulation of AMPA receptor extrasynaptic insertion by 4.1N, phosphorylation and palmitoylation. *Nature Neuroscience*, 12(7), pp.879–887.
- Lin, J. et al., 2005. Characterization of Mesenchyme Homeobox 2 (MEOX2) transcription factor binding to RING finger protein 10. *Molecular and Cellular Biochemistry*, 275(1–2), pp.75–84.
- Lin, Z. et al., 2013. Adiponectin Mediates the Metabolic Effects of FGF21 on Glucose Homeostasis and Insulin Sensitivity in Mice. *Cell Metabolism*, 17(5), pp.779–789.
- Linden, A. et al., 2002. Increased anxiety-related behavior in mice deficient for metabotropic glutamate 8 (mGlu8) receptor. *Neuropharmacology*, 43, pp.251–259.
- Di Luca, M. et al., 2000. Platelets as a peripheral district where to study pathogenetic mechanisms of Alzheimer disease: the case of amyloid precursor protein. *European journal of immunology*, 405, pp.277–283.
- Luchkina, N. V. et al., 2014. Developmental switch in the kinase dependency of long-term potentiation depends on expression of GluA4 subunit-containing AMPA receptors. *Proceedings of the National Academy of Sciences*, 111(11), pp.4321–4326.
- Ma, H. et al., 2014.  $\gamma$ CaMKII shuttles Ca<sup>2+</sup>/CaM to the nucleus to trigger CREB phosphorylation and gene expression. *Cell*, 159(2), pp.281–294.
- Mahmoud, R.R. et al., 2015. Spatial and working memory is linked to spine density and mushroom spines. *PLoS ONE*, 10(10), pp.1–15.
- Malik, Y.S. et al., 2013. RING finger protein 10 regulates retinoic acid-induced neuronal differentiation and the cell cycle exit of P19 embryonic carcinoma cells. *Journal of Cellular*

- Biochemistry*, 114(9), pp.2007–2015.
- Malinverno, M. et al., 2010. Synaptic Localization and Activity of ADAM10 Regulate Excitatory Synapses through N-Cadherin Cleavage. *Journal of Neuroscience*, 30(48), pp.16343–16355.
- Mannaioni, G. et al., 2001. Metabotropic Glutamate Receptors 1 and 5 Differentially Regulate CA1 Pyramidal Cell Function. *The Journal of Neuroscience*, 21(16), pp.5925–5934.
- Marcello, E., Di Luca, M. & Gardoni, F., 2018. Synapse-to-nucleus communication: from developmental disorders to Alzheimer’s disease. *Current Opinion in Neurobiology*, 48, pp.160–166.
- Marcora, E. & Kennedy, M.B., 2010. The Huntington’s disease mutation impairs Huntingtin’s role in the transport of NF- $\kappa$ B from the synapse to the nucleus. *Human Molecular Genetics*, 19(22), pp.4373–4384.
- Mateu-Huertas, E. et al., 2014. Blood expression profiles of fragile X premutation carriers identify candidate genes involved in neurodegenerative and infertility phenotypes. *Neurobiology of Disease*, 65, pp.43–54.
- Matsuzaki, M. et al., 2001. Dendritic spine geometry is critical for AMPA receptor expression in hippocampal CA1 pyramidal neurons. *Nature Neuroscience*, 4, p.1086.
- McKay, S. et al., 2018. The Developmental Shift of NMDA Receptor Composition Proceeds Independently of GluN2 Subunit-Specific GluN2 C-Terminal Sequences. *Cell Reports*, 25(4), p.841–851.e4.
- McKee, A.C. et al., 1990. Hippocampal Neurons Predisposed to Neurofibrillary Tangle Formation Are Enriched in Type II Calcium/Calmodulin-Dependent Protein Kinase. *Journal of neuropathology and experimental neurology*, 49(1), pp.49–63.
- Meffert, M.K. et al., 2003. NF- $\kappa$ B functions in synaptic signaling and behavior. *Nature Neuroscience*, 6(10), pp.1072–1078.
- Menéndez-González, M. et al., 2005. APP processing and the APP-KPI domain involvement in the amyloid cascade. *Neuro-degenerative diseases*, 2(6), pp.277–83.
- Monaghan, D.T. et al., 2012. Pharmacological Modulation of NMDA Receptor Activity and the Advent of Negative and Positive Allosteric Modulators. *Neurochem Int.*, 61(4), pp.581–592.
- Muguruza, C., Meana, J.J. & Callado, L.F., 2016. Group II Metabotropic Glutamate Receptors as Targets for Novel Antipsychotic Drugs. *Frontiers in Pharmacology*, 7(May), pp.1–12.
- Neet, K.E. & Campenot, R.B., 2001. Receptor binding, internalization, and retrograde transport of neurotrophic factors. *Cellular and Molecular Life Sciences*, 58(8), pp.1021–1035.
- Nicoletti, F. et al., 2011. Metabotropic glutamate receptors: From the workbench to the bedside. *Neuropharmacology*, 60(0), pp.1017–1041.
- Nishimune, A. et al., 1998. NSF binding to GluR2 regulates synaptic transmission. *Neuron*, 21(1),

pp.87–97.

- Niswender, C.M. & Conn, P.J., 2010. Metabotropic Glutamate Receptors: Physiology, Pharmacology, and Disease. *Annual Review of Pharmacology and Toxicology*, 50(1), pp.295–322.
- Nordstedt, C. et al., 1993. Identification of the Alzheimer  $\beta$ /A4 Amyloid Precursor Protein in Clathrin-coated Vesicles Purified from PC12 Cells. *The Journal of Biological Chemistry*, 268, pp.608–612.
- Palade, G. & Palay, S., 1954. Electron microscope observations of interneuron and neuromuscular synapses. *The Anatomical Record*, 118((oral presentation)), p.336.
- Panayotis, N. et al., 2015. Macromolecular transport in synapse to nucleus communication. *Trends in Neurosciences*, 38(2), pp.108–116.
- Paoletti, P., 2011. Molecular basis of NMDA receptor functional diversity. *European Journal of Neuroscience*, 33(8), pp.1351–1365.
- Parliament, T.E., 2011. *European initiative on Alzheimer's disease and other dementias*.
- Parra-Damas, A. et al., 2014. Crtc1 Activates a Transcriptional Program Deregulated at Early Alzheimer's Disease-Related Stages. *Journal of Neuroscience*, 34(17), pp.5776–5787.
- Parra-Damas, A. & Saura, C.A., 2019. Synapse-to-nucleus signaling in neurodegenerative and neuropsychiatric disorders. *Biological Psychiatry*.
- Pekhletski, R. et al., 1996. Impaired Cerebellar Synaptic Plasticity and Motor Performance in Mice Lacking the mGluR4 Subtype of Metabotropic Glutamate Receptor. *The Journal of Neuroscience*, 16(20), pp.6364–6373.
- Perl, D.P., 2010. Neuropathology of Alzheimer's Disease. *Mount Sinai Journal of Medicine: A Journal of Translational and Personalized Medicine*, 77(1), pp.32–42.
- Pinto, D. et al., 2010. Functional impact of global rare copy number variation in autism spectrum disorders. *Nature*, 466(7304), pp.368–372.
- Pitt, D., Werner, P. & Raine, C.S., 2000. Glutamate excitotoxicity in a model of multiple sclerosis. *Nature Medicine*, 6(1), pp.67–70.
- Pitteloud, N. et al., 2007. Digenic mutations account for variable phenotypes in idiopathic hypogonadotropic hypogonadism. *Journal of Clinical Investigation*, 117(2), pp.457–463.
- Postina, R. & Fahrenholz, F., 2013. Chapter 251 - ADAM10, Myelin-associated Metalloendopeptidase. In N. D. Rawlings & G. B. T.-H. of P. E. (Third E. Salvesen, eds. Academic Press, pp. 1108–1114.
- Prince, M. et al., 2013. The global prevalence of dementia: a systematic review and metaanalysis. *Alzheimer's & dementia : the journal of the Alzheimer's Association*, 9(1), p.63–75.e2.
- Proepper, C. et al., 2007. Abelson interacting protein 1 (Abi-1) is essential for dendrite

- morphogenesis and synapse formation. *EMBO Journal*, 26(5), pp.1397–1409.
- Purves, D. et al., 2018. *Neuroscience, 6th Edition*,
- Ramakers, G.J.A. et al., 2012. Dysregulation of Rho GTPases in the  $\alpha$ Pix/Arhgef6 mouse model of X-linked intellectual disability is paralleled by impaired structural and synaptic plasticity and cognitive deficits. *Human Molecular Genetics*, 21(2), pp.268–286.
- Raymond, F.L., 2006. X linked mental retardation: A clinical guide. *Journal of Medical Genetics*, 43(3), pp.193–200.
- Reese, L.C. et al., 2011. Dysregulated phosphorylation of Ca<sup>2+</sup>/calmodulin-dependent protein kinase II- $\alpha$  in the hippocampus of subjects with mild cognitive impairment and Alzheimer's disease. *Journal of Neurochemistry*, 119(4), pp.791–804.
- Reinders, N.R. et al., 2016. Amyloid- $\beta$  effects on synapses and memory require AMPA receptor subunit GluA3. *Proceedings of the National Academy of Sciences*, 113(42), pp.E6526–E6534.
- Reiss, K. et al., 2005. ADAM10 cleavage of N-cadherin and regulation of cell-cell adhesion and  $\beta$ -catenin nuclear signalling. *EMBO Journal*, 24(4), pp.742–752.
- Robbins, M.J. et al., 2007. Evaluation of the mGlu8 receptor as a putative therapeutic target in schizophrenia. *Brain research*, 1152, pp.215–227.
- De Robertis, E.D. & Bennett, H.S., 1955. Some features of the submicroscopic morphology of synapses in frog and earthworm. *Journal of Biophysical and Biochemical Cytology*, 1(1), pp.47–58.
- Roberts, S.B. et al., 1994. Non-amyloidogenic cleavage of the  $\beta$ -amyloid precursor protein by an integral membrane metalloendopeptidase. *The Journal of biological chemistry*, 269(4), pp.3111–6.
- Robinson, J.L. et al., 2014. Perforant path synaptic loss correlates with cognitive impairment and Alzheimer's disease in the oldest-old. *Brain : a journal of neurology*, 137, pp.2578–2587.
- Rönicke, R. et al., 2011. Early neuronal dysfunction by amyloid  $\beta$  oligomers depends on activation of NR2B-containing NMDA receptors. *Neurobiology of Aging*, 32(12), pp.2219–2228.
- Rosenberg, O.S. et al., 2005. Structure of the autoinhibited kinase domain of CaMKII and SAXS analysis of the holoenzyme. *Cell*, 123(5), pp.849–860.
- Roskoski Jr, R., 2012. ERK1/2 MAP kinases : Structure, function, and regulation. *Pharmacological Research*, 66(2), pp.105–143.
- Sa-nguanmoo, P., Chattipakorn, N. & Chattipakorn, S.C., 2016. Potential roles of fibroblast growth factor 21 in the brain. *Metabolic Brain Disease*, 31(2), pp.239–248.
- Sala, C. & Segal, M., 2014. Dendritic Spines: The Locus of Structural and Functional Plasticity. *Physiological Reviews*, 94(1), pp.141–188.
- Salter, M.W. et al., 2009. *Regulation of NMDA Receptors by Kinases and Phosphatases*, CRC

- Press/Taylor & Francis.
- Satpute-Krishnan, P. et al., 2006. A peptide zipcode sufficient for anterograde transport within amyloid precursor protein. *Proceedings of the National Academy of Sciences*, 103(44), pp.16532–16537.
- Satpute-Krishnan, P., DeGiorgis, J.A. & Bearer, E.L., 2003. Fast anterograde transport of herpes simplex virus: role for the amyloid precursor protein of Alzheimer's disease. *Aging cell*, 2(6), pp.305–318.
- Scheuner, D. et al., 1996. Secreted amyloid  $\beta$ -protein similar to that in the senile plaques of Alzheimer's disease is increased in vivo by the presenilin 1 and 2 and APP mutations linked to familial Alzheimer's disease. *Nature medicine*, 2(8), pp.864–870.
- Schlüter, O.M., Xu, W. & Malenka, R.C., 2006. Alternative N-Terminal Domains of PSD-95 and SAP97 Govern Activity-Dependent Regulation of Synaptic AMPA Receptor Function. *Neuron*, 51(1), pp.99–111.
- Screaton, R.A. et al., 2004. The CREB coactivator TORC2 functions as a calcium- and cAMP-sensitive coincidence. *Cell*, 119(1), pp.61–74.
- Segev, Y. et al., 2015. Neurobiology of Disease PKR Inhibition Rescues Memory Deficit and ATF4 Overexpression in ApoE  $\epsilon$ 4 Human Replacement Mice. *The Journal of Neuroscience*, 35(38), pp.12986–12993.
- Seidenman, K.J. et al., 2003. Glutamate receptor subunit 2 Serine 880 phosphorylation modulates synaptic transmission and mediates plasticity in CA1 pyramidal cells. *The Journal of neuroscience : the official journal of the Society for Neuroscience*, 23(27), pp.9220–8.
- Seki, N., Hattori, A. & Sugano, S., 2000. cDNA cloning , expression profile , and genomic structure of human and mouse RNF10 / Rnf 10 genes , encoding a novel RING finger protein. , pp.38–42.
- Selkoe, D., 1998. The cell biology of  $\beta$ -amyloid precursor protein and presenilin in Alzheimer's disease. *Trends in Cell Biology*, 8(11), pp.447–453.
- Seubert, P. et al., 1992. Isolation and quantification of soluble Alzheimer's bold beta-peptide from biological fluids. *Nature*, 359, pp.325–327.
- Shankar, G.M. & Walsh, D.M., 2009. Alzheimer's disease: synaptic dysfunction and A $\beta$ . *Molecular neurodegeneration*, 4, p.48.
- Sheng, M. & Kim, E., 2011. The postsynaptic organization of synapses. *Cold Spring Harbor Perspectives in Biology*, 3(12), pp.1–20.
- Sinha, S. et al., 1999. Purification and cloning of amyloid precursor protein  $\beta$ -secretase from human brain. *Nature*, 402, p.537.
- Sisodia, S.S., 1992.  $\beta$ -Amyloid precursor protein cleavage by a membrane-bound protease.

- Proceedings of the National Academy of Sciences of the United States of America*, 89(July), pp.6075–6079.
- Sisodia, S.S. & Tanzi, R.E., 2007. *Alzheimer's Disease: Advances in Genetics, Molecular and Cellular Biology*,
- Small, D.H., Klaver, D.W. & Foa, L., 2010. Presenilins and the  $\gamma$ -secretase: still a complex problem. *Molecular brain*, 3, p.7.
- Sobolevsky, A.I., Rosconi, M.P. & Gouaux, E., 2009. X-ray structure, symmetry and mechanism of an AMPA-subtype glutamate receptor. *Nature*, 462(7274), pp.745–756.
- Solans, A., Estivill, X. & de la Luna, S., 2000. A new aspartyl protease on 21q22.3, BACE2, is highly similar to Alzheimer's amyloid precursor protein  $\beta$ -secretase. *Cytogenetic and Genome Research*, 89(3–4), pp.177–184.
- Spilker, C. et al., 2016. A Jacob/Nsmf Gene Knockout Results in Hippocampal Dysplasia and Impaired BDNF Signaling in Dendritogenesis. *PLoS Genetics*, 12(3), pp.1–32.
- Srivastava, S. & Ziff, E.B., 1999. ABP: A novel AMPA receptor binding protein. *Annals of the New York Academy of Sciences*, 868, pp.561–564.
- Stradal, T. et al., 2001. The Abl interactor proteins localize to sites of actin polymerization at the tips of lamellipodia and filopodia. *Current Biology*, 11(11), pp.891–895.
- Sun, X. et al., 2013. ATF4 Protects Against Neuronal Death in Cellular Parkinson's Disease Models by Maintaining Levels of Parkin. *Journal of Neuroscience*, 33(6), pp.2398–2407.
- Takashima, a et al., 1998. Presenilin 1 associates with glycogen synthase kinase-3beta and its substrate tau. *Proceedings of the National Academy of Sciences of the United States of America*, 95(16), pp.9637–41.
- Takasugi, N., Tomita, T. & Hayashi, I., 2003. The role of presenilin cofactors in the  $\gamma$ -secretase complex. *Nature*, 422(March), pp.2114–2117.
- Talukdar, S. et al., 2015. FGF21 Regulates Sweet and Alcohol Preference. *Cell Metabolism*, 23(2), pp.344–349.
- Tani, K. et al., 2003. Abl interactor 1 promotes tyrosine 296 phosphorylation of mammalian enabled (Mena) by c-ABL kinase. *Journal of Biological Chemistry*, 278(24), pp.21685–21692.
- Tindi, J.O. et al., 2015. ANKS1B Gene Product AIDA-1 Controls Hippocampal Synaptic Transmission by Regulating GluN2B Subunit Localization. *Journal of Neuroscience*, 35(24), pp.8986–8996.
- Tirupathi, C. et al., 2014. The transcription factor DREAM represses the deubiquitinase A20 and mediates inflammation. *Nature Immunology*, 15(3), pp.239–247.
- Traynelis, S.F. et al., 2010. Glutamate Receptor Ion Channels: Structure, Regulation, and Function. *Pharmacological Reviews*, 62(3), pp.405–496.
- Valenti, O., Jeffrey Conn, P. & Marino, M.J., 2002. Distinct physiological roles of the Gq-coupled

- metabotropic glutamate receptors co-expressed in the same neuronal populations. *Journal of Cellular Physiology*, 191(2), pp.125–137.
- Vassar, R., 2004. BACE1 - The  $\beta$ -secretase Enzyme in Alzheimer's Disease. *Journal of Molecular Neuroscience*, 23, pp.105–113.
- Vassar, R. et al., 1999.  $\beta$ -Secretase Cleavage of Alzheimer's Amyloid Precursor Protein by the Transmembrane Aspartic Protease BACE. *Science*, 286(5440), p.735 LP-741.
- Voglis, G. & Tavernarakis, N., 2006. The role of synaptic ion channels in synaptic plasticity. *EMBO Reports*, 7(11), pp.1104–1110.
- Volk, L. et al., 2010. Developmental regulation of protein interacting with C kinase 1 (PICK1) function in hippocampal synaptic plasticity and learning. *Proceedings of the National Academy of Sciences*, 107(50), pp.21784–21789.
- Wang, J. et al., 2013. Abnormal Hyperphosphorylation of Tau : Sites , Regulation , and Molecular Mechanism of Neurofibrillary Degeneration. *Journal of Alzheimers Disease*, 33, pp.S123–S139.
- Wang, Y.J. et al., 2005. The expression of calcium/calmodulin-dependent protein kinase II- $\alpha$  in the hippocampus of patients with Alzheimer's disease and its links with AD-related pathology. *Brain Research*, 1031(1), pp.101–108.
- Wee, K.S.L. et al., 2008. Immunolocalization of NMDA receptor subunit NR3B in selected structures in the rat forebrain, cerebellum, and lumbar spinal cord. *Journal of Comparative Neurology*, 509(1), pp.118–135.
- Wellmann, H., Kaltschmidt, B. & Kaltschmidt, C., 2001. Retrograde Transport of Transcription Factor NF- $\kappa$ B in Living Neurons. *Journal of Biological Chemistry*, 276(15), pp.11821–11829.
- Wiegert, J.S., Bengtson, C.P. & Bading, H., 2007. Diffusion and not active transport underlies and limits ERK1/2 synapse-to-nucleus signaling in hippocampal neurons. *Journal of Biological Chemistry*, 282(40), pp.29621–29633.
- Wilson, E.N. et al., 2017. Intraneuronal Amyloid Beta Accumulation Disrupts Hippocampal CRTG1-Dependent Gene Expression and Cognitive Function in a Rat Model of Alzheimer Disease. *Cerebral Cortex*, 27(2), pp.1501–1511.
- Won, S.-Y. et al., 2016. Nigral dopaminergic PAK4 prevents neurodegeneration in rat models of Parkinson's disease. *Science Translational Medicine*, 8(367), p.367ra170-367ra170.
- Wortzel, I. & Seger, R., 2011. The ERK Cascade: Distinct Functions within Various Subcellular Organelles. *Genes & Cancer*, 2(3), pp.195–209.
- Wu, C. et al., 2009. The coming of age of axonal neurotrophin signaling endosomes. *Journal of Proteomics*, 72(1), pp.46–55.
- Wu, Z. et al., 2006. Transducer of regulated CREB-binding proteins (TORCs) induce PGC-

- 1 transcription and mitochondrial biogenesis in muscle cells. *Proceedings of the National Academy of Sciences*, 103(39), pp.14379–14384.
- Wyllie, D.J.A., Livesey, M.R. & Hardingham, G.E., 2013. Influence of GluN2 subunit identity on NMDA receptor function. *Neuropharmacology*, 74, pp.4–17.
- Xia, J. et al., 1999. Clustering of AMPA Receptors by the Synaptic PDZ Domain–Containing Protein PICK1 Recent studies have revealed that the synaptic protein PSD-95/SAP90 and its family members, SAP102 and PSD-93/Chapsyn-110, physically associate with NMDA. *Neuron*, 22, pp.179–187.
- Xu, H. et al., 1997. Generation of Alzheimer  $\beta$ -amyloid protein in the trans-Golgi network in the apparent absence of vesicle formation. *Proceedings of the National Academy of Sciences of the United States of America*, 94(April), pp.3748–3752.
- Xue, Z.-C. et al., 2015. CREB-regulated transcription coactivator 1 : important roles in neurodegenerative disorders. *Acta Physiologica Sinica*, 67(81171036), pp.155–162.
- Yan, R. et al., 2001. BACE2 Functions as an Alternative  $\alpha$ -Secretase in Cells. *Journal of Biological Chemistry*, 276(36), pp.34019–34027.
- Yan, R. et al., 1999. Membrane-anchored aspartyl protease with Alzheimer's disease  $\beta$ -secretase activity. *Nature*, 402, p.533.
- Yasuda, H. et al., 2002. A developmental switch in the signaling cascades for LTP induction. *Nature Neuroscience*, 6, p.15.
- Yu, G. et al., 2018. RING finger protein 10 prevents neointimal hyperplasia by promoting apoptosis in vitro and in vivo. *Life Sciences*, 208, pp.325–332.
- Zhang, Y. et al., 2011. APP processing in Alzheimer ' s disease. *Molecular Brain*, 4(1), p.3.
- Zheng, H. & Koo, E.H., 2011. Biology and pathophysiology of the amyloid precursor protein. *Molecular Neurodegeneration*, 6(1), p.27.

# PhD Research activity

Student Name: Ana Ribeiro

Student Number: R11496

Tutor: Prof. Fabrizio Gardoni

Co-Tutors: Prof. Elena Marcello and Prof. Monica Di Luca

Coordinator: Prof. Alberico L. Catapano

Academic year: 2017-2018

## Poster presentations:

1. **European Synapse meeting (ESM), December 2017, MILAN, ITALY**  
Ribeiro A, Musardo S, Carrano N, Marcello E, Gardoni F, Di Luca M. *A spine to nucleus signaling pathway in Alzheimer's disease.*
2. **Federation of European Neuroscience societies (FENS), July 2018, BERLIN, GERMANY**  
Ribeiro A, Musardo S, Carrano N, Barthet G, Mülle C, Marcello E, Gardoni F, Di Luca M. *A spine to nucleus signaling pathway in Alzheimer's disease.*
3. **American Society for Neuroscience (SfN), November 2018, SAN DIEGO, USA**  
Ribeiro A, Musardo S, Carrano N, Barthet G, Mülle C, Marcello E, Gardoni F, Di Luca M. *A spine to nucleus signaling pathway in Alzheimer's disease.*

## Data presentations:

<b>University of Milan</b> June 15th 2016	Data presentation during "Next Step 7" conference. (200 people)
<b>DZNE, Bonn, Germany</b> May 9th-10th 2017	SyDAD Annual meeting Data presentation for EU committee. (European committee + SyDAD committee)
<b>University of Milan</b> April 26th-28th 2017	Data presentation during PhD Spring Camp in Gargnano. (50 people)
<b>University of Milan</b> June 15th 2017	Data presentation during "Next Step 8" conference. (300 people)

<b>University of Milan</b> April 7th-8th 2018	SyDAD annual Meeting Data presentation. (European committee + SyDAD committee)
<b>University of Milan</b> April 14th 2018	Skype Data presentation during PhD Spring Camp. (50 people)
<b>Bordeaux, France</b> July 7th-11th 2018	SyDAD final annual Meeting Data presentation. (European committee + SyDAD committee)

## Attended courses/workshops:

### 2016

- Kick-off Meeting, Karolinska Institutet, April 21-22<sup>th</sup>
- Innovation Workshops, Serendipity Innovations and Axon Neuroscience, April 23<sup>th</sup>
- Alzheimer Disease Course, Karolinska Institutet, April 25-29<sup>th</sup> (ETCS 1,5)
- Neuropsychopharmacology course, University of Milan, June 6-10<sup>th</sup> (ECTS 2)
- Pharmacological properties of biotechnological drugs, University of Milan, June 14-17<sup>th</sup> (ETCS 2)
- Transversal competence courses, Course A: Open access, University of Milan, September 26<sup>th</sup>
- Transversal competence courses, Course B: Evaluation of research, University of Milan, October 3<sup>rd</sup>

### 2017

- Synapse Methodology course Bordeaux, January 18-26<sup>th</sup> (ETCS 1,5)
- Drug Discovery Course, Axon Neuroscience, March 26-28<sup>th</sup> (ETCS 1,5)
- Molecular Pharmacology and Applied Statistics, University of Milan, June 21<sup>st</sup> - 22<sup>nd</sup> (ECTS 1)
- Molecular Biology Course, University of Milan, 19<sup>th</sup> June; 4<sup>th</sup> July and 10<sup>th</sup> July (ECTS 1)
- Genetic toxicological issues and methodological approaches in vitro and in vivo, University of Milan, July 13<sup>th</sup> (ECTS 2)

### 2018

- Workshop Project Management and career plan, University of Milano, May 9<sup>th</sup> (ETCS 1)

## Other activities and Outreach activities:

- Italian language course, University of Milan, September 2016 – February 2017
- MEETmeTONIGHT – Faccia a faccia con la scienza, Milan, September 2017

- Instructor in the Workshop on Advanced Methods for Preclinical Alzheimer Disease Research, Bordeaux School of Neuroscience, January 21<sup>th</sup> - February 2<sup>nd</sup> (ETCS 3)

### Publication in preparation:

**“A spine to nucleus signaling pathway in Alzheimer’s disease”**

Ribeiro A, Musardo S, Carrano N, Barthet G, Mulle C, Marcello E, Gardoni F, Di Luca M.

### PhD Secondment:

- March 2017 – September 2017 in the IINS in Bordeaux – Electrophysiology: patch clamp technique in PP/GC in WT and RNF10 KO mice
- March 2019 in the IINS in Bordeaux – Electrophysiology: field LTP recordings in CA1 in WT and RNF10 KO mice